

Pharmaceutical development and clinical application
of
radiolabeled rituximab

ISBN/EAN 9789490122881

© Ly Tran

Printed by Gildeprint Drukkerijen, Enschede, The Netherlands
Cover designed by Pieter Frank de Jong, www.pieterfrank.com

**Pharmaceutical development and clinical application
of
radiolabeled rituximab**

Farmaceutische ontwikkeling en klinische toepassing
van
radioactief gelabeld rituximab

(met een samenvatting in het Nederlands)

Proefschrift

ter verkrijging van de graad van doctor aan de Universiteit Utrecht
op gezag van de rector magnificus, prof. dr. J.C. Stoof,
ingevolge het besluit van het college voor promoties
in het openbaar te verdedigen op
vrijdag 11 december 2009 des ochtends te 10.30 uur

door

Thi Hoang Ly Tran
geboren op 12 december 1978
te Vung Tau (Vietnam)

Promotor: Prof. dr. J.H. Beijnen

Co-promotoren: Dr. A.D.R. Huitema
Dr. J.W. Baars

The research described in this thesis was performed at

the department of pharmacy & pharmacology of the Slotervaart Hospital/the Netherlands Cancer Institute-Antoni van Leeuwenhoek Hospital, Amsterdam, the Netherlands

&

the department of medical oncology of the Netherlands Cancer Institute-Antoni van Leeuwenhoek Hospital, Amsterdam, the Netherlands

&

the department of nuclear medicine of the Netherlands Cancer Institute-Antoni van Leeuwenhoek Hospital, Amsterdam, the Netherlands

Printing of this thesis was financially supported by

The Netherlands Laboratory for Anticancer Drug Formulation, Amsterdam, the Netherlands

Dutch Arthritis Association, Amsterdam, the Netherlands

Roche Nederland B.V., Woerden, the Netherlands

Boehringer Ingelheim Nederland B.V., Alkmaar, the Netherlands

BV Cyclotron VU, Amsterdam, the Netherlands

IBA Pharma SA, Louvain-La-Neuve, Belgium

Merck Sharp & Dohme B.V., Haarlem, the Netherlands

J.E. Jurriaanse stichting, Rotterdam, the Netherlands

Amgen Nederland B.V., Breda, the Netherlands

Veenstra Instruments, Joure, the Netherlands

Von Gahlen Nederland B.V., Zevenaar, the Netherlands

“Laugh, and the world laughs with you”

Ella Wheeler Wilcox

Voor mijn ouders

Contents

Preface		11
Chapter 1	Radiolabeling of rituximab	
1.1	The preparation of radiolabeled monoclonal antibodies for human use	17
1.2	A simple and safe method for ¹³¹ I radiolabeling of rituximab for myeloablative high-dose radioimmunotherapy	37
1.3	Three spectroscopic techniques evaluated as a tool to study the effects of iodination of monoclonal antibodies, exemplified by rituximab	51
Chapter 2	Pharmacokinetics of unlabeled rituximab	
2.1	The pharmacokinetics of rituximab in patients with CD20 positive B-cell malignancies	67
Chapter 3	¹³¹I-rituximab in patients with CD20 positive B-cell malignancies	
3.1	Lack of tumor uptake of ¹³¹ I-rituximab in a patient with a CD20 positive lymphoma lesion	79
3.2	Pharmacokinetics of ¹³¹ I-rituximab in a patient with CD20 positive B-cell non-Hodgkin lymphoma: evaluation of the effect of radioiodination of the biological properties of rituximab	87
Chapter 4	¹²⁴I-rituximab in patients with rheumatoid arthritis	
4.1	The pharmacokinetics of ¹²⁴ I-rituximab as a radio-diagnostic in patients with rheumatoid arthritis	97
4.2	CD20 antigen imaging with ¹²⁴ I-rituximab in patients with rheumatoid arthritis	109
Conclusions and perspectives		121
Summary		127
Samenvatting		133
Dankwoord & Curriculum vitae		139

Preface

Rituximab is a chimeric monoclonal antibody against the CD20 antigen. The antigen is expressed on pre-B and mature B-cells. Rituximab is approved for the treatment of CD20 positive B-cell non-Hodgkin lymphoma as more than 90% of the B-cell non-Hodgkin lymphomas show CD20 antigen expression.

Since 2006, rituximab has also been approved for the treatment of patients with rheumatoid arthritis non-responsive to tumor necrosis factor antagonists. Rheumatoid arthritis is a destructive inflammatory joint disorder characterized by chronic inflammation of the synovial membrane. The precise pathogenesis of rheumatoid arthritis is unknown, but it is evident that B-cells play an important role in the inflammatory process.

Next to its therapeutic role, like other monoclonal antibodies, rituximab offers the application of procedures called radioimmunosintigraphy and radioimmunotherapy. The basic concept is to use monoclonal antibodies as a carrier to target the radionuclide to the target sites, B-cells involved in the underlying disease.

The aim of this thesis was the development of a labeling procedure for radioimmunotherapy and radioimmunosintigraphy with rituximab, and clinical application of radiolabeled rituximab.

For the preparation of radiolabeled monoclonal antibodies for clinical use, several requirements should be met. First, the preparation of this radioconjugate has to be performed in accordance with the principles of Good Manufacturing Practice. Secondly, a labeling technique with minimal radiation exposure to involved personnel is necessary. **Chapter 1.1** gives an overview of the considerations that have to be made for the manufacturing of clinical grade radiolabeled monoclonal antibodies.

Because of the well-known chemistry, many years of experience, and the availability of different isotopes with different emitting characteristics, iodine was chosen as radionuclide. **Chapter 1.2** focuses on the radiolabeling of rituximab with iodine. In this chapter, the procedure for radiolabeling rituximab with iodine is described. **Chapter 1.3** outlines the evaluation of three spectroscopic methods to study the effects of radioiodination on the molecular structure of rituximab.

In **chapter 2**, the pharmacokinetics of rituximab in patients with a CD20 B-cell malignancy is discussed. In this chapter, factors that can influence the pharmacokinetics of rituximab in patients with a CD20 positive malignancy were investigated.

Chapter 3 consists of two case reports that illustrate the application and the pharmacokinetic behavior of ¹³¹I-rituximab as consolidation treatment after induction therapy in patients with CD20 positive non-Hodgkin lymphoma. Chapter 4 focuses on the application of ¹²⁴I-rituximab for imaging in patients with rheumatoid arthritis. First, it was investigated if the pharmacokinetics of ¹²⁴I-rituximab are suitable for imaging over several days (**Chapter 4.1**). Secondly, the feasibility of CD20 antigen imaging using ¹²⁴I-rituximab has to be investigated which is outlined in **chapter 4.2**.

Chapter 1

Radiolabeling of rituximab

Chapter 1.1

The preparation of
radiolabeled monoclonal antibodies
for human use

Ly Tran

Jos H. Beijnen

Alwin D.R. Huitema

Abstract

Modalities like antibody based radioimmunotherapy and radioimmunoscinigraphy require the development and the use of radiolabeled monoclonal antibodies. For this, a radiolabeling procedure has to be designed for the preparation of radiolabeled monoclonal antibodies. As the radioconjugate is intended for human use, it has to possess characteristics like preservation of the immunoreactivity, high (radio)chemical purity, and high specific activity. Therefore, the labeling procedure has to meet several requirements. To guarantee a reproducible quality of the radiolabeled product, the whole labeling procedure has to be performed according to the rules of Good Manufacturing Practice (GMP). In addition, to warrant the safety of involved personnel, safety measurements have to be taken into account, to minimize radiance exposure. This review describes selected methods for the preparation of radiolabeled monoclonal antibodies for human use emphasizing pharmaceutical issues such as manufacturing and quality control.

Introduction

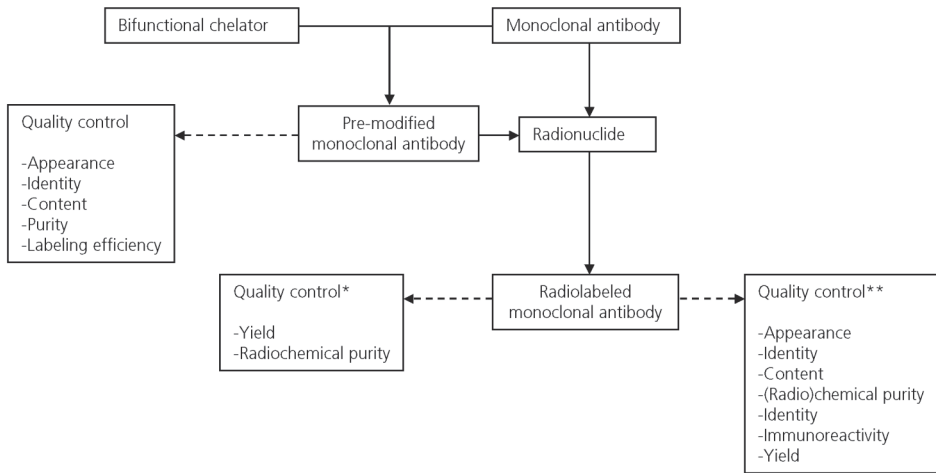
Monoclonal antibodies like trastuzumab and rituximab have proven their significant role in the treatment of malignant and benign diseases (1-4). Next to their therapeutic role, monoclonal antibodies also offer the application of radioimmunosciintigraphy and radioimmunotherapy. The basic concept is to use monoclonal antibodies as a carrier to transport a radionuclide to the target sites, exploiting the mechanism of selective binding of the antibody to an antigen (5-9). ⁹⁰Y-ibritumomab tiuxetan and ¹³¹I-tositumomab are the only commercially available radiolabeled monoclonal antibodies, and both are used for radioimmunotherapy of B-cell non-Hodgkin lymphoma (10,11). However, for many other applications, it is desirable to use radiolabeled monoclonal antibodies. Thus, for the application of (investigational) radioimmunotherapy or radioimmunosciintigraphy, a radiolabeling procedure has to be designed, usually in-house, to produce radiolabeled monoclonal antibodies. As the radioconjugate is intended for human use, it has to fulfill several pharmaceutical requirements. A high specific activity is required while the integrity, and thus the desired biological targeting and pharmacokinetic behavior, of the monoclonal antibody has to be preserved. A high radiochemical purity of the product is necessary as unbound radioactivity gives an unnecessary radiation exposure to the patient and decreases the imaging quality. For parenteral administration, the product needs to be sterile, pyrogen-free, and non-toxic. To guarantee a reproducible quality of the radiolabeled product, the manufacturing has to be performed according to Good Manufacturing Practice (GMP) (12). To warrant the safety of involved personnel, safety measurements have to be maintained concerning radianc exposure. The basic assumption is straightforward: the radianc exposure has to be As Low As Reasonably Achievable (ALARA, (13,14)). For this approach, four factors have to be taken into consideration for every step during manufacturing, quality control, and administration to achieve ALARA exposure: time, distance, shielding, and activity.

There are several methods available for radiolabeling of monoclonal antibodies. This review illustrates the most frequently used methods, and focuses on critical pharmaceutical steps when designing a procedure for the preparation, quality control and administration of radiolabeled monoclonal antibodies for human use.

Preparation process of radiolabeled monoclonal antibodies

Figure 1 shows a schematic overview of the manufacturing of radiolabeled monoclonal antibodies for human use.

An important item not included in the scheme is the quality control of the starting material. In many cases, however, the monoclonal antibody starting material is a commercially available, approved, pharmaceutical product. Nonetheless, specifications of all starting material should include details of their source, origin and (where applicable) method of manufacture and of the controls measures used to ensure



*Quality control of a radiolabeled pre-modified monoclonal antibody
 **Quality control of a radiohalogenated monoclonal antibody

Figure 1 A schematic overview of the manufacturing of radiolabeled monoclonal antibodies for human use

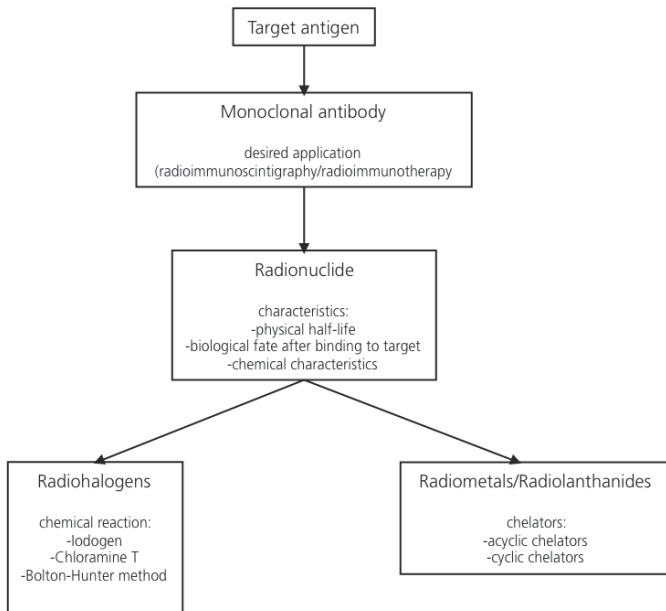


Figure 2 Choices in designing a new radiolabeled monoclonal antibody

For an optimal effect, the physical half-life has to be long enough for target uptake, and subsequently for target accumulation. The choice of the radionuclide also depends on the fate of the radiolabeled monoclonal antibody after binding to its target. For instance, radiometals and radiolanthanides are favored when the target antigen is internalized due to a better retention after lysosomal proteolysis (17). Knowledge about the chemical properties of the radionuclide as well as the monoclonal antibody is therefore required. The chosen radionuclide, subsequently, determines how the conjugation with the antibody can be accomplished.

Radiohalogens

Table 1 gives an overview of mostly applied methods of radiolabeling with radiohalogens.

Iodine is one of the most frequently used radiohalogens and, therefore, most of the described labeling methods for radiohalogens concern the radiolabeling with iodine. Several isotope forms are available (^{123}I , ^{124}I , ^{125}I , ^{131}I), with different emission characteristics, but the labeling chemistry remains the same (16,18-20).

Radiohalogens are generally obtained as their halide salt. Oxidation of radiohalogens enables covalent binding of the halogen to the monoclonal antibody. Because of the volatile nature of most radiohalogens, a closed labeling system is preferred which is also supported by GMP-guidelines.

1,3,4,6-tetrachloro-3 α ,6 α -diphenylglycouril (Iodogen) and *N*-chloro-*p*-toluenesulfonamide (Chloramine T) are commonly used to oxidize radiohalogens. In presence of Iodogen or Chloramine T, the radiohalogen is converted to a reactive specie which then attacks the most electronegative site on the monoclonal antibody. At a neutral pH, linkage of the radiohalogen on the tyrosine residues *ortho* to the hydroxyl group of phenolring predominates (21,22).

The oxidizing agent Iodogen is commonly used for radiohalogenation of monoclonal antibodies (21). The conventional method is to coat a reaction vial with Iodogen (coated vial method): Iodogen is dissolved in an organic solvent and is coated on the walls of a vial by evaporation of the solvent. The labeling reaction commences when the radiohalogen is added to the coated vial containing the monoclonal antibody. Iodogen is virtually insoluble in water, and thus the reaction can be stopped by transferring the reaction solution into another non-coated vial. Therefore, an advantage of Iodogen is that the radiolabeled monoclonal antibody can be readily separated from Iodogen, and a purification step is not always necessary. In addition, the possibility to use syringes and lines to transfer the solutions minimizes the radiation exposure.

As Iodogen is an oxidizing agent, it can also cause oxidation of amino acid residues of a monoclonal antibody and, therefore, Iodogen can affect the integrity of the monoclonal antibody which can decrease the binding affinity to the target antigen. Hayes showed a decrease in binding affinity when a 10-fold higher amount of

Iodogen was applied (23). The monoclonal antibody (MAb DF3) reacts with a family of large molecular weight glycoproteins expressed by 78% of breast cancer cells and 95% of epithelial ovarian cancer cells (24). The binding affinity to a breast cancer cell line, MCF-7, of unlabeled MAb DF3 was compared to that of MAb DF3 exposed to different concentrations of Iodogen in absence of radioactivity. The amount of MAb DF3 required to obtain half-maximal binding ($B_{1/2,max}$) for native MAb DF3 was 180 ng, while the $B_{1/2,max}$ for MAb DF3 exposed to an Iodogen:antibody ratio of 1:1 and 10:1 was 580 ng and 1800 ng, respectively. As no radioactivity was used, the decrease in binding affinity could neither be assigned to incorporation of iodine atoms into the functional regions nor to radiation damage. Therefore, the decrease in binding affinity was caused by chemical damage of MAb DF3 by oxidation of amino acid residues, and the concentration of Iodogen, which causes minimal damage to the monoclonal antibody and a sufficiently high specific activity has to be investigated.

Visser et al introduced a labeling method using a minimal amount of Iodogen in solution (Iodogen:antibody ratio 0.007:1) for high dose labeling of c-MOV18. To terminate the reaction, the reductant ascorbic acid was added. For comparison, ^{131}I labeled c-MOV18 batches were made using the coated vial method (Iodogen:antibody ratio 0.1:1). High-dose labeling of 5 mg c-MOV18 with 4.4 GBq ^{131}I resulted in a labeling yield of 60%, a radiochemical purity of 90%, and an immunoreactivity 25%. Using similar amounts of ^{131}I and c-MOV18 in the method introduced by Visser et al, 85%–89% overall radiochemical yield, a radiochemical purity larger than 99.7%, and an immunoreactivity of 72% were found. The results, thus, showed an improved preservation of the immunoreactivity by application of this improved method. For rituximab similar results have been obtained (25). However, compared to the coated vial method, the method introduced by Visser et al requires more manual handling. Considering the high dose of radioactivity, the hands are potentially exposed to a relatively large amount of radiation. Therefore, appropriate shielding, and, if possible, replacement of the manual handling is required to minimize the radiation exposure.

Chloramine T is a sodium salt of *N*-monochloro-*p*-toluenesulfonamide and is a water-soluble oxidizing agent. The monoclonal antibody for labeling is added to the radiohalogen in solution. The labeling reaction is evoked by the addition of a solution of Chloramine T. Chloramine T oxidizes the radiohalogen to a reactive specie, which then labels the monoclonal antibody (22). Reducing agents are required to terminate the reaction. It has been reported that sulphite based reducing agents also reduce amino acids residues of the monoclonal antibody and thereby contribute to a loss of immunoreactivity (26-28). Previous studies showed that the integrity of a radiolabeled monoclonal antibody was affected after incubation with sodium bisulphite. Phosphor imager quantification, after gel electrophoresis, showed, next to the intact radiolabeled monoclonal antibody c-MOV18, a degradation product which presented 18% of the radioactivity. The immunoreactivity

was reduced to 58%. Analogous incubation with ascorbic acid did not affect the integrity and gave an immunoreactivity of 72% (28). Termination of the reaction can be performed using gel-filtration with the advantage that also purification of the product from residual radiohalogen and Chloramine T is achieved (29).

Like Iodogen, Chloramine T is an oxidizing agent. Although the oxidizing effect of Iodogen has been investigated more extensively, damage to the monoclonal antibody due to the oxidizing effect of Chloramine T has to be considered. Therefore, like Iodogen, the optimal concentration of Chloramine T has to be investigated.

Iodogen and Chloramine T offer the application of a single vial to perform the labeling. Because of the simplicity of these methods, it is possible to adapt remote handling procedures into a closed system to minimize the safety hazards to those performing the labeling (26,30,31).

Bolton and Hunter introduced a method for labeling proteins which does not link the radionuclide to the tyrosine moiety. Moreover, the monoclonal antibody is not directly bound to the radiohalogen (20). The procedure consists of pretreatment of the radionuclide and subsequent labeling. First, the Bolton-Hunter reagent, a N-hydroxysuccinimide ester of 3-(4-hydroxyphenyl)propionic acid, is labeled with the radiohalogen using Chloramine T. The reaction is terminated by addition of a reducing agent (sodium metabisulphite (20)) Following steps involve extraction of the radiohalogenated ester and evaporation of the solvents. Subsequently, the ester can react with free amine groups of the monoclonal antibody to form amides. Commonly, the radiohalogenated ester is conjugated to lysine moieties of the monoclonal antibody (20). Purification from the products of the radiohalogenation reaction is necessary to obtain a (radio)chemical pure product.

Behr et al compared three approaches (Iodogen, Chloramine T and Bolton-Hunter) to radioiodinate several monoclonal antibodies (32). By using Iodogen and Chloramine T based radioiodination procedures, incorporation yields were observed between 60 and 90%. In addition, the immunoreactivity was larger than 85%, regardless whether Iodogen or Chloramine-T was used. Using Bolton-Hunter methodology, a lower incorporation yield of 20-55% was observed (32). The authors did not mention the immunoreactivity obtained using the Bolton-Hunter. Hayes et al claimed to achieve a higher immunoreactivity using the Bolton-Hunter method compared to Iodogen as oxidizing agent (23). Labeling of the monoclonal MAb DF3 showed an immunoreactivity of 24 % when a Iodogen:antibody ratio of 1:1 was used. An immunoreactivity of 65% was obtained when the Bolton-Hunter reagent was applied to the same amount monoclonal antibody. However, the applied Iodogen:antibody ratio of 1:1 is relatively high, as a ratio of 0.1:1 is regularly used.

Table 1 Methods for radiohalogenation

Reagent	Structure	Advantage	Disadvantage	References
Chloramine T	<p>Chloramine T + Tyrosine residue</p>	Simple Close vial Remote procedure	Purification required Reducing agent required Loss of immunoreactivity	(22,26,27, 29,31,32)
Iodogen	<p>Iodogen + Tyrosine residue</p>	Simple Close vial Remote procedure Purification not required*	Loss of immunoreactivity	(21,25,28, 32,76)
Bolton-Hunter method	<p>Bolton-Hunter reagent + Tyrosine residue + Lysine residue</p>	Application for protein lacking tyrosine groups	Labor-intensive High variability in labeling yield Open system	(20,23,32)

X: Radiohalogen

R: monoclonal antibody

*: Purification is not required when radiochemical purity is within the criteria.

Iodogen as well as Chloramine T substitute the radiohalogen into tyrosine residue of the monoclonal antibody. At a neutral pH, linkage of the radiohalogen on the tyrosine residues *ortho* to the hydroxyl group predominates (21,22). Although the complementary determining region represents less than one-tenth of the amino acid sequence, typically these regions include 20-30% of the tyrosines (33). Hence, binding of radiohalogens to the tyrosine residues in the antibody complementary-determining regions of the binding site can affect the immunoreactivity. Application of the Bolton-Hunter method, results in a linkage of the radionuclide via a lysine moiety of the monoclonal antibody, aiming for a preservation of the immunoreactivity as lysine moieties are uniformly distributed throughout the monoclonal antibody (33).

However, the low incorporation yield may be caused by the radiohalogenated hydroxysuccinimide ester of 3-(4-hydroxyphenyl)propionic acid (the Bolton-Hunter reagent) which is unstable under conditions of the radiohalogenation. Therefore, halogenation of the reagent has to be performed as quickly as possible to prevent hydrolysis (20). Because of the instability of the hydroxysuccinimide ester, the method has low reproducibility. Also, the method is labor-intensive and requires careful handling techniques concerning radiance safety. The pretreatment procedures of the radiohalogen enlarge the risk of (radioactive) contamination and radiance exposure. This method should, therefore, be restricted to its use of either monoclonal antibodies which could not be labeled using another method or monoclonal antibodies having abundant tyrosine moieties in the complementary-determining regions.

Several studies showed a correlation between immunoreactivity and specific activity. Schaffland et al demonstrated the relationship between specific activity and immunoreactivity using 2 different specific activities of ^{131}I labeled rituximab (32.8 MBq/mg vs 169.7 MBq/mg) (29). Binding was analyzed at maximally observed binding capacity on 10^7 cells of Raji and Daudi cells expressed as percentage of the added radioactivity. The results showed a statistically significant higher binding for ^{131}I rituximab with the lower specific activity (51.1 ± 7.9 vs 35.8 ± 11.1 for Raji cells and $57.1\% \pm 8.3$ vs $42.0 \pm 13.00\%$ for Daudi cells). Similar observations of higher immunoreactivity at a lower specific activity of ^{131}I have been described for anti-B1 which is also an anti-CD20 monoclonal antibody. The immunoreactivity was estimated to be 58% for a specific activity of 29.6 MBq/mg and 49% for a specific activity of 325.3 MBq/mg (15).

A radiohalogen as ^{131}I is a relatively large atom. Next to binding to a tyrosine moiety in a determining region which prevents binding to the binding site of a target antigen, incorporation of such a large molecule into a monoclonal antibody may cause a disruption of the structure. Disruption of the structure can lead to a reduced binding affinity. This effect may be larger at a higher specific activity due to a high number of incorporated atoms.

Therefore, to achieve optimal effect of the radiohalogenated monoclonal antibody, knowledge about the amino acid sequence, and the correlation of the specific activity (radionuclide/antibody ratio) with the immunoreactivity, are crucial in the development of effective therapeutic or diagnostic applications.

Radiometals and radiolanthanides

Radiometals and radiolanthanides are linked to the monoclonal antibody via a chelator. The binding process is thereby performed in two steps. First pre-modification (the conjugation of the chelator to the monoclonal antibody) and secondly the actual radiolabeling of the antibody via the chelator just before administration. The pre-modification of a monoclonal antibody can be performed in large scale. The pre-modified monoclonal antibody can be formulated into a ready-to-use kit, which can be stored until use. No radioactivity is involved during the manufacturing of the pre-modified monoclonal antibody. Radiation exposure is restricted to the actual labeling, which only consists of the addition of the radionuclide, and, if applicable some quality control testing. If needed, a purification step has to be included (17,34,35).

The most important factor in choosing an appropriate chelator is to produce a stable radioconjugate. The choice of chelator depends on the nature and oxidation state of the radionuclide. Therefore, a good understanding of the coordination chemistry of the radiometal to be labeled is crucial. For more comprehensive discussions of this subject, other reviews may be consulted (36,37).

The chelators can largely be divided into two categories: acyclic chelators and macrocyclic chelators. Among the acyclic chelators, active ester derivatives of diethylenetriaminepentaacetic acid (DTPA) are most commonly used (17,38-41). For the macrocyclic chelators, derivatives of 1,4,7,10-tetraazacyclododecanetetraacetic acid (DOTA) are the most frequently used chelators. The overall conjugation process of the chelator to the monoclonal antibody is similar for different chelators. In brief, the chelator is conjugated to the monoclonal antibody by incubation. Because the active ester of the chelating agent reacts with the neutral form of the lysine moiety, the monoclonal antibody has to be transferred into a buffer in which a proportion of the lysine side chains are uncharged (42). After the incubation step, the monoclonal antibody-chelator complex is purified and transferred into another buffer.

For the actual radiolabeling step, the pH of the reaction buffer is crucial. At pH>6, many metal ions form insoluble hydroxide complexes with water and become unavailable for binding to the chelator. At a pH between 4 and 6, the radionuclide remains in solution during the labeling procedure. The presence of weakly chelating ions, such as acetate or citrate, in the buffer reduces the possibility of hydrolysis (42,43). Anti-oxidants in the buffer can prevent radiolysis of the antibody after radiolabeling.

Difficulties have been encountered in the radiolabeling of DOTA-conjugated monoclonal antibodies. The slow rate of formation of radionuclide-DOTA-monoclonal antibody complexes requires a prolonged incubation time which can result in extensive radiolysis (42,44-48). Kukis et al investigated labeling conditions of ^{90}Y -DOTA immunoconjugates, and showed that at room temperature, 62% of ^{90}Y was conjugated in 30 minutes, while at 37°C 89% of ^{90}Y was conjugated within 5 minutes (49). Although elevated temperatures are needed for successful radiolabeling, higher temperatures may cause degradation as well as a loss of immunoreactivity of thermolabile monoclonal antibodies (50,51). Therefore, a drawback of using DOTA complexes is that some heating is often required for their formation, whereas DTPA complexes readily are formed at room temperature (52-54).

When a monoclonal antibody is conjugated with a bifunctional chelator, the site of attachment is often at a lysine moiety of the monoclonal antibody. Radiometals/radiolantanides conjugated via bifunctional chelator, therefore, often show a better distribution of the ligand over the entire monoclonal antibody compared to radiohalogens which are exclusively bounded to tyrosine moieties (55,56). Labeling of a monoclonal antibody (HuM195) with up to 7 chelate molecules per monoclonal antibody molecule resulted in minimal losses of immunoreactivity, whereas equivalent labeling with iodine molecules reduced binding to an immunoreactivity lower than 20% (33). Thus, radiometal chelates may be more suitable for high specific activity radiolabeling of monoclonal antibodies.

A higher incorporation yield requires more chelators per monoclonal antibody. However, it has been reported that the number of chelating groups influences the immunoreactivity and biodistribution. Zimmerman et al showed that with a chelator/antibody ratio of 11 an immunoreactivity of 100% was obtained (57). Substitution of 18 chelator groups (DO3A) per antibody (chCE7), however, led to an 25% lower immunoreactivity. In vivo tumor uptake was decreased by 80%, while accumulation in the liver showed an increase of 40%. Knogler et al showed that the highest specific activity (106 MBq/mg) was achieved with 12 chelator groups per monoclonal antibody molecule. When 15 chelator groups were attached, no increase of specific activity was found, while a substantially higher uptake in the liver was observed (58). This implies that an increase of chelator groups per monoclonal antibody molecule does not always lead to a higher specific activity. Therefore, determination of the stoichiometric ratio (chelator:antibody ratio) is essential to establish the most optimal construct.

Purification/buffer exchanging steps

As mentioned, several purification/buffer exchanging steps are required during the entire procedure (12).

When handling radioactive material, a rapid procedure is preferred because of the radioactive decay as well as for radiation safety. Most purification methods require extensive manual handling. When radioactivity is involved, monitoring of hand- and finger exposure is, therefore, necessary. Utilization of a closed system in a controlled area, under aseptic conditions, is often required.

Purification or buffer exchange by elution through gel filtration columns based on size exclusion chromatography results in a high recovery yield. The monoclonal antibody, either unlabeled, labeled, or conjugated is eluted with a new buffer, and low-weight molecular components can be washed off. However, collecting requires manual handling which can be problematic when radioactivity is involved. Collecting and pooling of fractions need to be optimized during the development phase to minimize number of steps, and current technologies offer the possibility for an automated system (59).

Centrifugal ultrafiltration is a commonly used method. The method is based on ultrafiltration through a membrane with a molecular mass cut-off. However, the method results in a low recovery yield. Therefore, for optimal purification and recovery, the antibody has to be diluted with exchange buffer and recentrifuged several times. For purification of a monoclonal-chelator conjugate (DTPA-hEGF), 8 dilution and ultrafiltration steps were necessary (59). For purification of the radiolabeled monoclonal antibody, the multiple steps of dilution and ultrafiltration enlarge the radiation exposure. Hence, the method requires optimization (e.g. number of dilution steps, dilution volume, time of centrifugation) to reduce the radiation exposure.

Dialysis facilitates purification and buffer exchange based on diffusion. The product is applied into a sterile dialysis cassette, and the cassette is placed in a vessel with the exchange buffer. Small molecules are diffused out of the cassette, and the buffer is exchanged (60). The exchange buffer has to be refreshed several times for optimal purification. The dialysis procedure often takes several hours. Considering the decay of radioactivity this method is usually not applicable for purification of radioconjugates (60). The method, however, is suitable for purification of pre-modified monoclonal antibodies.

Tangential flow filtration is commonly used in the biopharmaceutical industry to separate, purify, and to concentrate products (61,62). Tangential flow filtration is a separation technique that uses pressurized membrane systems with a certain cut-off value. While recirculating and replenishing the solution with the protein, along the membrane, solvent is pressed through the membrane pores into a waste container, taking molecules with higher molecular mass than the cut-off value along. The solution is recirculated until the required concentration is obtained. This method is applicable for buffer exchange and purification of the pre-modified monoclonal antibody as well as purification of the radiolabeled monoclonal antibody (25). Tangential flow filtration can be executed in a closed system using autoclavable material. The method is semi-automated, manual handling, however, is required for

the replenishing steps. Therefore, although the method can be performed remotely, radiation exposure to the hands has to be considered. Using a dose of 7400 MBq ^{131}I gives a maximum detected exposure to the hands of 1.9 mSv (25). Tangential flow filtration is expensive compared to the other mentioned methods.

Quality control

As the radioconjugate is intended for human use, it is imperative to implement quality controls.

All quality control procedures that are applied to non-radioactive parental products are also applicable for radiolabeled monoclonal antibodies. Because of the short shelf-life of the radiolabeled product, these tests are often performed in retrospect. Some of these tests can be restricted to the pharmaceutical development phase.

The integrity of the radiolabeled monoclonal antibody has to be preserved to retain binding to the target. The immunoreactivity of the radiolabeled monoclonal antibody is therefore important to be determined. A widely used method to determine the immunoreactivity of a radiolabeled antibody is described by Lindmo et al (63). They have presented a method in which the immunoreactive fraction is determined by extrapolation from conditions representing infinite antigen excess. The extrapolation is performed in a double-inverse linear plot which is a modification of the Lineweaver-Burk plot. The basic defect in the Lindmo method is that it uses extrapolation, and values can be produced that are clearly overestimated. Most monoclonal antibodies show a plateau in the fraction of monoclonal antibody binding, as the antigen-monoclonal antibody ratio is increased, therefore the actual binding is a reasonably good estimate of the immunoreactive fraction, and extrapolation is not required (23).

For determination of the binding of the radiolabeled monoclonal antibody, the availability of the target antigen is required. Cell-lines with an overexpression of the target antigen are usually used for this purpose (e.g. SKOV-3 cell line with HER2 overexpression, Raji and Daudi cell lines with CD20 antigen overexpression) (17,29). Bevacizumab is a humanized monoclonal antibody that recognizes and blocks vascular endothelial growth factor (VEGF). Radiolabeled bevacizumab has been used for noninvasive in vivo VEGF visualization in patients with colorectal cancer (64). VEGF is a soluble protein (65) and, hence, usage of cell lines for determination of the immunoreactivity is impossible. For determination of the binding properties for VEGF of radiolabeled bevacizumab a VEGF-coated enzyme-linked immunosorbent assay was designed, by Collingridge et al (66). Serial dilutions of radiolabeled bevacizumab were added to a fixed amount of VEGF. After incubation and washing steps, antigen bound radioactivity was measured.

Determination of the immunoreactivity is time-consuming (varying from 1 hr to >1 day) (17,25). Therefore, it is often restricted to the determination during the development and validation phase.

For optimal use of the radioconjugate, a high and persistent radioactivity uptake at the target site is important. This requires a high number of chelators or radionuclides coupled to the antibody in order to achieve high labeling yields and high specific activity. However, as mentioned, the number of incorporated groups can influence the immunoreactivity and biodistribution. Matzku et al observed that the effects of radiolabeling differ within a series of anti-melanoma monoclonal antibodies under similar labeling conditions (67). The unique primary, secondary and tertiary structures of these proteins may result in different sensitivities to various labeling conditions. Therefore, either steric hindrance or conformational changes may contribute to a decrease in binding affinity. Thus, in the development phase of a new radiolabeled monoclonal antibody, determination of the stoichiometric ratio and structural characterization is needed to get more insight into the correlation between the specific activity and immunoreactivity.

High performance liquid chromatography-size exclusion chromatography (HPLC-SEC) is an important tool in the analysis of samples as it provides separation of components with high resolution. When coupled to an ultraviolet (UV) and/or a radioactive detector, several characteristics (degradations products, (radio)chemical impurity, aggregates) can be determined. Coupled online with a mass spectrometer a protein specific charge envelope can be generated. Structural changes in the molecule and/or degradation patterns can be detected (68).

Far-ultraviolet circular dichroism (far-UV CD) has been applied to map the secondary structural stability of a monoclonal antibody during development, production and storage (50,51). Shifts in wavelengths or differences in the peak intensity could indicate an alteration in secondary structure of the monoclonal antibody.

Fluorescence emission spectrophotometry is a procedure, which uses changes in the intensity of protein fluorescence emission spectra as an indicator to observe alterations for the conformation of proteins (69). For monoclonal antibodies that are radiolabeled with Iodine, a decrease in fluorescence can be observed, as iodine is known for its quenching characteristics (70). Loss of incorporated iodine would result in less quenching and thus in a higher fluorescence intensity. Hence, fluorescence emission spectrophotometry can be a tool for stability monitoring.

The stability and storage conditions of the radioconjugate have to be investigated. Radiations emitted by the radionuclides can lead to radiolysis of the labeled compound. High specific activity can cause more radiolysis resulting in radiochemical impurities (71,72). Salako et al studied the impact of specific activity on the stability of ^{90}Y labeled Lym-1 antibody to establish a formulation at which radiolysis was acceptable (73). The monoclonal antibody was radiolabeled with different doses of ^{90}Y . The radiochemical purity, monitored daily with HPLC-SEC, and the immunoreactivity of each preparation were monitored for 3 days. The quality and purity profile of products at 3.7 and 7.4 MBq/mg were retained ($\geq 80\%$) as was the immunoreactivity for both doses ($\geq 75\%$) over 3 days. The radiochemical purity and immunoreactivity of the product at 14.8 MBq/mg declined to 65% and 28%,

respectively, by 3 days after preparation. In 48 hrs after preparation, the product with a specific activity of 34 MBq/mg had degraded to 21% in radiochemical purity with only 3% immunoreactivity remaining.

The presence of unbound radioactivity results in poor-quality images due to the high background which is unattractive for radioimmunoscintigraphic purposes. But moreover, unbound radioactivity gives unnecessary radiation dose to the patient. Unbound ^{111}In is taken up by the liver, ^{177}Lu and ^{90}Y possess high affinity for the bone (74). For iodine isotopes, thyroid uptake is a well-known phenomenon as ^{131}I is applied for thyroid therapy (75). Determination of the (radio)chemical purity of a compound is thus mandatory after each production.

Conclusions

Several considerations have to be taken into account when designing a procedure for radiolabeling of a monoclonal antibody. Guided by GMP and radiation safety guidelines, the procedure has to result in a reproducible, (radio)chemical pure product with preservation of its integrity. Knowledge about the labeling method is required, as the method itself can affect amino acid residues of the monoclonal antibody reflected in a deterioration of the immunoreactivity. Furthermore, the correlation between the specific activity and the immunoreactivity is an important factor, and needs to be investigated for optimization of the labeling procedure.

References

1. Slamon DJ, Leyland-Jones B, Shak S et al. Use of chemotherapy plus a monoclonal antibody against HER2 for metastatic breast cancer that overexpresses HER2. *N Engl J Med* 2001;344(11):783-792
2. Pegram MD, Lipton A, Hayes DF et al. Phase II study of receptor-enhanced chemosensitivity using recombinant humanized anti-p185HER2/neu monoclonal antibody plus cisplatin in patients with HER2/neu-overexpressing metastatic breast cancer refractory to chemotherapy treatment. *J Clin Oncol* 1998;16(8):2659-2671
3. Berinstein NL, Grillo-Lopez AJ, White CA et al. Association of serum Rituximab (IDEC-C2B8) concentration and anti-tumor response in the treatment of recurrent low-grade or follicular non-Hodgkin's lymphoma. *Ann Oncol* 1998;9(9):995-1001
4. McLaughlin P, Grillo-Lopez AJ, Link BK et al. Rituximab chimeric anti-CD20 monoclonal antibody therapy for relapsed indolent lymphoma: half of patients respond to a four-dose treatment program. *J Clin Oncol* 1998;16(8):2825-2833
5. van NJ, Jr., Kim E, Casper S et al. Radioimmunodetection of primary and metastatic ovarian cancer using radiolabeled antibodies to carcinoembryonic antigen. *Cancer Res* 1980;40(3):502-506
6. Goldenberg DM, Sharkey RM. Radioimmunotherapy of non-Hodgkin's lymphoma revisited. *J Nucl Med* 2005;46(2):383-384
7. Goldenberg DM, Sharkey RM. Advances in cancer therapy with radiolabeled monoclonal antibodies. *Q J Nucl Med Mol Imaging* 2006;50(4):248-264
8. Sharkey RM, Goldenberg DM. Perspectives on cancer therapy with radiolabeled monoclonal antibodies. *J Nucl Med* 2005;46 Suppl 1:115S-27S. 115S-127S
9. Larson SM. Radiolabeled monoclonal anti-tumor antibodies in diagnosis and therapy. *J Nucl Med* 1985;26(5):538-545
10. Horning SJ, Younes A, Jain V et al. Efficacy and safety of tositumomab and iodine-131 tositumomab (Bexxar) in B-cell lymphoma, progressive after rituximab. *J Clin Oncol* 2005;23(4):712-719
11. Witzig TE. Efficacy and safety of 90Y ibritumomab tiuxetan (Zevalin) radioimmunotherapy for non-Hodgkin's lymphoma. *Semin Oncol* 2003;30(6 Suppl 17):11-16
12. EudraLex, Good manufacturing practices: medicinal products for human and veterinary use. 2009;Volume 4 (http://ec.europa.eu/enterprise/pharmaceuticals/eudralex/vol4_en.htm)
13. International Commission on Radiological Protection. 1990 Recommendations of the international commission on radiological protection. ICRP publication 60. *Annals of the ICRP* 1991;21:1-3
14. Hendee WR, Edwards FM. ALARA and an integrated approach to radiation protection. *Semin Nucl Med* 1986;16(2):142-150
15. Kaminski MS, Zasadny KR, Francis IR et al. Radioimmunotherapy of B-cell lymphoma with [131I]anti-B1 (anti-CD20) antibody. *N Engl J Med* 1993;329(7):459-465
16. Verel I, Visser GW, Vosjan MJ et al. High-quality 124I-labelled monoclonal antibodies for use as PET scouting agents prior to 131I-radioimmunotherapy. *Eur J Nucl Med Mol Imaging* 2004;31(12):1645-1652
17. Lub-de Hooge MN, Kosterink JG, Perik PJ et al. Preclinical characterisation of 111In-DTPA-trastuzumab. *Br J Pharmacol* 2004;143(1):99-106
18. Blauenstein P, Locher JT, Seybold K et al. Experience with the iodine-123 and technetium-99m labelled anti-granulocyte antibody MAb47: a comparison of labelling methods. *Eur J Nucl Med* 1995;22(7):690-698
19. Vose JM, Bierman PJ, Enke C et al. Phase I trial of iodine-131 tositumomab with high-dose chemotherapy and autologous stem-cell transplantation for relapsed non-Hodgkin's lymphoma. *J Clin Oncol* 2005;23(3):461-467
20. Bolton AE, Hunter WM. The labelling of proteins to high specific radioactivities by conjugation to a 125I-containing acylating agent. *Biochem J* 1973;133(3):529-539
21. Fraker PJ, Speck JC, Jr. Protein and cell membrane iodinations with a sparingly soluble chloroamide, 1,3,4,6-tetrachloro-3a,6a-diphenylglycoluril. *Biochem Biophys Res Commun* 1978;80(4):849-857
22. Greenwood FC, Hunter WM, Glover JS. The preparation of I-131-labelled human growth hormone of high specific radioactivity. *Biochem J* 1963;89:114-23. 114-123
23. Hayes DF, Noska MA, Kufe DW et al. Effect of radioiodination on the binding of monoclonal antibody DF3 to breast carcinoma cells. *Int J Rad Appl Instrum B* 1988;15(3):235-241

24. Kufe D, Inghirami G, Abe M et al. Differential reactivity of a novel monoclonal antibody (DF3) with human malignant versus benign breast tumors. *Hybridoma* 1984;3(3):223-232
25. Tran L, Baars JW, Maessen HJ et al. A simple and safe method for ¹³¹I radiolabeling of rituximab for myeloablative high-dose radioimmunotherapy. *Cancer Biother Radiopharm* 2009;24(1):103-110
26. Weadock KS, Sharkey RM, Varga DC et al. Evaluation of a remote radioiodination system for radioimmunotherapy. *J Nucl Med* 1990;31(4):508-511
27. Robles AM, Balter HS, Oliver P et al. Improved radioiodination of biomolecules using exhaustive Chloramine-T oxidation. *Nucl Med Biol* 2001;28(8):999-1008
28. Visser GW, Klok RP, Gebbinck JW et al. Optimal quality (¹³¹I)-monoclonal antibodies on high-dose labeling in a large reaction volume and temporarily coating the antibody with IODO-GEN. *J Nucl Med* 2001;42(3):509-519
29. Schaffland AO, Buchegger F, Kosinski M et al. ¹³¹I-rituximab: relationship between immunoreactivity and specific activity. *J Nucl Med* 2004;45(10):1784-1790
30. Ferens JM, Krohn KA, Beaumier PL et al. High-level iodination of monoclonal antibody fragments for radiotherapy. *J Nucl Med* 1984;25(3):367-370
31. Weadock KS, Anderson LL, Kassis AI. A simple remote system for the high-level radioiodination of monoclonal antibodies. *J Nucl Med Allied Sci* 1989;33(1):37-41
32. Behr TM, Gotthardt M, Becker W et al. Radioiodination of monoclonal antibodies, proteins and peptides for diagnosis and therapy. A review of standardized, reliable and safe procedures for clinical grade levels kBq to GBq in the Gottingen/Marburg experience. *Nuklearmedizin* 2002;41(2):71-79
33. Nikula TK, Bocchia M, Curcio MJ et al. Impact of the high tyrosine fraction in complementarity determining regions: measured and predicted effects of radioiodination on IgG immunoreactivity. *Mol Immunol* 1995;32(12):865-872
34. Dijkers EC, de Vries EG, Kosterink JG et al. Immunoscintigraphy as potential tool in the clinical evaluation of HER2/neu targeted therapy. *Curr Pharm Des* 2008;14(31):3348-3362
35. Nagengast WB, de Vries EG, Hospers GA et al. In vivo VEGF imaging with radiolabeled bevacizumab in a human ovarian tumor xenograft. *J Nucl Med* 2007;48(8):1313-1319
36. Liu S. Bifunctional coupling agents for radiolabeling of biomolecules and target-specific delivery of metallic radionuclides. *Adv Drug Deliv Rev* 2008;60(12):1347-1370
37. Brechbiel MW. Bifunctional chelates for metal nuclides. *Q J Nucl Med Mol Imaging* 2008;52(2):166-173
38. Brechbiel MW, Gansow OA. Backbone-substituted DTPA ligands for ⁹⁰Y radioimmunotherapy. *Bioconjug Chem* 1991;2(3):187-194
39. Hnatowich DJ, Snook D, Rowlinson G et al. Preparation and use of DTPA-coupled antitumor antibodies radiolabeled with yttrium-90. *Targeted Diagn Ther* 1988;1:353-74.353-374
40. Roselli M, Schlom J, Gansow OA et al. Comparative biodistribution studies of DTPA-derivative bifunctional chelates for radiometal labeled monoclonal antibodies. *Int J Rad Appl Instrum B* 1991;18(4):389-394
41. Reilly R, Lee N, Houle S et al. In vitro stability of EDTA and DTPA immunoconjugates of monoclonal antibody 2G3 labeled with indium-111. *Int J Rad Appl Instrum A* 1992;43(8):961-967
42. Sosabowski JK, Mather SJ. Conjugation of DOTA-like chelating agents to peptides and radiolabeling with trivalent metallic isotopes. *Nat Protoc* 2006;1(2):972-976
43. Liu S, Ellars CE, Edwards DS. Ascorbic acid: useful as a buffer agent and radiolytic stabilizer for metaloradiopharmaceuticals. *Bioconjug Chem* 2003;14(5):1052-1056
44. Lewis MR, Raubitschek A, Shively JE. A facile, water-soluble method for modification of proteins with DOTA. Use of elevated temperature and optimized pH to achieve high specific activity and high chelate stability in radiolabeled immunoconjugates. *Bioconjug Chem* 1994;5(6):565-576
45. Camera L, Kinuya S, Garmestani K et al. Comparative biodistribution of indium- and yttrium-labeled B3 monoclonal antibody conjugated to either 2-(p-SCN-Bz)-6-methyl-DTPA (1B4M-DTPA) or 2-(p-SCN-Bz)-1,4,7,10-tetraazacyclododecane tetraacetic acid (2B-DOTA). *Eur J Nucl Med* 1994;21(7):640-646
46. Williams LE, Lewis MR, Bebb GG et al. Biodistribution of ¹¹¹In- and ⁹⁰Y-labeled DOTA and maleimidocysteineamido-DOTA conjugated to chimeric anticarcinoembryonic antigen antibody in xenograft-bearing nude mice: comparison of stable and chemically labile linker systems. *Bioconjug Chem* 1998;9(1):87-93

47. Lewis MR, Kao JY, Anderson AL et al. An improved method for conjugating monoclonal antibodies with N-hydroxysulfosuccinimidyl DOTA. *Bioconjug Chem* 2001;12(2):320-324
48. Lewis MR, Raubitschek A, Shively JE. A facile, water-soluble method for modification of proteins with DOTA. Use of elevated temperature and optimized pH to achieve high specific activity and high chelate stability in radiolabeled immunoconjugates. *Bioconjug Chem* 1994;5(6):565-576
49. Kukis DL, Denardo SJ, DeNardo GL et al. Optimized conditions for chelation of yttrium-90-DOTA immunoconjugates. *J Nucl Med* 1998;39(12):2105-2110
50. Hawe A, Kasper JC, Friess W et al. Structural properties of monoclonal antibody aggregates induced by freeze-thawing and thermal stress. *Eur J Pharm Sci* 2009;38(2):79-87
51. Harn N, Allan C, Oliver C et al. Highly concentrated monoclonal antibody solutions: direct analysis of physical structure and thermal stability. *J Pharm Sci* 2007;96(3):532-546
52. Paik CH, Ebbert MA, Murphy PR et al. Factors influencing DTPA conjugation with antibodies by cyclic DTPA anhydride. *J Nucl Med* 1983;24(12):1158-1163
53. Hnatowich DJ, Virzi F, Doherty PW. DTPA-coupled antibodies labeled with yttrium-90. *J Nucl Med* 1985;26(5):503-509
54. Paik CH, Hong JJ, Ebbert MA et al. Relative reactivity of DTPA, immunoreactive antibody-DTPA conjugates, and nonimmunoreactive antibody-DTPA conjugates toward indium-111. *J Nucl Med* 1985;26(5):482-487
55. Riechmann L, Clark M, Waldmann H et al. Reshaping human antibodies for therapy. *Nature* 1988;332(6162):323-327
56. Co MS, Avdalovic NM, Caron PC et al. Chimeric and humanized antibodies with specificity for the CD33 antigen. *J Immunol* 1992;148(4):1149-1154
57. Zimmermann K, Grunberg J, Honer M et al. Targeting of renal carcinoma with 67/64Cu-labeled anti-L1-CAM antibody chCE7: selection of copper ligands and PET imaging. *Nucl Med Biol* 2003;30(4):417-427
58. Knogler K, Grunberg J, Novak-Hofer I et al. Evaluation of 177Lu-DOTA-labeled aglycosylated monoclonal anti-L1-CAM antibody chCE7: influence of the number of chelators on the in vitro and in vivo properties. *Nucl Med Biol* 2006;33(7):883-889
59. Reilly RM, Scollard DA, Wang J et al. A kit formulated under good manufacturing practices for labeling human epidermal growth factor with 111In for radiotherapeutic applications. *J Nucl Med* 2004;45(4):701-708
60. Wu C, Gansow OA, Brechbiel MW. Evaluation of methods for large scale preparation of antibody ligand conjugates. *Nucl Med Biol* 1999;26(3):339-342
61. Eon-Duval A, MacDuff RH, Fisher CA et al. Removal of RNA impurities by tangential flow filtration in an RNase-free plasmid DNA purification process. *Anal Biochem* 2003;316(1):66-73
62. Kahn DW, Butler MD, Cohen DL et al. Purification of plasmid DNA by tangential flow filtration. *Biotechnol Bioeng* 2000;69(1):101-106
63. Lindmo T, Boven E, Cuttitta F et al. Determination of the immunoreactive fraction of radiolabeled monoclonal antibodies by linear extrapolation to binding at infinite antigen excess. *J Immunol Methods* 1984;72(1):77-89
64. Stollman TH, Scheer MG, Leenders WP et al. Specific imaging of VEGF-A expression with radiolabeled anti-VEGF monoclonal antibody. *Int J Cancer* 2008;122(10):2310-2314
65. Ferrara N. Role of vascular endothelial growth factor in physiologic and pathologic angiogenesis: therapeutic implications. *Semin Oncol* 2002;29(6 Suppl 16):10-14
66. Collingridge DR, Carroll VA, Glaser M et al. The development of [(124)I]iodinated-VG76e: a novel tracer for imaging vascular endothelial growth factor in vivo using positron emission tomography. *Cancer Res* 2002;62(20):5912-5919
67. Matzku S, Kirchgessner H, Dippold WG et al. Immunoreactivity of monoclonal anti-melanoma antibodies in relation to the amount of radioactive iodine substituted to the antibody molecule. *Eur J Nucl Med* 1985;11(6-7):260-264
68. Damen CW, Rosing H, Schellens JH et al. Quantitative aspects of the analysis of the monoclonal antibody trastuzumab using high-performance liquid chromatography coupled with electrospray mass spectrometry. *J Pharm Biomed Anal* 2008;46(3):449-455
69. Jovanovic N, Bouchard A, Hofland GW et al. Stabilization of IgG by supercritical fluid drying: optimization of formulation and process parameters. *Eur J Pharm Biopharm* 2008;68(2):183-190

70. Lakowicz JR, Weber G. Quenching of protein fluorescence by oxygen. Detection of structural fluctuations in proteins on the nanosecond time scale. *Biochemistry* 1973;12(21):4171-4179
71. Chakrabarti MC, Le N, Paik CH et al. Prevention of radiolysis of monoclonal antibody during labeling. *J Nucl Med* 1996;37(8):1384-1388
72. DeNardo GL, Denardo SJ, Wessels BW et al. ¹³¹I-Lym-1 in mice implanted with human Burkitt's lymphoma (Raji) tumors: loss of tumor specificity due to radiolysis. *Cancer Biother Radiopharm* 2000;15(6):547-560
73. Salako QA, O'Donnell RT, Denardo SJ. Effects of radiolysis on yttrium-90-labeled Lym-1 antibody preparations. *J Nucl Med* 1998;39(4):667-670
74. Mohsin H, Fitzsimmons J, Shelton T et al. Preparation and biological evaluation of ¹¹¹In-, ¹⁷⁷Lu- and ⁹⁰Y-labeled DOTA analogues conjugated to B72.3. *Nucl Med Biol* 2007;34(5):493-502
75. Maxon HR, III, Smith HS. Radioiodine-131 in the diagnosis and treatment of metastatic well differentiated thyroid cancer. *Endocrinol Metab Clin North Am* 1990;19(3):685-718
76. Saha GB, Whitten J, Go RT. Conditions of radioiodination with iodogen as oxidizing agent. *Int J Rad Appl Instrum B* 1989;16(4):431-433

Chapter 1.2

A simple and safe method
for
¹³¹I radiolabeling of rituximab
for myeloablative high-dose
radioimmunotherapy

Ly Tran

Joke W. Baars

Cornelis A. Hoefnagel

Harry Maessen

Jos H. Beijnen

Alwin D.R. Huitema

Abstract

Aim of this study was to develop a safe and simple radiolabeling and purification procedure for high dose ^{131}I -rituximab for treatment of patients with non-Hodgkin lymphoma. As starting point, the conventional lodogen coated vial method was applied. Afterwards, the lodogen coated MAb method, a labeling method involving much lower amounts of lodogen was assessed. Subsequently, ^{131}I -rituximab was purified with a tangential flow filtration system. Quality control of the final product was performed using size exclusion chromatography with UV detection and by instant high performance thin layer chromatography. Immunoreactivity was determined using a cell-binding assay. During the labeling procedure, radiation exposure was monitored. The coated vial method resulted in a low radiation exposure but immunoreactivity was highly compromised (37%). Also, formation of aggregates was observed. The maximal observed effective dose was 18 μSv , finger TLD's revealed hand dose measurement of 0.8 mSv. The second method resulted in an immunoreactivity of 70%. Radiochemical purity was >97% after purification. The maximal measured effective dose was 31 μSv , detected exposure to the hands was 1.9 mSv. We have developed a simple labeling technique for the preparation of high dose ^{131}I -rituximab. The method offers a high purity and retained immunoreactivity with minimal radiation exposure for involved personnel.

Introduction

Radioimmunotherapy is an emerging treatment modality as the radiopharmaceuticals ^{131}I -tositumomab and ^{90}Y -ibritumomab tiuxetan have shown considerable activity in the treatment of B-cell non-Hodgkin lymphoma (B-cell NHL) (1-3). As more than 90% of the B-cell NHL show CD20 antigen expression, the CD20 antigen is an excellent target for the treatment of B-cell NHL (4). Rituximab is a chimeric monoclonal antibody (MAb) that specifically targets the CD20 antigen and induces anti-tumor activity through antibody-mediated mechanisms. Treatment with unlabeled rituximab has resulted in significant responses in patients with B-cell NHL (5,6). ^{131}I is a suitable nuclide for radioimmunotherapy. Its chemistry is well known, it is readily available, and it is relative inexpensive. The β -emitting characteristics promote cytotoxic activity while the γ -rays can serve for diagnostic purposes.

Therefore, ^{131}I -rituximab was considered an appropriate agent for radioimmunotherapy for the treatment of B-cell NHL. In a low radioactive dose of 185 MBq, ^{131}I -rituximab can serve as a diagnostic compound for dosimetric purposes. Scaling up the radioactive dose up to 3.7 GBq may be used in the treatment of B-cell NHL (7).

For the preparation of ^{131}I -rituximab for clinical use, several requirements should be met. Firstly, for the efficacy and safety of the therapy, the integrity of the MAb has to be maintained during labeling. Secondly, a labeling technique with minimal radiation exposure to involved personnel is necessary. Finally, the preparation of this radioconjugate has to be performed in accordance with the principles of good manufacturing practice.

Conjugation of iodine to a MAb can be obtained with several methods. The lodogen method has most widely been applied and this method has most of the properties required for the preparation of radiopharmaceuticals (8,9).

Conjugation with iodine can be carried out using the lodogen coated vial method, in which the MAb is added to a vial coated with lodogen. The method is simple, rapid, and can largely be performed with remote handling (10). However, for this method, relatively high amounts of lodogen are necessary, which may have impact on the integrity of the MAb.

Visser et al described a relative mild reaction procedure, also known as the lodogen-coated MAb method, in which a small amount of lodogen dissolved in acetonitril was added to a solution containing the MAb and ^{131}I (11). Although this method may lead to a more immunoreactive conjugate, purification of the product is necessary, which makes the method more laborious which increases radiation exposure.

The aim of our study was to develop a simple and safe method for the preparation of high dose radiolabeled rituximab for clinical purposes, with adequate immunoreactivity.

Material and methods

Rituximab, a murine/humane chimeric anti-CD20 monoclonal antibody (Mabthera®, 10 mg/mL) was commercially obtained from Roche (Basle, Switzerland). Carrier-free ^{131}I was purchased (GE Healthcare Buchler, Braunschweig, Germany) as Na^{131}I in 0.05 mol/L NaOH, with a specific activity larger than 370 GBq/mg. The volume of ^{131}I was established at 1 mL, provided in a 10 mL delivery vial. 1,3,4,6-tetrachloro-3 α ,6 α -diphenylglycouril (Iodogen) was obtained from Sigma-Aldrich (St. Louis, MO, USA). 0.9% NaCl was purchased from B. Braun Medical (Melsungen, Germany). Phosphate buffered saline (PBS), for labeling and cell-binding assay, was also purchased from B. Braun Medical (Melsungen, Germany). Ascorbic acid was purchased from BUFA (Uitgeest, The Netherlands). 0.50 mol/L phosphate buffer and 0.05 mol/L NaOH were manufactured in-house (Department of Pharmacy & Pharmacology, The Netherlands Cancer Institute / Slotervaart Hospital, Amsterdam, The Netherlands) and the used chemicals were obtained from BUFA (Uitgeest, The Netherlands). Methanol, dichloromethane, acetonitrile, and PBS, for quality control, were obtained from Merck (Darmstadt, Germany). Iscove's modified Dulbecco's medium (IMDM) was purchased from Invitrogen GIBCO (Carlsbad, CA, USA). Foetal Calf Serum (FCS) was obtained from PAA Laboratories GmbH (Pasching, Austria). Bovine Serum Albumine (BSA) was purchased from Sigma-Aldrich (St. Louis, MO, USA). All chemicals used for quality control were of analytical grade and used without further purification.

The coated vial method

A closed system was applied, using underpressure to transfer the solutions (Figure 1). A 10 mL glass vial was coated with Iodogen by evaporating dichloromethane containing 1 mg/mL Iodogen. A magnetic stirring rod was placed in the coated vial and rituximab was added. The vial was capped with a rubber stopper and was sealed with an aluminum closure. The vials were connected using sterile syringes and infusion lines. All the vials were provided with a lead shield for radiation protection. Underpressure was created and ^{131}I was transferred to the coated vial, followed by 0.9% NaCl to rinse the ^{131}I delivery vial. After stirring for at least 15 minutes, the solution was transferred through a sterile filter (0.2 μm , Sartorius, Goettingen, Germany) into an infusion flask with 0.9% NaCl. The labeling was performed under aseptic conditions, in a class 100 laminar air flow cabinet layered with lead walls with a minimum thickness of 3 cm (MNT-Kwint International B.V., Culemborg, The Netherlands). Also, the cabinet was provided with a movable front shield lead glass window equivalent to 3 cm of lead. For labeling 185 MBq ^{131}I , 200 μg Iodogen, 5 mg rituximab, and an incubation time of 15 minutes were applied. These factors were varied to optimize the labeling procedure. Hereafter, the optimal conditions were used to scale up the labeling for 3.7 GBq ^{131}I .

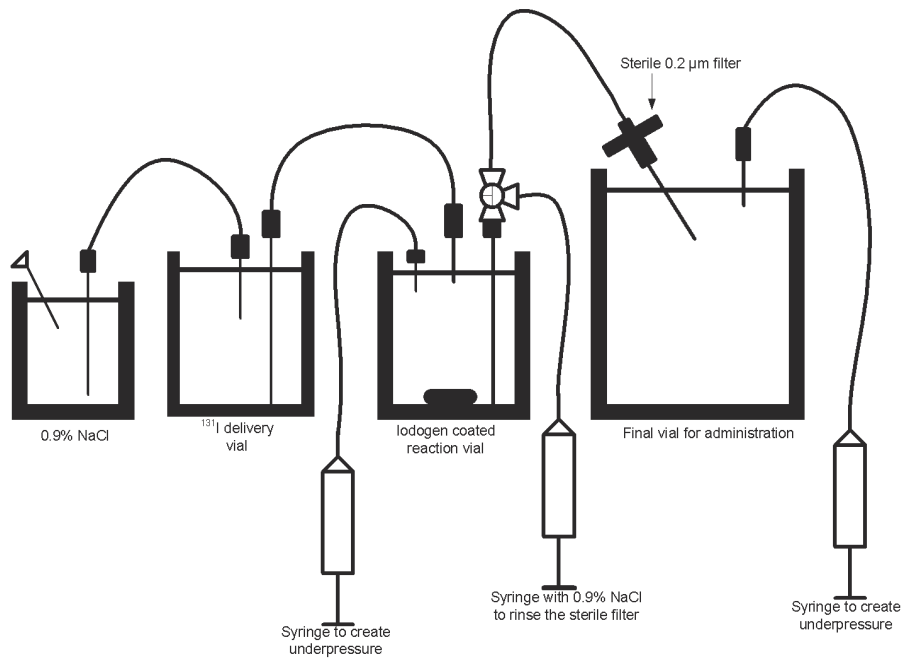


Figure 1 System for the coated vial method

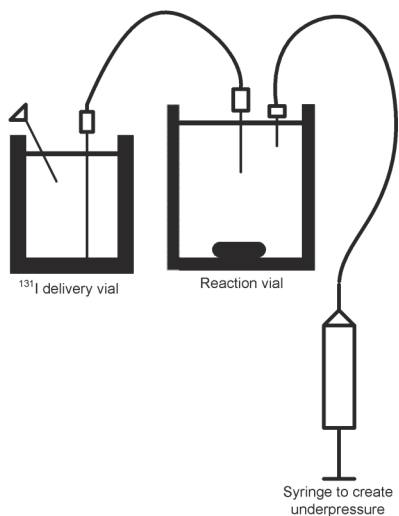


Figure 2 Transferring ^{131}I from the delivery vial to the reaction vial using underpressure for the iodogen coated MAb method

Iodogen coated MAb method

As second method for radiolabeling rituximab, the method described by Visser et al. was used as starting point (11) (see Table 1). Most of the manual handlings were altered into remote handling procedures, by using underpressure for transfer of the solutions, to promote radiation safety. Briefly 7.4 GBq ^{131}I was pretreated to neutralize to oxidative effect of aging with 30 μl 1.41 mg/mL ascorbic acid. 0.05 mol/L NaOH was added to adjust to volume of ^{131}I to 3 mL which could be transferred properly into the 20 mL reaction vial using underpressure as described above. The labeling was provoked by addition of 70 μl of a 1 mg/mL solution of iodogen in acetonitrile to a reaction vial with 20 mg rituximab and ^{131}I . After 3 minutes, the reaction was terminated by addition 1 mL of 50 mg/mL ascorbic acid. The labeling was performed in a class 100 glovebox incorporated with laminar air flow system (MNT–Kwint International B.V., Culemborg, The Netherlands). The glovebox shielding consisted of a 3-cm-thick layer of lead.

Table 1 Technical protocol for ^{131}I labeling of rituximab (7.4 GBq)

- ^{131}I was pretreated with 2-2.5 mL 50 mM NaOH and 30 μL 1.41 mg/ml ascorbic acid
- ^{131}I was transferred to the reaction vial
 - 2 mL Phosphate buffer, 5 mL phosphate buffered saline, and 2 mL rituximab were added
 - t=0 min: The labeling was provoked by adding 70 μL Iodogen solution (1 mg/ml)
 - t=3 min: The reaction was terminated by 1 mL 50 mg/ml ascorbic acid
 - t=10 min: The reaction was completed
 - The product was purified with a Tangential Flow Filtration system
 - Sterile filtration of the product

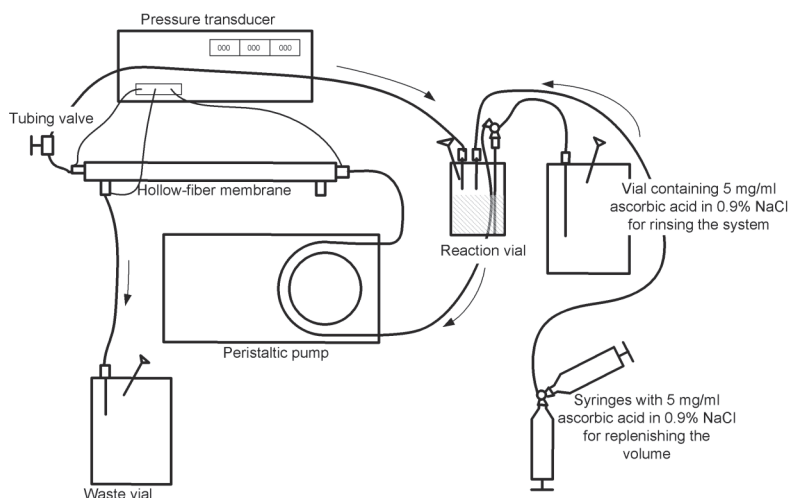


Figure 3 Purification of ^{131}I -rituximab using the tangential flow filtration system

Purification of the product

The tangential flow filtration system consisted of an autoclavable, disposable hollow-fiber membrane (GE Healthcare, Diegem, Belgium) with a pore opening of 50,000 Dalton, a pressure transducer (GE Healthcare, Diegem, Belgium), and a peristaltic pump (323S/RL, Watson Marlow, Rotterdam, The Netherlands) (Figure 2). The volume of the product solution was replenished to 20 mL with 5 mg/mL ascorbic acid in 0.9% NaCl. The membrane was pressurized and, while pumping the solution along the membrane, solvent was pressed through the membrane pores into a waste container, taking molecules smaller than 50,000 Dalton along until the volume of the product solution was reduced to 10 mL, and next, the volume was replenished to 20 mL. This procedure of replenishing and pumping the solution through the system was repeated for five times. Subsequently, the solution was transferred through a sterile filter (0.2 μm , Soartorius, Goettingen, Germany), into an infusion flask. The final volume was adjusted to 50 mL with 5 mg/mL ascorbic acid in 0.9% NaCl (Figure 3). The tangential flow filtration system was a closed system. The system was equipped with vent needles to prevent overpressure. The purification was conducted in the laminar air flow cabinet. A lead box surrounded the hollow fiber membrane and all vials were provided with a lead shield

Quality control

Identification of the product was determined by size exclusion chromatography (SEC-HPLC) with ultraviolet (UV) detection. The HPLC system (Beckman Coulter, Inc., Fullerton, CA, USA) consisted of a manual injector with a 20 μL injection loop and a UV detector. The column used was a Phenomenex BioSep-SEC-s3000, 300 x 7.8 mm column (Torrance, CA, USA). The mobile phase was 0.01 mol/L PBS, the flow was 1.0 mL/min and the UV detection was performed at $\lambda = 280 \text{ nm}$. Radiochemical purity was determined by instant thin layer chromatography (iTPTLC). From a diluted sample of the final product, 2 μL was applied to an iTPTLC strip (1 x 10 cm², aluminium High Performance Thin Layer Chromatography plates, coated with silicagel 60 F254, Merck, Darmstadt, Germany) that was developed with methanol 85% v/v until the solvent front was migrated to approximately 1.5 cm from the top of the strip. ¹³¹I-rituximab remains at the start position, unbound ¹³¹I migrates to the front. Subsequently, the plate was dried and cut into half. Both halves were counted for 60 seconds in an automatic gamma counter (Wizard 1480, Perkin Elmer, Waltham, MA, USA) and the amount of radioactivity was expressed in counts per minute. Radiochemical purity was determined by dividing the activity present on the lower half of the plate by the total activity of both halves. For a patient's dose, a radiochemical purity of more than 95% was considered acceptable.

The immunoreactivity was determined using a cell-binding assay at infinite antigen excess, described by Lindmo et al (12). Briefly, Epstein Barr Virus-transfected human B-lymphocytes were cultured in IMDM /10% FCS, in a humidified atmosphere with

5% CO₂ at 37°C. The cells were harvested by centrifugation, counted, and resuspended in PBS/0.5% BSA. 5 ng of the product was added to increasing numbers of cells and incubated overnight. After incubation, cells were washed twice with PBS/ 0.5% BSA to remove unbound antibodies and cell-bound radioactivity was measured with the automatic gamma counter. Specific binding was calculated as the ratio of cell-bound to total applied radioactivity minus non-specific binding, which was determined in the presence of 100 ng of unlabeled rituximab. For the overall quality of the product, high preservation of the immunoreactivity was necessary; the minimum immunoreactivity was set at 60%.

GMP and radiation safety

Glassware and materials used were sterilized (15 minutes at 121°C). Process simulation using tryptone soy broth was conducted to evaluate the aseptic handling. The final product was tested for pyrogen content (Ph. Eur. Specification < 175 EU/vial). Personnel were appropriately trained regarding the radiation safety and GMP aspects. Involved personnel were equipped with an electronic personal dosimeter (EPD) (DMC 2000, MGP instruments SA, Lamanon, France) which measured the effective dose. Finger thermoluminescence dosimeters (TLD's) (NRG, Petten, The Netherlands) were attached to the thumb and ring finger, on both hands of the person who conducted the labeling procedure. The monitoring was conducted under surveillance of the radiation protection officer. According to European guidelines, the annual permitted effective dose for a radiation worker category A, is 20 mSv. An annual cumulative hand dose of maximally 500 mSv was considered to be acceptable (13,14).

Results

Labeling with the coated vial method

Finger dose received during labeling with 185 MBq was under the detectable range. The measured effective dose was 3 µSv. An effective dose during the labeling process of 3.7 GBq ¹³¹I of 18 µSv was detected. Hand dose measurements revealed a dose of 0.2 mSv on the left hand. Both finger TLD's on the right hand showed a dose of 0.3 mSv.

Labeling of rituximab with 185 MBq ¹³¹I resulted in a mean radiochemical yield of 91 % (Table 2). Radiochemical purity, immediately after labeling, was 98%(±0.75)% and immunoreactivity was 34%. Scaling up the radioactive dose to 3.7 GBq resulted in a radiochemical yield of 86% and an immunoreactivity of 37%. SEC-HPLC analysis showed that the integrity of rituximab was maintained, but formation of aggregates was observed (6.9%) which is also visible in the chromatogram (Figure 4). iTPLC analysis showed a radiochemical purity of 89% when a radioactive dose of 3.7 GBq was applied, which was insufficient for clinical purposes. Additionally, after 24 hours

storage, the radiochemical purity was 81% and the immunoreactivity was decreased to 8.7%.

Attempts to improve on this result by increasing the amount of Iodogen, reaction time, and amount of rituximab (Table 3), were unsuccessful. Radiochemical purity decreased when the ^{131}I dose was increased. This purity may be increased by further purification of the product. However, immunoreactivity was strongly decreased with the coated vial method probably due to the high amounts of Iodogen used. Although the coated vial method could be performed with sufficient radiation protection for involved personnel, the method did not meet the requirements for a product for clinical purposes.

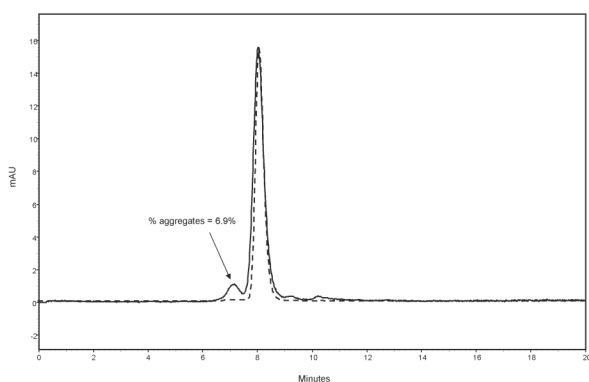


Figure 4 SEC-HPLC-UV chromatogram of ^{131}I -rituximab (solid line), labeled according to the coated vial method. The retention time of ^{131}I -rituximab corresponds with the retention time of unlabeled rituximab (dotted line). The small peak before the rituximab peak is assigned as formation of aggregates

Table 2 Overview labeling according to the coated vial method, using ± 185 MBq ^{131}I and 5 mg rituximab

Start activity (MBq)	Final activity (MBq)	Yield (%)	Radiochemical purity* (%)	Immunoreactivity (%)
177	168	95	98	36
144	141	98	98	ND
165	159	96	98	37
188	170	90	97	ND
187	162	87	97	ND
177	145	82	99	30

ND: not determined

*: without purification

Table 3 Overview of the radiochemical purity of the products when alterations of the reaction conditions (Iodogen, rituximab, incubation time) were applied

Radioactive dose (MBq)	Amount Iodogen (μg)	Amount rituximab (mg)	Incubation time (minutes)	Radiochemical purity*
3700	1000	10	30	91
	2000	10	30	92
	2000	20	40	94
	2000	40	40	93

*without purification

Iodogen coated MAb method

The effective dose received during labeling with 185 MBq was 12 μSv , finger dose during labeling was under the detectable range. During the high dose labeling procedure of 7.4 GBq ^{131}I , a maximum effective dose of 31 μSv was measured. Maximum detected exposure to the hands was 1.9 mSv in total.

Labeling rituximab with 185 MBq ^{131}I resulted in a mean radiochemical yield of 80%, a radiochemical purity of 92% and cell-binding tests before and after purification showed an immunoreactivity of 70% (Table 4). Purification with the tangential flow filtration system was necessary. After purification, the purity was >99%. Labeling rituximab with a high dose of 7.4 GBq resulted in a mean radiochemical yield of 85% (Table 5). Radiochemical purity before purification was 93% and after the purification step the radiochemical purity was $\geq 97\%$. Cell-binding assays revealed a substantially increased immunoreactivity of 72% (Figure 5 and 6). For both the low dose (185 MBq) as high-dose (7.4 GBq), the immunoreactivity was consistently between 69 and 75%. After 24 hours storage of the product at room temperature, the radiochemical purity of the product was $\geq 95\%$ and the immunoreactivity was 70%. The retention time of ^{131}I -rituximab corresponded to the retention time of unlabeled rituximab (Figure 7). The second peak in the chromatogram was identified as ascorbic acid, which was confirmed by SEC-HPLC analysis of a solution of 5 mg/mL ascorbic acid in 0.9% NaCl. The formation of aggregates was not observed.

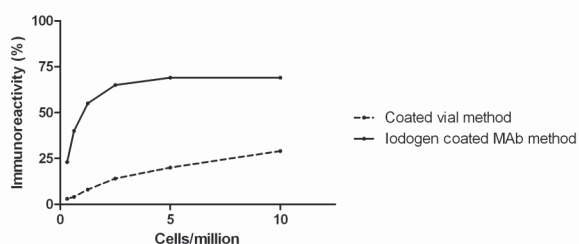


Figure 5 Cell-binding assay

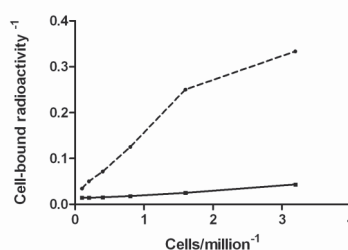


Figure 6 The inverse of cell-bound radioactivity in function of the inverse of cell concentration

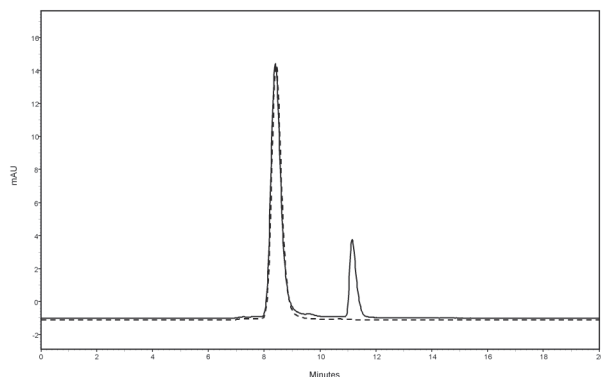


Figure 7 SEC-HPLC-UV chromatogram of ^{131}I -rituximab (solid line), labeled according to the Iodogen coated MAb method. The retention time of ^{131}I -rituximab corresponds with the retention time of unlabeled rituximab (dotted line). The small peak before the rituximab peak is assigned as formation of aggregates

Table 4 Overview labeling according to the Iodogen coated MAb method, using ± 185 MBq ^{131}I and 5 mg rituximab

Start activity (MBq)	Activity final product (MBq)	Yield (%)	Radiochemical purity* (%)	Immunoreactivity (%)
195	140	72	92	ND
122	90	74	90	ND
188	162	86	92	70
215	188	87	92	70

*: without purification

ND: not determined

Table 5 Overview labeling according to the Iodogen coated MAb method, using ± 7400 MBq ^{131}I and 20 mg rituximab

Start activity (MBq)	Activity final product (MBq)	Yield (%)	Radiochemical purity* (%)	Immunoreactivity (%)
7080	6380	90	93	74
6520	6040	93	94	71
7550	5970	79	94	69
7380	5840	79	92	75

*: without purification

Discussion

Since its introduction in 1978 by Fraker and Speck, the Iodogen method is the most frequently utilized method for the radioiodination of MAbs. The coated vial method is the most known variant of the Iodogen method. The procedure is straightforward. The method results in high labeling yield, and is adaptable to remote handling procedures for therapy-level labeling to promote the radiation safety. The method had shown to be safe for involved personnel. However, for rituximab, this method resulted in an unacceptable decrease of the immunoreactivity of rituximab.

Visser et al described a labeling procedure for high dose radioiodination of MAbs, also using Iodogen as oxidizing agent (11). The labeling was conducted by adding a solution of Iodogen in acetonitril into an aqueous mixture containing the MAb and ^{131}I . The reaction was abrogated by adding a high concentration of ascorbic acid. Also, before, during and after purification, ascorbic acid, in a lower concentration, was used as radioprotectant to reduce potential, reactive damage to the MAb (11,15). This method resulted in a preservation of the integrity and immunoreactivity of rituximab. Additionally, quality control revealed that the product was stable for at least 24 hours. Addition of ascorbic acid to the initially used method, the coated vial method, would improve the stability, but would not improve the immunoreactivity.

However, the previously described Iodogen coated MAb method, required intensive manual handling. Gel filtration was applied as purification step, requiring numerous gel filtration columns to purify the product. This method involved manual handling of the columns and collection of the eluted fractions, both of which may lead to a high exposure of the hands.

We have altered most of the manual handling into a remote handling procedure to promote radiation safety. Furthermore, we have introduced a remote method for purification of the product. This method, tangential flow filtration, is commonly used in the biopharmaceutical industry to harvest, purify, and concentrate products (16,17). For this study, this system was used to remove unbound ^{131}I and excipients from the product. Despite of the remote handling procedures, during the whole labeling procedure, radiation exposure was observed. As previously mentioned, the annual permitted effective dose for a radiation worker category A, is 20 mSv and an annual cumulative hand dose of 500 mSv is acceptable. During the labeling procedure, the radiation exposure remained far below the acceptable range, and permits a radiation worker category A to carry out the high dose procedure for multiple times daily.

Conclusion

With the developed method for labeling and purification, therapeutic amounts of ^{131}I labeled rituximab can be safely and reproducibly prepared for clinical applications, with high efficiency while the integrity and immunoreactivity of rituximab are largely

preserved. The labeling process was accompanied with low and acceptable exposure to the labeling personnel.

Acknowledgements

The authors like to thank prof. dr. G.A.M.S. van Dongen and dr. G.W. Visser for sharing their knowledge and Mrs. M.J.W.D. Vosjan for her continuous support.

References

1. Fisher RI, Kaminski MS, Wahl RL et al. Tositumomab and iodine-131 tositumomab produces durable complete remissions in a subset of heavily pretreated patients with low-grade and transformed non-Hodgkin's lymphomas. *J Clin Oncol* 2005;23(30):7565-7573
2. Winter JN. Combining yttrium 90-labeled ibritumomab tiuxetan with high-dose chemotherapy and stem cell support in patients with relapsed non-Hodgkin's lymphoma. *Clin Lymphoma* 2004;5 Suppl 1S22-S26
3. Witzig TE. Efficacy and safety of 90Y ibritumomab tiuxetan (Zevalin) radioimmunotherapy for non-Hodgkin's lymphoma. *Semin Oncol* 2003;30(6 Suppl 17):11-16
4. Anderson KC, Bates MP, Slaughenhoupt BL et al. Expression of human B cell-associated antigens on leukemias and lymphomas: a model of human B cell differentiation. *Blood* 1984;63(6):1424-1433
5. Shan D, Ledbetter JA, Press OW. Apoptosis of malignant human B cells by ligation of CD20 with monoclonal antibodies. *Blood* 1998;91(5):1644-1652
6. McLaughlin P, Grillo-Lopez AJ, Link BK et al. Rituximab chimeric anti-CD20 monoclonal antibody therapy for relapsed indolent lymphoma: half of patients respond to a four-dose treatment program. *J Clin Oncol* 1998;16(8):2825-2833
7. Behr TM, Griesinger F, Riggert J et al. High-dose myeloablative radioimmunotherapy of mantle cell non-Hodgkin lymphoma with the iodine-¹³¹-labeled chimeric anti-CD20 antibody C2B8 and autologous stem cell support. Results of a pilot study. *Cancer* 2002;94(4 Suppl):1363-1372
8. Fraker PJ, Speck JC, Jr. Protein and cell membrane iodinations with a sparingly soluble chloroamide, 1,3,4,6-tetrachloro-3a,6a-diphrenylglycoluril. *Biochem Biophys Res Commun* 1978;80(4):849-857
9. *Handbook of Radiopharmaceuticals*. 2003;(13):423-440
10. Weadock KS, Anderson LL, Kassis AI. A simple remote system for the high-level radioiodination of monoclonal antibodies. *J Nucl Med Allied Sci* 1989;33(1):37-41
11. Visser GW, Klok RP, Gebbinck JW et al. Optimal quality (131)I-monoclonal antibodies on high-dose labeling in a large reaction volume and temporarily coating the antibody with IODO-GEN. *J Nucl Med* 2001;42(3):509-519
12. Lindmo T, Boven E, Cuttitta F et al. Determination of the immunoreactive fraction of radiolabeled monoclonal antibodies by linear extrapolation to binding at infinite antigen excess. *J Immunol Methods* 1984;72(1):77-89
13. International Commission on Radiological Protection. 1990 Recommendations of the international commission on radiological protection. ICRP publication 60. *Annals of the ICRP* 1991;211-3
14. Goldstone KE. Principles and control methods. 2002;(6):79-87
15. Chakrabarti MC, Le N, Paik CH et al. Prevention of radiolysis of monoclonal antibody during labeling. *J Nucl Med* 1996;37(8):1384-1388
16. Eon-Duval A, MacDuff RH, Fisher CA et al. Removal of RNA impurities by tangential flow filtration in an RNase-free plasmid DNA purification process. *Anal Biochem* 2003;316(1):66-73
17. Kahn DW, Butler MD, Cohen DL et al. Purification of plasmid DNA by tangential flow filtration. *Biotechnol Bioeng* 2000;69(1):101-106

Chapter 1.3

Three spectroscopic techniques
evaluated as a tool
to study the effects of iodination
of monoclonal antibodies,
exemplified by rituximab

Ly Tran
Joke W. Baars
Carola W.N. Damen
Jos H. Beijnen
Alwin D.R. Huitema

Abstract

Radioiodinated monoclonal antibodies have been used for radioimmunotherapeutic and radiodiagnostic purposes. Radioiodination of monoclonal antibodies may lead to deterioration of the immunoreactivity of the monoclonal antibody. Methods for the determination of the immunoreactivity, however, do not provide information about any structural changes of the radioconjugate which may influence the binding properties of the protein to the target antigen. Within this study we demonstrated the potential role of three alternative spectroscopic analytical techniques to characterize the structural changes emerging after iodination of rituximab. We conclude that techniques as liquid chromatography coupled to mass spectrometry, fluorescence emission spectrophotometry, and circular dichroism can provide valuable information about structural changes of a radiolabeled compound, e.g. during pharmaceutical development and for quality control.

Introduction

Radioiodinated monoclonal antibodies have been used for radioimmunotherapeutic and radiodiagnostic purposes (1-4). Several methods are available for iodination of monoclonal antibodies. Methods using Iodogen for iodination of the protein are most frequently applied. In previous studies, it has been shown that the reaction conditions may have a large impact on the immunoreactivity of the resulting iodinated monoclonal antibody, which can be considered as a measure of protein integrity (5). By using Iodogen as oxidizing agent, linkage of the iodine on the tyrosine residues ortho to the hydroxyl group of the phenolic moiety predominates when conducting the reaction at neutral pH (Figure 1) (6). For the optimal use of the radioconjugate, a high specific activity is required while the integrity, and thus the desired biological targeting, of the monoclonal antibody has to be preserved. High specific activity can be reached by using techniques which ensure relatively strong reaction conditions, but this may impair the integrity of the monoclonal antibody.

The most widely applied method for the determination of the immunoreactivity has been reported by Lindmo et al (7). They have described a method in which the immunoreactive fraction is determined by extrapolation from conditions representing infinite antigen excess. The extrapolation is performed in a double-inverse linear plot which is a modification of the Lineweaver-Burk plot. The inverse of the intercept of the y-axis then represents the immunoreactive fraction. The method provides information about the immunoreactivity of the monoclonal antibody, but does not provide insight into potential structural changes of the radioconjugate which may cause changes of the binding properties of the protein to a target antigen. Furthermore, this method is labor-intensive and time-consuming and, therefore, difficult to be used during pharmaceutical development and quality control.

Within this study we demonstrated the potential role of three alternative analytical techniques, liquid chromatography coupled to mass spectrometry (LC-MS), fluorescence emission and circular dichroism spectrometry, to characterize the structural changes during iodination of rituximab.

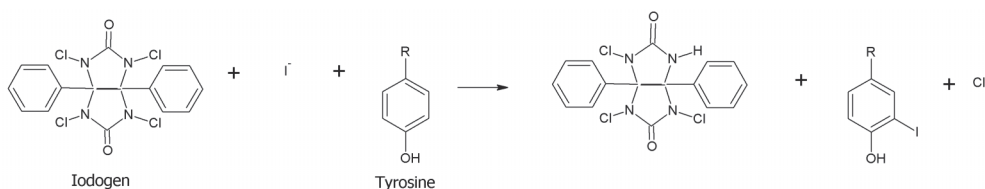


Figure 1 Incorporation of Iodine into proteins and peptides. Application of Iodogen mainly leads to iodinated tyrosines moieties

Methods

Rituximab, an approved murine/humane chimeric anti-CD20 monoclonal antibody (Mabthera®, 10 mg/mL) was commercially obtained from Roche (Basle, Switzerland). 1,3,4,6-tetrachloro-3 α ,6 α -diphenylglycouril (Iodogen) originated from Sigma-Aldrich (St. Louis, MO, USA). 0.9% NaCl and phosphate buffered saline (PBS) was purchased from B. Braun Medical (Melsungen, Germany). Sodium iodide and ascorbic acid were from BUFA (Uitgeest, The Netherlands). 0.50 mol/L phosphate buffer and 0.05 mol/L NaOH were manufactured in-house (Department of Pharmacy & Pharmacology, The Netherlands Cancer Institute / Slotervaart Hospital, Amsterdam, The Netherlands) and all other chemicals used were from BUFA (Uitgeest, The Netherlands). Methanol, dichloromethane and acetonitrile for quality control, were obtained from Merck (Darmstadt, Germany). All other chemicals used for quality control experiments were of analytical grade and used without further purification.

Sample preparation of unlabeled rituximab

Rituximab was isolated and purified from the commercially available Mabthera® solution. A PD-10 sephadex column (GE Healthcare, Diegem, Belgium) was equilibrated with 0.9% NaCl. 2 mL of the Mabthera® solution was subjected to the column and was eluted with 0.9% NaCl. Fractions were collected with rituximab eluting between 0.5 and 3.5 mL.

Preparation of the iodinated rituximab

To exclude the effect of radiolysis on the monoclonal antibody, ^{127}I was used instead of radioactive ^{131}I . The labeling procedure was simulated using a ^{127}I concentration corresponding to a specific activity of 185 GBq/mg ^{131}I in 0.05 M NaOH.

Rituximab iodinated according to the Iodogen coated vial method

20 mg rituximab was iodinated according to the Iodogen coated vial method (8) with an amount of ^{127}I corresponding to 3700 MBq. A 10 mL glass vial was coated with 2 mg Iodogen by evaporating 2.0 mL dichloromethane containing 1 mg/mL Iodogen. Rituximab and 200 μL sodium iodide (0.116 mg/mL 0.05 M NaOH) were added and the volume was adjusted to 10 mL with 0.9% NaCl. After 30 minutes incubation at room temperature with constant stirring, the reaction was terminated by transferring the reaction solution to another, non-coated, vial followed by sterile filtration of the solution. The product was stored at room temperature.

Rituximab iodinated according to the Iodogen coated mab method

20 mg rituximab was iodinated using the Iodogen coated mab method with an amount of ^{127}I corresponding with 7400 MBq. The preparation was performed as described previously (8,9). Briefly, 400 μL sodium iodide solution (0.116 mg/mL 0.05

M NaOH) was added to a reaction vial with 2 mL rituximab (10 mg/mL) and the labeling reaction was initiated by addition of 70 μ l 1 mg/mL Iodogen in acetonitrile to the reaction vial. After 3 minutes, 1 mL 50 mg/mL ascorbic acid was added. The reaction was completed after 10 minutes. Purification was performed using PD10 sephadex columns equilibrated and eluted with 5 mg/ml ascorbic acid in 0.9% NaCl. Fractions were collected with iodinated rituximab eluting between 0.5 and 3.5 mL. The product was stored at room temperature. Prior to each analysis, buffer exchange of the iodinated rituximab, using PD-10 sephadex columns, was performed as described earlier.

Liquid chromatography coupled to mass spectrometry

(Iodinated) rituximab was diluted to a concentration of 200 μ g/mL in 10% v/v acetonitrile in water and was used immediately for analysis. The analysis was performed as described by Damen et al (10) for the monoclonal antibody trastuzumab under identical chromatographic conditions. In brief, separation of the monoclonal antibody was performed using a high performance liquid chromatography (HPLC) system consisting of an 1100 series binary pump with mobile-phase degasser, column heater and a thermostated autosampler (Agilent Technologies Santa Clara, CA, USA). A POROS R2/10 2000 Å column was used at a flow rate of 0.2 mL/min. For the MS analysis, the eluent was directed to an API365 triple-quadrupole mass spectrometer equipped with a turbo ion spray source (Sciex, Thornhill, ON, Canada).

Circular dichroism

The analysis was performed on the day of the labeling (day 0), and one and seven days after the labeling after storage at room temperature (respectively day 1 and 7). Prior to each analysis, unlabeled rituximab, iodinated rituximab prepared according to the Iodogen coated vial method, and iodinated rituximab according to the Iodogen coated mab method were diluted with 0.9% NaCl to similar concentrations (0.5 mg/mL) as verified by measurement of the UV absorption at 280 nm (Eppendorf BioPhotometer, Hamburg, Germany). Far-ultraviolet circular dichroism (Far-UV CD) (195-260 nm) was performed at room temperature in a 0.02-cm quartz cuvette with a dual beam DSM 1000 CD spectroscopy instrument (On-Line Instrument Systems, Bogart, GA, USA). The subtractive double-graded monochromator was equipped with a fixed disk, holographic gratins (2400 lines/mm, blaze wavelength 230) and 1.24 mm slits. Each measurement was the average of 5 repeated scans. Data were plotted over the range from 205 to 250 nm. 0.9% NaCl was used as buffer, whereas chloride ions interfere with data collection at wavelengths beneath 205 nm (11).

Fluorescence spectroscopy

Fluorescence emission spectra were recorded on a Fluorlog fluorimeter (Horiba, Kyoto, Japan). The analysis was performed immediately after iodination (day 0), on day 1 and day 7 to monitor the stability. Prior to each analysis, the samples were diluted with 0.9% NaCl to similar concentrations (0.05 mg/mL) as confirmed by UV spectrometry. The excitation slits were set at 5 nm. Measurements were executed a room temperature in a quartz cuvette (1 cm path length). The excitation wavelength was set at 280 nm and emission scans were performed at a range of 300-450 nm.

Results

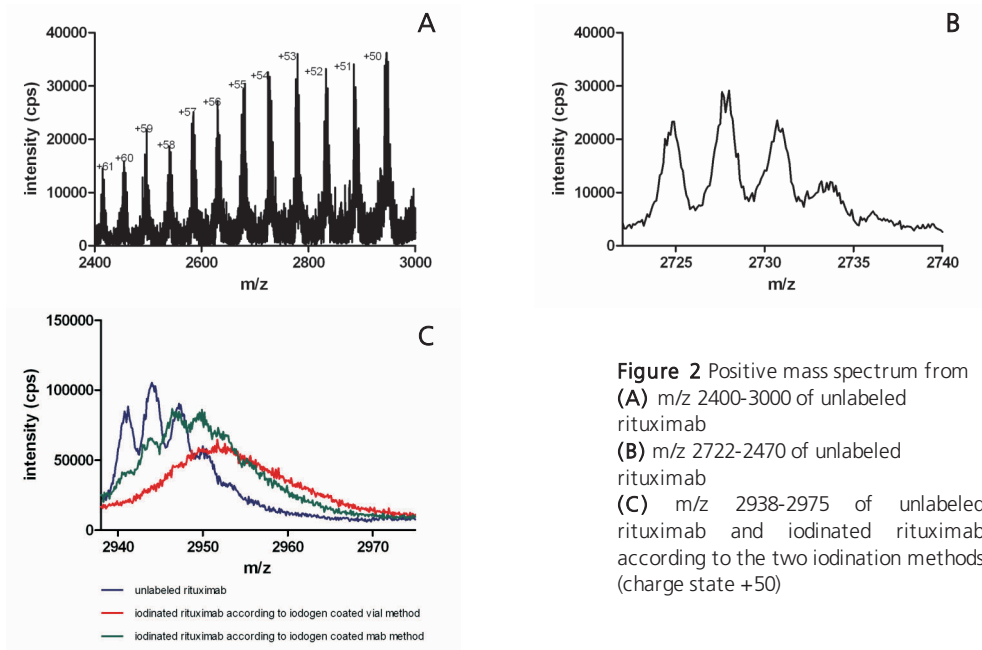


Figure 2 Positive mass spectrum from (A) m/z 2400-3000 of unlabeled rituximab (B) m/z 2722-2470 of unlabeled rituximab (C) m/z 2938-2975 of unlabeled rituximab and iodinated rituximab according to the two iodination methods (charge state +50)

Liquid chromatography coupled to mass spectrometry

Chromatographic analyses of (iodinated) rituximab resulted in a single peak with a retention time of 5.5 minutes (not shown). Subsequently, MS spectra were taken of rituximab, and iodinated rituximab prepared according to the two methods. Figure 2A shows a full spectrum scan of unlabeled rituximab across the range from m/z 2400-3000. The different peaks correspond to the different charge states of rituximab, as indicated in figure 2A. Figure 2B depicts the zoomed spectrum of unlabeled rituximab for the +54 charge state. Four distinctive peaks, corresponding to a mass of 147,088; 147,250; 147,414 and 147,558 Da respectively, were observed due to glycosylation heterogeneity. Figure 2C depicts the zoomed spectra (+50 charge state) of unlabeled rituximab and iodinated rituximab prepared

according to the two methods. The spectra of iodinated rituximab showed a shift to higher m/z values which indicates an increase in mass of the molecule. In the spectrum of iodinated rituximab according to the Iodogen coated mab method, four peaks were still observed but with less resolution. The shift in m/z values corresponded with a mass difference of 361 Da between unlabeled and iodinated rituximab. The line representing iodinated rituximab according to the Iodogen coated vial method showed a larger shift in m/z values with a mass difference of 495 Da. The four distinctive peaks converged into a single broad peak.

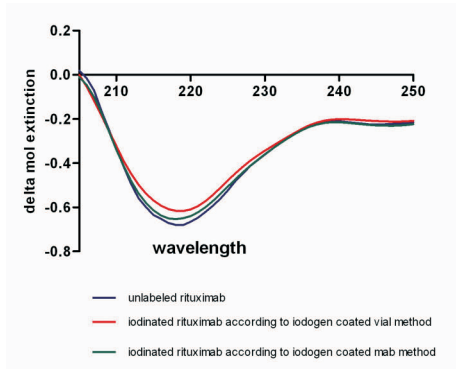


Figure 3 Far-UV CD spectroscopy

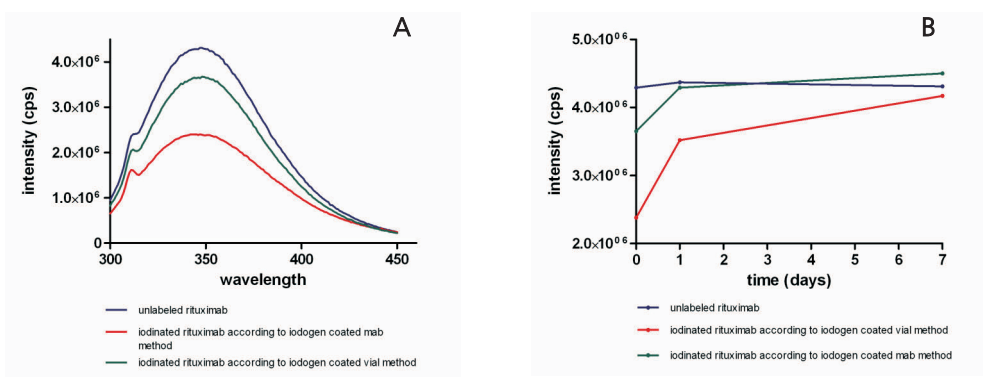


Figure 4 Fluorescence spectroscopy

(A) Fluorescence spectra of unlabeled and iodinated rituximab immediately after iodination at $\lambda=280$ nm for excitation
 (B) Emission of (iodinated) rituximab at $\lambda=350$ nm measured immediately after iodination and storage for 1 and 7 days at room temperature

Circular dichroism

Far-UV CD represents the peptide bond absorption and information on the secondary structure of rituximab can be obtained (12). Figure 3 shows Far-UV CD spectra of on day 0 of unlabeled rituximab, iodinated rituximab according to the lodogen coated vial method, and iodinated rituximab according to the lodogen coated mab method. The spectra of iodinated rituximab were comparable to the spectrum of the unlabeled rituximab. At 218 nm a peak minimum is visible. A variation in peak intensity was observed. Unlabeled rituximab showed a larger negative ellipticity compared to the two iodinated forms whereby iodinated rituximab prepared according to the lodogen coated vial method showed less intensity. Isobestic points at 209 nm and 234 nm were seen. At day 1 and 7, the spectra remained constant (data not shown).

Fluorescence spectroscopy

The emission spectra of unlabeled rituximab, iodinated rituximab prepared according to the lodogen coated vial method, and iodinated rituximab prepared according to the lodogen coated mab method are depicted in figure 4A. Unlabeled rituximab showed higher emission intensity than iodinated rituximab prepared according to both iodination methods. Figure 4B shows the emission of (iodinated) rituximab at $\lambda=350$ nm ($\lambda=280$ nm for excitation) at day 0, day 1, and day 7. For iodinated rituximab prepared according to the lodogen coated vial method, a low intensity at day 0 which increases in time was observed. This is also observed for iodinated rituximab prepared according to the lodogen coated mab method but with a higher intensity at day 0. For unlabeled rituximab, the emission intensity remains constant during the 7-day observation period.

Discussion

Radioiodinated monoclonal antibodies are used as imaging agents (3,13) and as radioimmunotherapeutic agents (1,14,15). The chemistry of radioiodination of monoclonal antibodies has been studied extensively and numerous methods are available for radioiodination. Among the several methods of iodination (6,16,17), the lodogen procedure is still the most frequently used method. By using lodogen as oxidizing agent, linkage of the iodine on the tyrosine residues ortho to the hydroxyl group of the phenol moiety predominates when conducting the reaction at neutral pH (6).

Previous studies already have shown that the method of radioiodination influences the immunoreactivity of rituximab (8,9). Even though less iodine atoms are incorporated when applying the lodogen coated vial method, this method results in a lower immunoreactivity compared to the lodogen coated mab method where twice as much iodine is applied. Therefore the immunoreactivity is proved to be not only dependent on the specific activity of the product.

The immunoreactivity is an important biological feature as it illustrates the binding capacity of the radiolabeled compound. The most widely used method to determine the immunoreactivity of a radiolabeled antibody is described by Lindmo et al (7). The method determines the immunoreactivity, but it does not give further explanation about any change of binding capacity of the radioiodinated analyte. Also, the method is laborious and time consuming. In this study, radioiodinated rituximab was used for further, structural, characterization. For this, three spectroscopic methods of analysis were evaluated which may give further insight into any structural changes following iodination.

By using liquid chromatography coupled online with mass spectrometry a protein specific charge envelope is generated and structural changes in the molecule can be detected (10). When zoomed in a single charge state of unlabeled rituximab, four distinctive peaks were observed. These peaks correspond to four different glycosylation forms with mass differences corresponding with the mass of one hexose residue (10). Compared to unlabeled rituximab, both spectra of iodinated rituximab showed a shift to higher m/z values which indicates an increase in the mass of the molecule. The spectrum of iodinated rituximab prepared according to the lodogen coated mab method resulted in a shift of 361 Da. The spectrum of iodinated rituximab prepared according to the lodogen coated vial method showed a shift of 495 Da. Based on the amount of iodine used in both methods, an average of 1-2 atoms iodine per molecule rituximab could be incorporated. This corresponds to a maximum mass increase of 254 Da. The increases in the mass of both iodinated forms could thus not only be attributed to the addition of iodine atoms as the observed mass differences were larger than 254 Da.

Next to the shift in m/z values, in the spectrum of iodinated rituximab prepared according to the lodogen coated mab method, the four distinctive peaks are observed but with less intensity. In the spectrum of iodinated rituximab prepared according to the lodogen coated vial method, the four peaks are converged into one single broad peak.

Most likely, incubation with the oxidizing agent lodogen also resulted in heterogeneous oxidation of the amino acid moieties of rituximab which results in a mass increase. Heterogeneous oxidation may explain the observed increase in mass as well as the converging of the four distinctive glycosylation peaks into a single broad peak, which subsequently attribute to the loss of immunoreactivity. We have shown earlier that immunoreactivity depends on the iodination method. The lodogen coated vial method resulted in a larger mass difference, but it also resulted in an immunoreactivity of only 30%. Iodinated rituximab, prepared according to the lodogen coated mab method, yielded a lower mass difference and in an immunoreactivity of 70% (8). In addition, in the spectra of rituximab iodinated according to the lodogen coated mab method, the four glycosylation peaks were preserved, though with less resolution. Compared to the lodogen coated vial method, the lodogen coated mab method is a relative mild reaction procedure.

Firstly, a shorter incubation time is required. Secondly, less Iodogen is needed to obtain a high labeling yield. These reaction conditions may lead to a more conserved monoclonal antibody than when applying the Iodogen coated vial method.

Next to the immunoreactivity, the biological clearance and activity of rituximab can be affected by heterogenous oxidation. Rituximab, an IgG molecule, consists of two identical Fab regions, and a Fc-region which is glycosylated through asparagine residue 297. The Fc-region expresses interaction sites for ligands that activate clearance mechanisms (18,19). A correlation was found between Fc-region glycosylation and the binding to these ligands (20). A structural change in the glycan moiety could therefore also cause a change in biological clearance and immunogenicity of rituximab.

Far-UV CD is used to map the secondary structural stability of a protein. The peak minimum seen at 218 nm suggests a high degree of β -sheet structure (21). The spectra of the iodinated rituximab, prepared according to the two methods, show less intensity suggesting the presence of less stable β -sheets. LC-MS data already showed that iodination of rituximab results in an increase in mass and structural changes due to the incorporation of iodine atoms and heterogeneous oxidation of amino acid moieties. Although the differences in CD spectra are subtle, the far-UV CD data supports these results by showing an alteration in secondary structure of the monoclonal antibody after iodination. In addition, the secondary structure remains intact after iodination for at least 7 days.

Fluorescence emission spectrophotometry is a simple procedure. Changes in the intensity of protein fluorescence emission spectra are widely used as indicators for alterations in the conformations of proteins (22). At an excitation wavelength of 280 nm, both tryptophan and tyrosine contribute to intrinsic protein fluorescence. Tryptophan dominates fluorescence among the aromatic amino acids. Tryptophan fluorescence is highly dependent on the polarity of the environment of the fluorophore. At the excitation wavelength of 295 nm, only tryptophan emission is observed (23). Because of the significant role of tyrosine in the iodination process, it was to perform this study with an excitation wavelength of 280 nm. Decreased fluorescence intensity was observed for the iodinated rituximab solutions. Iodinated rituximab according to the Iodogen coated vial method exhibited a larger decrease in intensity. The decrease in intensity can be assigned to quenching. Large halogens such as iodine are known for their quenching characteristics (24). In time, the spectra showed higher emission intensity. Previous study has shown the instability of the product during 24 hours after labeling (8). Loss of incorporated iodine would result in less quenching and thus in a higher fluorescence intensity. Hence, fluorescence emission spectrophotometry can be a tool for rapid stability monitoring.

Conclusions

For development of radiolabeling procedures of monoclonal antibodies for diagnostic and therapeutic properties, thorough investigation of the integrity of the radioconjugate is of importance. Next to the determination of the immunoreactivity, structural characterization is essential. Techniques as liquid chromatography coupled to mass spectrometry, circular dichroism and fluorescence emission spectrophotometry can provide valuable information about structural changes and stability of a radiolabeled compound, both during pharmaceutical development as for quality control.

References

1. Press OW, Eary JF, Gooley T, Gopal AK, Liu S, Rajendran JG et al. A phase I/II trial of iodine-131-tositumomab (anti-CD20), etoposide, cyclophosphamide, and autologous stem cell transplantation for relapsed B-cell lymphomas. *Blood* 2000; 96(9):2934-2942.
2. Behr TM, Griesinger F, Riggert J, Gratz S, Behe M, Kaufmann CC et al. High-dose myeloablative radioimmunotherapy of mantle cell non-Hodgkin lymphoma with the iodine-131-labeled chimeric anti-CD20 antibody C2B8 and autologous stem cell support. Results of a pilot study. *Cancer* 2002; 94(4 Suppl):1363-1372.
3. Blauenstein P, Locher JT, Seybold K, Koprivova H, Janoki GA, Macke HR et al. Experience with the iodine-123 and technetium-99m labelled anti-granulocyte antibody MAb47: a comparison of labelling methods. *Eur J Nucl Med* 1995; 22(7):690-698.
4. Verel I, Visser GW, Vosjan MJ, Finn R, Boellaard R, van Dongen GA. High-quality 124I-labelled monoclonal antibodies for use as PET scouting agents prior to 131I-radioimmunotherapy. *Eur J Nucl Med Mol Imaging* 2004; 31(12):1645-1652.
5. Konishi S, Hamacher K, Vallabhajosula S, Kothari P, Bastidas D, Bander N et al. Determination of immunoreactive fraction of radiolabeled monoclonal antibodies: what is an appropriate method? *Cancer Biother Radiopharm* 2004; 19(6):706-715.
6. Fraker PJ, Speck JC, Jr. Protein and cell membrane iodinations with a sparingly soluble chloroamide, 1,3,4,6-tetrachloro-3a,6a-diphrenylglycoluril. *Biochem Biophys Res Commun* 1978; 80(4):849-857.
7. Lindmo T, Boven E, Cuttitta F, Fedorko J, Bunn PA, Jr. Determination of the immunoreactive fraction of radiolabeled monoclonal antibodies by linear extrapolation to binding at infinite antigen excess. *J Immunol Methods* 1984; 72(1):77-89.
8. Tran L, Baars JW, Maessen HJ, Hoefnagel CA, Beijnen JH, Huitema AD. A simple and safe method for 131I radiolabeling of rituximab for myeloablative high-dose radioimmunotherapy. *Cancer Biother Radiopharm* 2009; 24(1):103-110.
9. Visser GW, Klok RP, Gebbinck JW, ter Linden T, van Dongen GA, Molthoff CF. Optimal quality (131I)-monoclonal antibodies on high-dose labeling in a large reaction volume and temporarily coating the antibody with IODO-GEN. *J Nucl Med* 2001; 42(3):509-519.
10. Damen CW, Rosing H, Schellens JH, Beijnen JH. Quantitative aspects of the analysis of the monoclonal antibody trastuzumab using high-performance liquid chromatography coupled with electrospray mass spectrometry. *J Pharm Biomed Anal* 2008; 46(3):449-455.
11. Ejima D, Tsumoto K, Fukada H, Yumioka R, Nagase K, Arakawa T et al. Effects of acid exposure on the conformation, stability, and aggregation of monoclonal antibodies. *Proteins* 2007; 66(4):954-962.
12. Hawe A, Friess W, Sutter M, Jiskoot W. Online fluorescent dye detection method for the characterization of immunoglobulin G aggregation by size exclusion chromatography and asymmetrical flow field flow fractionation. *Anal Biochem* 2008; 378(2):115-122.
13. Verel I, Visser GW, van Dongen GA. The promise of immuno-PET in radioimmunotherapy. *J Nucl Med* 2005; 46 Suppl 1:164S-171S.
14. Bienert M, Reisinger I, Srock S, Humplik BI, Reim C, Kroessin T et al. Radioimmunotherapy using 131I-rituximab in patients with advanced stage B-cell non-Hodgkin's lymphoma: initial experience. *Eur J Nucl Med Mol Imaging* 2005; 32(10):1225-1233.
15. Kaminski MS, Tuck M, Estes J, Kolstad A, Ross CW, Zasadny K et al. 131I-tositumomab therapy as initial treatment for follicular lymphoma. *N Engl J Med* 2005; 352(5):441-449.
16. Bolton AE, Hunter WM. A new method for labelling protein hormones with radioiodine for use in the radioimmunoassay. *J Endocrinol* 1972; 55(2).
17. Greenwood FC, Hunter WM, Glover JS. The preparation of I-131-labelled human growth hormone of high specific radioactivity. *Biochem J* 1963; 89:114-23:114-123.
18. Indik ZK, Park JG, Hunter S, Schreiber AD. Structure/function relationships of Fc gamma receptors in phagocytosis. *Semin Immunol* 1995; 7(1):45-54.
19. Kim JK, Firan M, Radu CG, Kim CH, Ghetie V, Ward ES. Mapping the site on human IgG for binding of the MHC class I-related receptor, FcRn. *Eur J Immunol* 1999; 29(9):2819-2825.
20. Krapp S, Mimura Y, Jefferis R, Huber R, Sondermann P. Structural analysis of human IgG-Fc glycoforms reveals a correlation between glycosylation and structural integrity. *J Mol Biol* 2003; 325(5):979-989.
21. Harn N, Allan C, Oliver C, Middaugh CR. Highly concentrated monoclonal antibody solutions: direct analysis of physical structure and thermal stability. *J Pharm Sci* 2007; 96(3):532-546.

22. Jovanovic N, Bouchard A, Hofland GW, Witkamp GJ, Crommelin DJ, Jiskoot W. Stabilization of IgG by supercritical fluid drying: optimization of formulation and process parameters. *Eur J Pharm Biopharm* 2008; 68(2):183-190.
23. Neves-Petersen MT, Gryczynski Z, Lakowicz J, Fojan P, Pedersen S, Petersen E et al. High probability of disrupting a disulphide bridge mediated by an endogenous excited tryptophan residue. *Protein Sci* 2002; 11(3):588-600.
24. Lakowicz JR, Weber G. Quenching of protein fluorescence by oxygen. Detection of structural fluctuations in proteins on the nanosecond time scale. *Biochemistry* 1973; 12(21):4171-4179.

Chapter 2

Pharmacokinetics of rituximab

Chapter 2.1

Pharmacokinetics of rituximab in patients with CD20 positive B-cell malignancies

Ly Tran

Joke W. Baars

Lucien A. Aarden

Jos H. Beijnen

Alwin D.R. Huitema

Submitted for publication

Abstract

Background

Rituximab is used for the treatment of CD20 positive non-Hodgkin lymphoma. Although the drug has proven efficacy and safety, considerable variability in response and side effects are regularly observed. In this study, we investigated the pharmacokinetics of rituximab in patients with CD20 positive non-Hodgkin lymphoma, to get more insight into the factors that influence the pharmacokinetics of rituximab. This may aid to understand variability of treatment outcome, in patients with a CD20 positive malignancy treated with rituximab.

Methods

In this study, patients with a CD20 positive B-cell malignancy who were treated with rituximab containing regimens were included. Induction treatment schedules consisted of a 2, 3 or 4-weekly schedule of 375 mg/m² rituximab intravenously in combination with chemotherapy for 4-8 cycles. Maintenance treatment consisted of a 2 or 3-monthly dose of 375 mg/m² rituximab intravenously for 2 years. On the day of the treatment with rituximab, preinfusion blood samples were taken. Also, after the end of treatment, selected blood samples were taken. Rituximab levels were measured with a validated enzyme-linked immunosorbent assay (ELISA). An antigen-binding assay was applied for determination of human-antibodies against chimeric-antibodies (HACAs)

Results

Eight patients were on induction therapy. Rituximab levels of one patient on induction therapy remained very low after the first course. This patient had a chronic lymphoid leukemia with circulating tumor cells and a high tumor burden. Apart from one patient with mantle cell lymphoma, all patients on induction therapy had a complete response.

Five patients were on maintenance therapy.

Trough levels of 4 patients on three-monthly schedule maintenance therapy remained constant, with a median concentration of 6 µg/mL (range 0.5–11.7 µg/mL). One patient had a relapse during his maintenance treatment.

The elimination half-life at steady state of rituximab in all patients was estimated to be 19.2 (±15.2%) days with a between-subject variability of 54%, indicating wide variability.

In a patient with relapse and a patient who had no response, the rituximab serum levels declined or remained low, suggesting that a decline or low rituximab serum level is not the cause but the result of the presence of malignant CD20+ B-cells that bind but not react to rituximab.

For all patients, concentration of HACAs remained below the quantification limit.

Summary/conclusion

Considerable inter-individual variability of rituximab levels was observed. No HACAs were observed in these patients. Although the patient population was small, the results support the need for more research into the pharmacokinetics and factors that might influence the pharmacokinetic-pharmacodynamic relationships of rituximab in patients with non-Hodgkin lymphoma.

Introduction

Non-Hodgkin lymphomas are neoplastic transformations of normal lymphoid cells that reside predominantly in lymphoid tissues. Molecular studies have shown that most lymphomas are derived from mature B-cells which are characterized by the CD20 antigen. The CD20 antigen is expressed on more than 90% of the B-cell population, and is therefore an ideal target for the treatment of CD20 positive B-cell NHL (1). Rituximab is a chimeric monoclonal antibody against the CD20 antigen. Rituximab eliminates CD20 positive cells via antibody-dependent cellular cytotoxicity (ADCC), complement-dependent cytotoxicity (CDC), and direct effects induced by rituximab binding to the CD20 antigen, including apoptosis (2,3).

Although rituximab has proven efficacy and safety, several studies have demonstrated a large inter-individual variability of rituximab exposure, response, and side effects which may be influenced by factors like tumor burden, amount of antigen expression, presence of circulating antigen, and the development of antibodies against rituximab (4-10).

To get more insight into the factors that can influence the pharmacokinetics of rituximab in patients with a CD20 positive malignancy, and possible relation between rituximab levels and treatment response, we have investigated this in patients with CD20 positive non-Hodgkin lymphoma who are on induction or maintenance therapy.

Methods

Patients, treatment, and sample collection

Eligible patients were patients with a CD20 positive B-cell malignancy scheduled for treatment with rituximab containing regimens or on rituximab maintenance therapy. The patients were informed by their treating physicians in line with the rules of good clinical practice. Written informed consent was obtained from all patients. The study protocol was approved by the medical ethics committee of the hospital.

Induction treatment schedules consisted of a 2-, 3-, or 4-weekly schedule of 375 mg/m² rituximab intravenously in combination with chemotherapy for 4-8 cycles. Table 1 shows an overview of the applied chemotherapeutic regimens. Maintenance treatment consisted of a 2- or 3-monthly dose of 375 mg/m² rituximab intravenously for 2 years. All patients were on maintenance therapy for more than 6 months. On the day of the treatment with rituximab, preinfusion blood samples were taken.

After the end of treatment, selected blood samples were taken up to 11 days after the last infusion. For determination of rituximab levels and antibodies against rituximab, blood samples were taken in serum separating tubes (BD, Franklin Lakes, NJ, USA), after blood sampling and coagulation for 30 minutes at room temperature, the samples were centrifuged at 1500 g for 10 minutes at room temperature. Serum was collected and stored at -20°C until analysis.

Table 1 Treatment regimen

Treatment	Dose regimen
R-CHOP	Rituximab (375 mg/m ²) day 1, cyclophosphamide (750 mg/m ²) day 1, doxorubicin 50 mg/m ² day 1, vincristine 1.4 mg/m ² day 1, prednisone 100 mg day 1-5
R-CVP	Rituximab (375 mg/m ²) day 1, cyclophosphamide (750 mg/m ²) day 1, vincristine 2 mg day 1, prednisone (40 mg/m ²) day 1-5
R-PECC	Rituximab (375 mg/m ²), prednisone (40 mg/m ²) day 2-6, etoposide (100 mg/m ²) day 2-6, CCNU (lomustine) 40 mg/m ² day 1, chlorambucil (8 mg/m ²) day 2-6
R-FC	Rituximab (375 mg/m ²), fludrabine (30 mg/m ²) day 2, 3, 4, cyclophosphamide (200 mg/m ²) day 2,3,4

Determination of serum rituximab levels

Rituximab concentrations in serum were measured by an enzyme-linked immunosorbent assay. The assay was designed and performed as described by Damen et al for the monoclonal antibody trastuzumab under identical conditions (11). In brief, anti-idiotypic antibodies raised in rabbits immunized with F(ab)₂ fragments of rituximab were coated on Maxisorp plates (Nunc, Roskilde, Denmark). After washing, patient sera, diluted in high performance ELISA buffer (HPE, Sanquin, Amsterdam, The Netherlands), were incubated with biotinylated rabbit anti-idiotypic IgG. Subsequently, streptavidin–poly-horseradishperoxidase (Sanquin, Amsterdam, The Netherlands) was added. The samples were allowed to incubate for 30 minutes. After three washing steps, (3,5,3',5')-tetramethylbenzidine (TMB) ELISA peroxidase substrate (Uptima, Interchim, Montluçon, France) was added. The reaction was stopped by addition of 100 µL 2 M H₂SO₄ (Merck, Darmstadt, Germany). Rituximab levels were quantified by measuring the absorbance at 450 nm against a calibration curve. The minimum quantifiable concentration was 7.8 ng/mL. Samples above 5,000 ng/mL were diluted 10 times with HPE buffer. Samples above 50,000 ng/mL were diluted 100 times with HPE buffer. The accuracy was 12.7% and 5.78% for 10 and 100 times dilutions, respectively and the precision was 7.87% and 10.7% for the 10 and 100 times dilutions, respectively.

Determination of antibodies against rituximab

Antibodies against rituximab were measured by an antigen-binding test as described for adalimumab (12). Briefly, serum was incubated with sepharose-immobilised protein A (Pharmacia/GE Healthcare, Uppsala, Sweden) in Freeze buffer (Sanquin, Amsterdam, the Netherlands). Non-bound serum components were removed before ¹²⁵I labeled F(ab)₂ fragments of rituximab were added. After washing, bound radioactivity was compared with a reference serum and was converted into arbitrary units (AU). The lower limit of quantification was 12 AU/mL.

Population pharmacokinetics

Pharmacokinetic data were analyzed using NONMEM software (version VI; Icon Development Solutions, Ellicott City, Maryland, USA). Since only trough levels were

collected, only the elimination half-life of rituximab could be estimated. Volume of distribution was fixed at 2.98 L (13). The elimination half-life at steady state and the associated between-subject variability was estimated. To account for rapid antigen mediated elimination after the first rituximab dose, a fraction of the dose eliminated above the elimination at steady state was estimated for patients showing a slow accumulation of rituximab. Body weight, sex, and treatment schedule were tested for their influence on rituximab pharmacokinetics (log-likelihood ratio test, $p=0.05$)

Results

Table 2 shows the patient's characteristics. All patients had a normal liver function and no patient had a splenomegaly. Median renal function was 86 mL/min (range 62-120 mL/min) and was considered normal for all patients. Figure 1A depicts the rituximab levels vs time for the patients on induction therapy. Eight patients were on induction therapy with a mean age of 62.3, ranging from 40 to 74 years. A wide variation was observed in the rituximab levels after the first course: 38.3-50.6 $\mu\text{g/mL}$ for patients on a 2-weekly schedule (3 patients), 19.4-83 $\mu\text{g/mL}$ for patients on a 3-weekly schedule (3 patients), and 1.45-26.7 $\mu\text{g/mL}$ on a 4-weekly schedule (2 patients). In part, this could be explained by a high tumor burden.

Patient 2 had small lymphoid leukemia/ chronic lymphoid leukemia, for which he received a four-weekly schedule for rituximab containing chemotherapy. The patient had a tumor load of $>20 \text{ cm}^2$, bone marrow infiltration and circulating tumor cells. A low trough level of rituximab (1.45 $\mu\text{g/mL}$) was detected, prior to the second rituximab cycle.

Apart from one patient (patient 4), all patients had a complete response. Patient 4 had a Mantle cell lymphoma and received a 4-weekly schedule R-PECC. This patient showed the lowest serum levels of rituximab. 83 days after the last rituximab infusion, a rituximab serum level of 20.2 $\mu\text{g/mL}$ was measured. Cytological puncture in the remaining lesion showed of a CD20 positive B-cells population.

Five patients were on maintenance therapy, with a mean age of 61 (38-71) years. The characteristics are given in table 2. One patient received two-monthly maintenance treatment. Trough levels of four patients on 3-monthly schedule remained constant, with a median concentration of 6 $\mu\text{g/mL}$ (range 0.5–11.7 $\mu\text{g/mL}$) (Figure 1B). One patient had a relapse after 9 months of maintenance therapy. The patient had hairy cell leukemia while no splenomegaly was detected. Pathology showed a massive CD20 positive B-cell infiltration with hairy cells. At the point of relapse the patient had a declining rituximab level compared to prior trough levels, possibly explained by increased number CD20 positive B-cells.

The elimination half-life at steady state of all patients was estimated to be 19.2 ($\pm 15.2\%$) days with a between-subject variability of 54%, indicating wide variability. For patient 2, only 1.4% of the first dose administered was ultimately detected in the central circulation, indicating that the majority of the administered rituximab was

bound to CD20 positive B-cells. Besides the tumor load of patient 2, none of the other co-variables could explain the observed variability. No antibodies against rituximab were detectable in all patients. No rituximab-related toxicities were observed in the patients on induction therapy as well as the maintenance therapy.

Table 2 Patient's characteristics

Patient	Gender	Age	Diagnose	Treatment	Dose interval	Cycles	Tumour load cm ²	Bone marrow infiltration	Circulating tumour cells	Outcome
1	female	50	DLBCL	R-CHOP	two weekly	8	2.45	no	no	CR
2	male	67	CLL/SLL	R-FC	four weekly	4	>20	yes	yes	CR
3	male	40	FL	R-CHOP	two weekly	8	8.2	yes	no	CR
4	male	68	MCL	R-PECC	four weekly	4	9	no	no	PR
5	female	64	FL	R-CVP	three weekly	4	7	yes	no	CR
6	male	74	DLBCL	R-CHOP	two weekly	8	>20	no	no	CR
7	female	61	FL	R-CVP	three weekly	8	19	no	no	CR
8	male	74	FL	R-CHOP	three weekly	6	>20	no	no	CR
9	male	66	FL	maintenance	three monthly	14	ND	no	no	CR
10	female	71	MCL	maintenance	two monthly	6	ND	no	no	CR
11	female	60	FL	maintenance	three monthly	6	ND	no	no	CR
12	male	70	HCL	maintenance	three monthly	9	ND	no	no	relapsed
13	male	38	FL	maintenance	three monthly	4	ND	no	no	CR

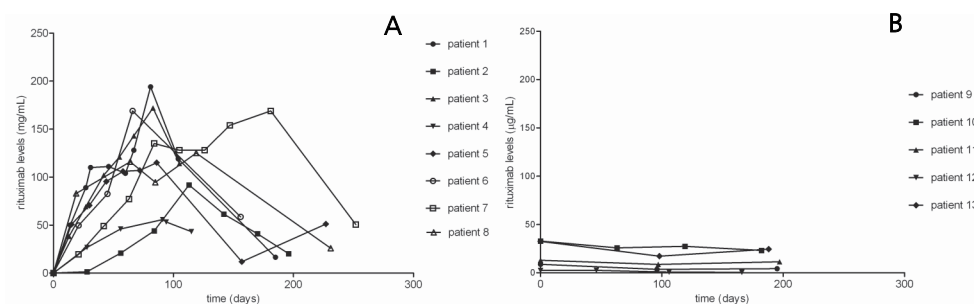


Figure 1 Rituximab serum levels in time. **(A)** Patient 1-8 received induction therapy. **(B)** Patient 9-13 were in maintenance therapy

Discussion

Within this study, rituximab serum levels of patients with different B-cell lymphoid malignancies were analyzed. A large variability (54%) in elimination half-life was found.

A correlation has been reported between mean rituximab levels and response by Berinstein et al. The authors reported that rituximab levels of responders during induction treatment of four cycles, once weekly, were higher than the levels of the non-responders (7,14). Three months after the last infusion, median rituximab levels of 5.9 µg/mL were found for non-responders and 25.4 µg/mL for responders (7,14).

In the study outlined herein, except one patient, all patients had a complete response even though the large variability in rituximab serum levels. Although a patient with small lymphoid leukemia/ chronic lymphoid leukemia showed initial low rituximab levels, the patient had a complete remission. One patient only had a partial remission after 4 cycles of induction therapy. Almost three months after the last rituximab infusion, a serum level of 20.2 µg/mL was measured. These results cannot be compared to previous reported results as this patient was treated according to a different treatment schedule. Nevertheless, the rituximab levels remained low compared to the other patients who did respond. Cytological puncture in the remaining lesion showed of a CD20 positive B-cells population. Most likely, circulating rituximab was bound to CD20 positive B-cells, and subsequently the amount of rituximab in the circulation was depleted. The low levels of rituximab could therefore also be caused by the presence of CD20 positive B-cells due to relapse.

CD20 antigen expression is heterogeneous between and within different lymphoma subtypes and might even be different in various tumor localizations (15,16). In addition, some studies have suggested that the amount of CD20 antigen either determined by tumor burden or by level of CD20 antigen expression did not play a major role in rituximab pharmacokinetics variability (17-19).

It has been reported that the number of lymphoid B-cells prior to treatment in patients with chronic lymphoid leukemia is correlated to the rate of rituximab concentration decline after the first administration and a dose of 375 mg/m² might provide an initial low response rate (10,20). A loading dose of rituximab could be considered for neutralizing the circulating antigen. However, severe first infusion reactions have been reported (9,21). Therefore, a more frequent dosing regimen would be preferred. Byrd et al have examined the possibility to administer rituximab three times in a week, with a total duration of 4 weeks, in patients with chronic lymphoid leukemia. The study demonstrated minimal detectable rituximab levels after the first infusion that began to accumulate after the third dose of therapy. The study showed an overall response of 50%, and suggested, albeit that the study was uncontrolled, that frequent dosing is more effective against chronic lymphoid leukemia (9).

Patients on maintenance therapy received a 2- or 3-monthly dose of 375 mg/m² rituximab. The efficacy of rituximab maintenance therapy has been reported by several groups (22-25). However, the desirable therapeutic levels are not yet fully elucidated. Of the five monitored patients, one patient had a relapse after 9 months maintenance therapy. The patient had hairy cell leukemia, while no splenomegaly was detected. At the time of relapse, a decrease in rituximab serum levels was observed. Pathology showed a massive CD20 positive B-cell infiltration with hairy cells and this could explain the decline in rituximab levels.

Most likely, when a patient has already been treated with rituximab for a certain period with a stable dose, a decline of the serum level of rituximab is not the cause but more the result of a relapse of the non-Hodgkin lymphoma.

As rituximab is a chimeric monoclonal antibody, it can induce an immune response which is reflected in the development of antibodies against rituximab evoking systemic inflammatory effects. Thus, there is a risk for the development of human anti-chimeric antibodies (HACAs). HACA formation can cause a rapid elimination of rituximab, decreases subsequently the extent of B-cell depletion, and therefore decreases therapeutic response. HACA formation has occurred in a high rate in patients with auto-immune diseases who were treated with rituximab (27% of patients with Sjögren's syndrome, 35% in patients systemic lupus erythematosus, and 4.3% of patients with rheumatoid arthritis (5,26,27)) Most likely, the high incidence of HACAs formation in autoimmune diseases is caused by the highly activated B-cells.

The incidence of the development of HACAs in patients with non-Hodgkin lymphoma proved to be low, but most observations were only performed during short-term induction therapy (14,28). Therefore, it was of interest to investigate the presence of HACAs in patients on longer treatment duration. In our study, no HACAs were detected in the patients on induction therapy as well as in patients who were on maintenance therapy for more than 6 months. Therefore, in this study, the pharmacokinetics of rituximab were not influenced by the development of HACAs. Furthermore, treatment with rituximab is safe in patients with a CD20 positive malignancy as the formation of HACAs is rarely observed in these patients.

Conclusion

This study shows a considerable inter-individual variability in rituximab pharmacokinetics. Although the patient population is small, several cases are presented which support the need for more research to investigate the pharmacokinetics of rituximab and its relationships with tumor response, HACA formation and toxicity.

Acknowledgements

The authors wish to thank Kim van Houten en Henk de Vrieze from Sanquin, Amsterdam, The Netherlands, for their indispensable help with the analysis of the rituximab levels and for the determination of antibodies against rituximab.

References

1. Anderson KC, Bates MP, Slaughenhaupt BL et al. Expression of human B cell-associated antigens on leukemias and lymphomas: a model of human B cell differentiation. *Blood* 1984;63(6):1424-1433
2. Maloney DG, Grillo-Lopez AJ, Bodkin DJ et al. IDEC-C2B8: results of a phase I multiple-dose trial in patients with relapsed non-Hodgkin's lymphoma. *J Clin Oncol* 1997;15(10):3266-3274
3. Reff ME, Carner K, Chambers KS et al. Depletion of B cells in vivo by a chimeric mouse human monoclonal antibody to CD20. *Blood* 1994;83(2):435-445
4. McLaughlin P, Grillo-Lopez AJ, Link BK et al. Rituximab chimeric anti-CD20 monoclonal antibody therapy for relapsed indolent lymphoma: half of patients respond to a four-dose treatment program. *J Clin Oncol* 1998;16(8):2825-2833
5. Pijpe J, van Imhoff GW, Spijkervet FK et al. Rituximab treatment in patients with primary Sjogren's syndrome: an open-label phase II study. *Arthritis Rheum* 2005;52(9):2740-2750
6. Tobinai K, Kobayashi Y, Narabayashi M et al. Feasibility and pharmacokinetic study of a chimeric anti-CD20 monoclonal antibody (IDEC-C2B8, rituximab) in relapsed B-cell lymphoma. The IDEC-C2B8 Study Group. *Ann Oncol* 1998;9(5):527-534
7. Berinstein NL, Grillo-Lopez AJ, White CA et al. Association of serum Rituximab (IDEC-C2B8) concentration and anti-tumor response in the treatment of recurrent low-grade or follicular non-Hodgkin's lymphoma. *Ann Oncol* 1998;9(9):995-1001
8. Huh YO, Keating MJ, Saffer HL et al. Higher levels of surface CD20 expression on circulating lymphocytes compared with bone marrow and lymph nodes in B-cell chronic lymphocytic leukemia. *Am J Clin Pathol* 2001;116(3):437-443
9. Byrd JC, Murphy T, Howard RS et al. Rituximab using a thrice weekly dosing schedule in B-cell chronic lymphocytic leukemia and small lymphocytic lymphoma demonstrates clinical activity and acceptable toxicity. *J Clin Oncol* 2001;19(8):2153-2164
10. Manshouri T, Do KA, Wang X et al. Circulating CD20 is detectable in the plasma of patients with chronic lymphocytic leukemia and is of prognostic significance. *Blood* 2003;101(7):2507-2513
11. Damen CW, de Groot ER, Heij M et al. Development and validation of an enzyme-linked immunosorbent assay for the quantification of trastuzumab in human serum and plasma. *Anal Biochem* 2009;391(2):114-120
12. Bartelds GM, Wijbrandts CA, Nurmohamed MT et al. Clinical response to adalimumab: relationship to anti-adalimumab antibodies and serum adalimumab concentrations in rheumatoid arthritis. *Ann Rheum Dis* 2007;66(7):921-926
13. Ng CM, Bruno R, Combs D et al. Population pharmacokinetics of rituximab (anti-CD20 monoclonal antibody) in rheumatoid arthritis patients during a phase II clinical trial. *J Clin Pharmacol* 2005;45(7):792-801
14. McLaughlin P, Grillo-Lopez AJ, Link BK et al. Rituximab chimeric anti-CD20 monoclonal antibody therapy for relapsed indolent lymphoma: half of patients respond to a four-dose treatment program. *J Clin Oncol* 1998;16(8):2825-2833
15. Dayde D, Ternant D, Ohresser M et al. Tumor burden influences exposure and response to rituximab: pharmacokinetic-pharmacodynamic modeling using a syngeneic bioluminescent murine model expressing human CD20. *Blood* 2009;113(16):3765-3772
16. Johnson NA, Boyle M, Bashashati A et al. Diffuse large B-cell lymphoma: reduced CD20 expression is associated with an inferior survival. *Blood* 2009;113(16):3773-3780
17. Regazzi MB, Iacona I, Avanzini MA et al. Pharmacokinetic behavior of rituximab: a study of different schedules of administration for heterogeneous clinical settings. *Ther Drug Monit* 2005;27(6):785-792
18. Mangel J, Buckstein R, Imrie K et al. Pharmacokinetic study of patients with follicular or mantle cell lymphoma treated with rituximab as 'in vivo purge' and consolidative immunotherapy following autologous stem cell transplantation. *Ann Oncol* 2003;14(5):758-765
19. Blasco H, Chatelut E, de Bretagne IB et al. Pharmacokinetics of rituximab associated with CHOP chemotherapy in B-cell non-Hodgkin lymphoma. *Fundam Clin Pharmacol* 2009;
20. O'Brien SM, Kantarjian H, Thomas DA et al. Rituximab dose-escalation trial in chronic lymphocytic leukemia. *J Clin Oncol* 2001;19(8):2165-2170
21. O'Brien SM, Kantarjian HM, Cortes J et al. Results of the fludarabine and cyclophosphamide combination regimen in chronic lymphocytic leukemia. *J Clin Oncol* 2001;19(5):1414-1420

22. Ghielmini M, Schmitz SF, Cogliatti SB et al. Prolonged treatment with rituximab in patients with follicular lymphoma significantly increases event-free survival and response duration compared with the standard weekly x 4 schedule. *Blood* 2004;103(12):4416-4423
23. Van Oers MH, Hagenbeek A, Van Glabbeke M et al. Chimeric anti-CD20 monoclonal antibody (Mabthera) in remission induction and maintenance treatment of relapsed follicular non-Hodgkin's lymphoma: a phase III randomized clinical trial--Intergroup Collaborative Study. *Ann Hematol* 2002;81(10):553-557
24. Hainsworth JD, Litchy S, Barton JH et al. Single-agent rituximab as first-line and maintenance treatment for patients with chronic lymphocytic leukemia or small lymphocytic lymphoma: a phase II trial of the Minnie Pearl Cancer Research Network. *J Clin Oncol* 2003;21(9):1746-1751
25. Brugger W, Hirsch J, Grunebach F et al. Rituximab consolidation after high-dose chemotherapy and autologous blood stem cell transplantation in follicular and mantle cell lymphoma: a prospective, multicenter phase II study. *Ann Oncol* 2004;15(11):1691-1698
26. Looney RJ, Anolik JH, Campbell D et al. B cell depletion as a novel treatment for systemic lupus erythematosus: a phase I/II dose-escalation trial of rituximab. *Arthritis Rheum* 2004;50(8):2580-2589
27. Edwards JC, Szczepanski L, Szechinski J et al. Efficacy of B-cell-targeted therapy with rituximab in patients with rheumatoid arthritis. *N Engl J Med* 2004;350(25):2572-2581
28. Berinstein NL, Grillo-Lopez AJ, White CA et al. Association of serum Rituximab (IDEC-C2B8) concentration and anti-tumor response in the treatment of recurrent low-grade or follicular non-Hodgkin's lymphoma. *Ann Oncol* 1998;9(9):995-1001

Chapter 3

¹³¹I-rituximab in patients
with
CD20 positive B-cell malignancies

Chapter 3.1

Lack of tumor uptake of ^{131}I -rituximab
in a patient
with a CD20 positive lymphoma lesion

Ly Tran

Alwin D.R. Huitema

Wouter V. Vogel

Jos H. Beijnen

Joke W. Baars

Submitted for publication

Abstract

Radioimmunotherapy has emerged as treatment modality for patients with CD20 positive B-cell non-Hodgkin lymphoma. Prior to administration of a therapeutic dose, confirmation of uptake of the radiolabeled compound in tumor locations and calculation of an appropriate dose can be performed using a diagnostic dose and subsequent imaging. We report the case of a 69-year old male with a relapsed mantle cell lymphoma scheduled for radioimmunotherapy, where diagnostic imaging with ^{131}I -rituximab revealed unexpected new insights with implications for treatment.

Persistence of the mantle cell lymphoma in a lymph node in the left arm was demonstrated by a ^{18}F -fluorodeoxyglucose scan. However, a scan after a diagnostic dose of ^{131}I -rituximab did not show any uptake of the tracer, even though subsequent cytological analysis unequivocally confirmed a CD20 positive B-cell population in the lesion. The administration of a therapeutic dose of ^{131}I -rituximab was therefore cancelled. We here discuss the mechanisms that may explain lack of targeting in a proven CD20 positive lymphoma, and provide recommendations for further studies.

Background

Radiolabeled monoclonal antibodies have been used as radioimmunotherapeutic agent for patients with non-Hodgkin lymphoma (1-4). Radioimmunotherapy offers targeted irradiation to CD20 positive cells and promotes cytotoxic activity by the crossfire-effect to neighboring tumor cells with none or insufficient antigen expression (5). Encouraging results have been reported about this targeted therapy strategy, but this case report illustrates a patient with a relapsed mantle cell lymphoma with a vital and CD20 positive lesion who did not show any tumor uptake of ^{131}I -rituximab. We here report the results of our investigations and provide recommendations for further studies.

Case representation

The patient was a 69-year-old male with a relapsed mantle cell lymphoma. At the time of diagnosis, histological and flow cytometric analysis had confirmed the presence of CD20 positive B-cells. The patient relapsed after several rituximab containing treatment regimens, in a lymph node in the left elbow and in the left axilla. Remission induction treatment was given in a 4-weekly schedule of 3 cycles R-PECC (rituximab 375 mg/m² intravenously at day 1, prednisone 40 mg/m² orally at day 1-6, etoposide 100 mg/m² orally at day 2-6, CCNU (lomustine) 40 mg/m² orally at day 1 and chlorambucil 8 mg/m² orally day 2-6). A ^{18}F -FDG scan was performed after the second cycle, which showed a complete metabolic remission of the lymphadenopathy in the left axilla, but a metabolically active localization of the lymph node in the left elbow indicating a persistent vital tumor site. The patient was considered to be in partial response. After written informed consent was obtained, the patient was scheduled for consolidation treatment with ^{131}I -rituximab in a clinical trial approved by our medical ethical committee.

The patient received a pretreatment dose of 2.5 mg/kg unlabeled rituximab, followed by a diagnostic dose of 185 MBq ^{131}I -rituximab to perform dosimetry prior to radioimmunotherapy. Wholebody scans after 24 hrs and 48 hrs showed circulation of the tracer with no obvious clearance. No accumulation of ^{131}I -rituximab could be detected in the tumor lesion in the left elbow. Due to this finding a beneficial effect of radioimmunotherapy was considered unlikely, and thus, administration of the therapeutic dose was cancelled.

Cytological biopsy of the tumor location in the left elbow was performed. Flow cytometric analysis showed a population of CD20 positive B-cells, and therefore the lack of targeting of the antibody remained unexplained. At the time of administration of the diagnostic dose, the patient had a rituximab serum concentration of 20.2 µg/mL, measured using an enzyme-linked immunosorbent assay (ELISA). Further treatment of the patient consisted of local radiation therapy of the left elbow and axilla. Hereafter the patient was in complete remission, 8 months to date.

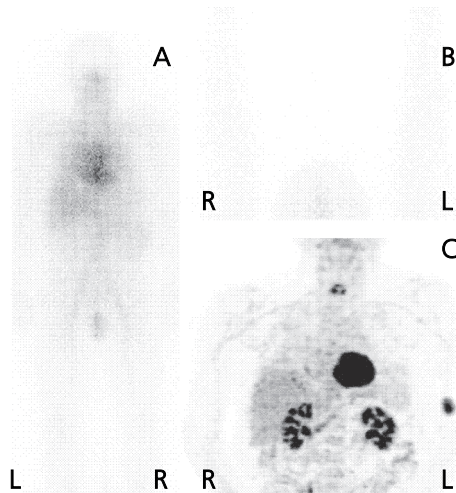


Figure 1 Imaging of ¹³¹I-rituximab
(A) Wholebody scan from anterior 48 hrs p.i. shows the biodistribution of the antibody
(B) Scans of the arms from posterior show no accumulation in the vital and CD20 positive lymphoma location, that can be seen on the ¹⁸F- FDG-PET scan

Discussion

Radioimmunotherapy has emerged as a promising treatment modality in patients with a CD20 positive non-Hodgkin lymphoma. Encouraging results have been reported for both non-myeloablative and myeloablative treatment regimens (1-4). Our case illustrates a patient scheduled for radioimmunotherapy as consolidation therapy after remission induction treatment, who unexpectedly showed no targeting of ¹³¹I-rituximab in a remaining proven vital and CD20 positive lesion.

This case shows that several factors have to be taken in account for the optimal use of radio-immunotherapy with radiolabeled anti-CD20 monoclonal antibodies in patients with non-Hodgkin lymphoma who are pretreated with rituximab containing chemotherapy. These factors are: the heterogeneity of CD20 antigen expression, the method by which CD20 antigen positivity has been determined (e.g. flow cytometry, immunochemistry), prior regimens, especially prior doses of rituximab that can saturate the CD20 antigen, possible change of the CD20 antigen by pretreatment of rituximab, change of configuration of the monoclonal antibody by radiolabeling, tumor load and the variability of the pharmacokinetics of rituximab.

The CD20 antigen expression, as assessed by flow cytometric analysis, is heterogeneous between and within different lymphoma subtypes and might even be different in tumor localizations. These differences may correlate with clinical responses to rituximab and to radioimmunotherapy (6,7). The method at which the CD20 expression has been determined has to be taken into consideration. Apart from this, in our patient, the positive CD20 antigen expression of the non-Hodgkin lymphoma was determined by flow cytometry and was strongly positive.

The pretreatment of rituximab prior to the administration of radioimmunotherapy with ¹³¹I-rituximab can also be a critical factor for the success of this treatment. Both preclinical and clinical data support the value of pretreatment with unlabeled

rituximab to improve tumor targeting and extend the residence time of the radio-immunoconjugates in the circulation. However, a too high dose of unlabeled rituximab may compete with the ^{131}I -rituximab and compromise selective uptake of ^{131}I -rituximab in tumor sites (8). Our patient had a relapse after administration of several rituximab containing regimens. Gopal et al evaluated the impact of prior rituximab on the binding of a secondary administration of anti-CD20 monoclonal antibodies (9). The authors found that, in vitro and in animal studies, sequential use of anti-CD20 monoclonal antibodies resulted in almost complete inhibition of binding of the second anti-CD20 monoclonal antibody. This suggests that high circulating rituximab concentrations may impair the clinical efficacy of anti-CD20 radioimmunotherapy. Clinical studies have shown the efficacy of radioimmunotherapy in rituximab refractory patients with measurable serum rituximab levels prior to treatment (10). However, results from other studies had suggested that therapeutic responses were caused by nontargeted radiation, induced by radioimmunotherapy (11,12). At the time of administration of the diagnostic dose of ^{131}I -rituximab, the patient had a rituximab serum concentration of 20.2 $\mu\text{g}/\text{mL}$ corresponding to a circulating amount of rituximab of approximately 100 mg. It is questionable if ^{131}I -rituximab would be efficacious as consolidation therapy for patients who have received extensive pretreatment with rituximab. Thus, more studies are required to estimate the optimal time point for radioimmunotherapy. Additionally, previous studies have shown the deterioration of the binding capacity, the immunoreactivity, of rituximab to the CD20 antigen after radiolabeling (13-15). A reduced immunoreactivity can cause less binding to the CD20 antigen. However, quality control of the radioconjugate showed a product with high preservation of its integrity (14).

Another possible explanation for the lack of binding could be a change in the configuration of the CD20 antigen. It is known that therapies may lead to selection of treatment resistant subpopulations with specific characteristics that differ from the original tumor cell population (16,17). The remaining lesion in the presented patient was the only lesion not responding to the R-PECC induction treatment. In retrospect, it is impossible to determine differences in the CD20 epitope in the remaining lesion before and after induction remission treatment, or between the remaining lesion and lesions that did respond to treatment. Therefore, unexpected (changes in) tumor behavior with respect to antibody binding may occur and remain unexplained in future cases as well.

However, radiolabeled rituximab can be used for diagnostic imaging in order to select patients with proper binding, who might profit from addition of rituximab to their chemotherapeutic regimen. In addition, by administering a diagnostic dose of ^{131}I -rituximab the biodistribution of the radiolabeled compound can be observed in a wholebody approach. Based on the results of this procedure, we decided not to administer a therapeutic dose of ^{131}I -rituximab to the patient presented here. Similar procedures have already been included in the treatment strategy for ^{90}Y -ibritumomab

tiuxetan and ^{131}I -tositumomab to exclude patients with unfavorable biodistribution (18-20), and we conclude that this approach is mandatory for ^{131}I -rituximab as well. A downside of ^{131}I -rituximab as a diagnostic imaging agent is that it is limited to gamma-camera imaging, with relatively poor image resolution and suboptimal quantification. Recent developments has allowed the preparation of ^{124}I -rituximab for positron emission tomography (PET) as has been proposed before (21), for diagnostic imaging with superior sensitivity and quantification. We conclude that radiolabeled rituximab as radiodiagnostic imaging agent can have an additive value in the selection of patients with CD20-positive non-Hodgkin lymphoma for treatment with CD20 targeted monoclonal antibodies.

References

1. Fisher RI, Kaminski MS, Wahl RL et al. Tositumomab and iodine-131 tositumomab produces durable complete remissions in a subset of heavily pretreated patients with low-grade and transformed non-Hodgkin's lymphomas. *J Clin Oncol* 2005;23(30):7565-7573
2. Witzig TE. Efficacy and safety of 90Y ibritumomab tiuxetan (Zevalin) radioimmunotherapy for non-Hodgkin's lymphoma. *Semin Oncol* 2003;30(6 Suppl 17):11-16
3. Press OW, Eary JF, Gooley T et al. A phase I/II trial of iodine-131-tositumomab (anti-CD20), etoposide, cyclophosphamide, and autologous stem cell transplantation for relapsed B-cell lymphomas. *Blood* 2000;96(9):2934-2942
4. Kaminski MS, Tuck M, Estes J et al. 131I-tositumomab therapy as initial treatment for follicular lymphoma. *N Engl J Med* 2005;352(5):441-449
5. Maloney DG, Grillo-Lopez AJ, White CA et al. IDEC-C2B8 (Rituximab) anti-CD20 monoclonal antibody therapy in patients with relapsed low-grade non-Hodgkin's lymphoma. *Blood* 1997;90(6):2188-2195
6. Johnson NA, Boyle M, Bashashati A et al. Diffuse large B-cell lymphoma: reduced CD20 expression is associated with an inferior survival. *Blood* 2009;113(16):3773-3780
7. Dayde D, Ternant D, Ohresser M et al. Tumor burden influences exposure and response to rituximab: pharmacokinetic-pharmacodynamic modeling using a syngeneic bioluminescent murine model expressing human CD20. *Blood* 2009;113(16):3765-3772
8. Sharkey RM, Press OW, Goldenberg DM. A re-examination of radioimmunotherapy in the treatment of non-Hodgkin lymphoma: prospects for dual-targeted antibody/radioantibody therapy. *Blood* 2009;113(17):3891-3895
9. Gopal AK, Press OW, Wilbur SM et al. Rituximab blocks binding of radiolabeled anti-CD20 antibodies (Ab) but not radiolabeled anti-CD45 Ab. *Blood* 2008;112(3):830-835
10. Illidge TM, Bayne M, Brown NS et al. Phase 1/2 study of fractionated (131I)-rituximab in low-grade B-cell lymphoma: the effect of prior rituximab dosing and tumor burden on subsequent radioimmunotherapy. *Blood* 2009;113(7):1412-1421
11. Iagaru A, Gambhir SS, Goris ML. 90Y-ibritumomab therapy in refractory non-Hodgkin's lymphoma: observations from 111In-ibritumomab pretreatment imaging. *J Nucl Med* 2008;49(11):1809-1812
12. Conti PS, White C, Pieslor P et al. The Role of Imaging with 111In-ibritumomab Tiuxetan in the Ibritumomab Tiuxetan (Zevalin) Regimen: Results from a Zevalin Imaging Registry. *J Nucl Med* 2005;46(11):1812-1818
13. Visser GW, Klook RP, Gebbinck JW et al. Optimal quality (131I)-monoclonal antibodies on high-dose labeling in a large reaction volume and temporarily coating the antibody with IODO-GEN. *J Nucl Med* 2001;42(3):509-519
14. Tran L, Baars JW, Maessen HJ et al. A simple and safe method for 131I radiolabeling of rituximab for myeloablative high-dose radioimmunotherapy. *Cancer Biother Radiopharm* 2009;24(1):103-110
15. Schaffland AO, Buchegger F, Kosinski M et al. 131I-rituximab: relationship between immunoreactivity and specific activity. *J Nucl Med* 2004;45(10):1784-1790
16. Jilani I, O'Brien S, Manshuri T et al. Transient down-modulation of CD20 by rituximab in patients with chronic lymphocytic leukemia. *Blood* 2003;102(10):3514-3520
17. Cragg MS, Bayne MC, Illidge TM et al. Apparent modulation of CD20 by rituximab: an alternative explanation. *Blood* 2004;103(10):3989-3990
18. Wiseman GA, Leigh B, Erwin WD et al. Radiation dosimetry results for Zevalin radioimmunotherapy of rituximab-refractory non-Hodgkin lymphoma. *Cancer* 2002;94(4 Suppl):1349-1357
19. Rajendran JG, Fisher DR, Gopal AK et al. High-dose (131I)-tositumomab (anti-CD20) radioimmunotherapy for non-Hodgkin's lymphoma: adjusting radiation absorbed dose to actual organ volumes. *J Nucl Med* 2004;45(6):1059-1064
20. Morschhauser F, Illidge T, Huglo D et al. Efficacy and safety of yttrium-90 ibritumomab tiuxetan in patients with relapsed or refractory diffuse large B-cell lymphoma not appropriate for autologous stem-cell transplantation. *Blood* 2007;110(1):54-58
21. Verel I, Visser GW, Vosjan MJ et al. High-quality 124I-labelled monoclonal antibodies for use as PET scouting agents prior to 131I-radioimmunotherapy. *Eur J Nucl Med Mol Imaging* 2004;31(12):1645-1652

Chapter 3.2

The pharmacokinetics of
¹³¹I-rituximab
in a patient
with CD20 positive Non-Hodgkin lymphoma:
evaluation of the effect of radioiodination on
the biological properties of rituximab

Ly Tran

Alwin D.R. Huitema

Wouter V. Vogel

Jos H. Beijnen

Joke W. Baars

Submitted for publication

Abstract

Purpose

To report the pharmacokinetics of ^{131}I -rituximab a patient with a CD20 positive non-Hodgkin lymphoma who has received ^{131}I -rituximab as consolidation treatment after remission induction and to evaluate the effect of radioiodination on the biological properties of rituximab.

Results

The patient was a 65-year-old male with a relapsed CD20 positive follicular non-Hodgkin lymphoma. After induction therapy the patient was in partial remission. Following administration of a diagnostic dose of 185 MBq ^{131}I -rituximab, remaining lesions were identified on the wholebody scans. The patient then received a therapeutic dose of 1000 MBq ^{131}I -rituximab. The uptake by the tumor in the right axilla was 0.17-0.21% of the injected dose. The calculated biological half-life of ^{131}I -rituximab was 684 hrs. This biological half-life corresponded well with the half-life of unlabeled rituximab which was approximately 720 hrs.

Discussion and conclusion

Even though radioiodination of rituximab results in a reduced binding capacity, whole body scans demonstrated localization of ^{131}I -rituximab in the tumor area. This observation supports the specific targeting of ^{131}I -rituximab. The half-life of ^{131}I -rituximab corresponded to the half-life of unlabeled rituximab. Hence, the pharmacokinetics of ^{131}I -rituximab was not relevantly affected by the radioiodination process.

Case report

The patient was a 65-year-old male with a relapsed CD20 positive follicular non-Hodgkin's lymphoma with localization in the lymph nodes of the right axillar and right parasternal region. Skin biopsy of the right axillar showed a transformation to CD20 positive diffuse large B-cell non-Hodgkin lymphoma. The patient received induction therapy of 3 cycles consisting of ifosfamide (3 g/m² day 1, 2), etoposide (100 mg/m² day 1, 2, 3), and rituximab (375 mg/m² intravenously day 1), every 3 weeks. After 2 cycles a partial remission was observed. ¹⁸F-fluorodeoxyglucose (FDG) positron emission tomography (PET) scintigraphy showed a slightly higher metabolic uptake in the right axilla and supraclavicular compared to normal tissue.

Administration of ¹³¹I-rituximab

Prior to administration of both the diagnostic and the therapeutic dose of ¹³¹I-rituximab, the patient received 2.5 mg/kg unlabeled rituximab. The diagnostic dose of 185 MBq ¹³¹I-rituximab confirmed findings of the localization of the lesions on the ¹⁸F-FDG PET scan. The calculated maximum tolerable therapeutic dose was 1875 MBq ¹³¹I-rituximab corresponding to a non-myeloablative maximum tolerated dose of 75 cGy to the total body. To reduce hospitalization to 7 days, a dose of 1000 MBq ¹³¹I-rituximab was ultimately administered.

Pharmacokinetic sampling and analysis

Whole body imaging scans were performed every 24 hrs until discharge of the patient. By delineating regions of interest on the scans (Syngo MI applications, Siemens), tracer accumulation in the lesion as well as the total body retention were estimated.

Blood samples were taken every 24 hours during the residence time in the isolation facility. After discharge, blood samples were taken weekly. Serum rituximab levels were measured by an enzyme-linked immunosorbent assay (ELISA). The lower limit of quantification was 7.8 ng/mL. Possible antibodies against rituximab were measured with a lower limit of quantification of 12 AU/mL.

1 mL heparinized wholeblood was counted for 60 seconds in an automatic gamma counter (Wizard 1480, Perkin Elmer, Waltham, MA, USA). From the radioactivity vs. time curve, based on the time of blood sampling, the effective half-life was estimated. The effective half-life represents the half-life by means of the physical half-life of ¹³¹I (192 hrs) and the biological half-life (biological elimination) of ¹³¹I-rituximab. Subsequently, the biological half-life was determined by:

$$1/t_{1/2,b} = 1/t_{1/2,e} - 1/t_{1/2,p}$$

$t_{1/2,b}$ = biological half-life of ¹³¹I-rituximab

$t_{1/2,p}$ = physical half-life of ¹³¹I (=192 hr)

$t_{1/2,e}$ = effective half-life of ¹³¹I-rituximab

Results

The scans were performed at 24, 48, 72, and 138 hrs after administration of the therapeutic ^{131}I -rituximab dose. Total body retention was respectively 104%, 103%, 92% and 92% of the injected dose. Figure 1 shows the effective decay, the biological decay (corrected for physical decay) and the serum rituximab levels as measured by ELISA. The effective half-life of ^{131}I -rituximab could be derived from figure 1 and was estimated to be 150 hrs. The calculated biological half-life was 684 hrs.

Before administration of the therapeutic dose, the rituximab serum level was 67.8 $\mu\text{g/mL}$. Total amount of ^{131}I -rituximab (2.7 mg) administered was negligible compared to the amount of unlabeled rituximab administered. Therefore, the measured serum concentration was equal to the concentration of unlabeled rituximab. The estimated half-life of unlabeled rituximab was approximately 720 hrs (figure 1).

Uptake in the right axilla was visible on the whole body scans. The determined uptake of ^{131}I -rituximab in the right axilla was between 0.17 and 0.21% of the injected dose.

No antibodies against rituximab were detected. Additionally, at the time of the administration of the therapeutic dose, no B-cells in peripheral blood were present. An elevated thyroid stimulating hormone level was present during 4 weeks after administration of the therapeutic dose of ^{131}I -rituximab. Hematological toxicity was observed during 5 months of follow-up; anemia (grade 1), trombocytopenia (grade 1), neutropenia (grade 3), and leucopenia (grade 3). The lesions remained stable for three months. Hereafter, the lesion in the right axilla increased. Also, destruction of the surrounding skin was observed. The lesion in the right supraclavicular region remained stable. Cytological punction in the right axilla was performed and showed vital CD20 positive transformed follicular non-Hodgin lymphoma. The patient received local radiation therapy of the right axilla and right supraclavicular. The patient deceased 10 months after administration of the ^{131}I -rituximab therapy due to progression of the disease.

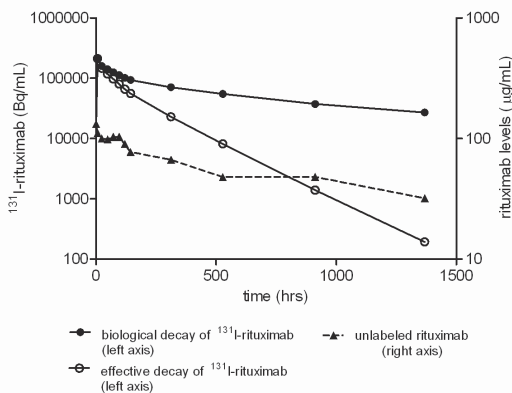


Figure 1 Effective decay and biological decay of ^{131}I -rituximab in time and serum rituximab levels of the presented case.

Discussion

The CD20 antigen is a 33-kDa unglycosylated transmembrane phosphoprotein that is expressed on pre-B, resting, activated, or malignant B cells but that is absent of plasma cells (1). It does not internalize nor does it shed into the blood circulation. Therefore, the CD20 antigen is an ideal target for treatment of B-cell malignancies. Because of their specific targeting, anti-CD20 monoclonal antibodies have already been used for radioimmunotherapy (2-5). By conjugating a radionuclide to a monoclonal antibody specific for the CD20 antigen, radioimmunotherapy offers targeted irradiation to CD20 positive cells by promoting cytotoxic activity by the crossfire-effect to neighboring tumor cells with none or insufficient antigen expression (5).

Radioiodination of rituximab, however, causes deterioration of the binding capacity which also may influence the tumor uptake and the pharmacokinetics. By radiolabeling of rituximab with ^{131}I , iodine atoms are conjugated to rituximab by using Iodogen as an oxidizing agent (6), causing linkage of the iodine to the tyrosine residues (7). Iodination of tyrosines moieties that are involved in a specific biological region of a monoclonal antibody can contribute to the impairment of the binding of a monoclonal antibody to a target antigen (8,9). Consequences of structural changes are reflected by an impairment of the binding capacity, also known as the immunoreactivity (10). Quality control showed that the administered ^{131}I -rituximab had an immunoreactivity of 70% (11).

Next to the immunoreactivity, the biological clearance and activity of rituximab can be affected by the radioiodination. Incubation with Iodogen may also result in heterogeneous oxidation of the amino acid moieties of rituximab. Rituximab, an IgG molecule, consists of two identical Fab regions, and a Fc-region which is glycosylated through asparagine residue 297. The Fc-region expresses interaction sites for ligands that activate clearance mechanisms (12,13). A correlation was found between Fc-region glycosylation and the binding to these ligands (14). A structural change in the glycan moiety could therefore also cause a change in biological clearance and immunogenicity of rituximab.

Although the binding capacity was reduced, specific uptake of the radiolabeled compound was confirmed visually. For this patient, the determined uptake of ^{131}I -rituximab in the tumor (0.17-0.21% of injected dose) was constant for 6 days. In vitro studies have revealed that rituximab depleted CD20 positive B cells via complement dependent cytotoxicity and through antibody dependent cellular toxicity (15). Binding to the target B cell leads to cell apoptosis which would result in elimination of radiolabeled rituximab/B-cell complex, subsequently leading to removal of ^{131}I -rituximab from the tumor site. This would entail that the mechanism of action of rituximab, after radiolabeling with ^{131}I , is still intact. Additionally, the constant

uptake in the tumor site could imply a continuous supply of ^{131}I -rituximab to the tumor site from the circulation.

In conclusion, even though a reduced binding of ^{131}I -rituximab to the CD20 antigen, specific uptake of ^{131}I -rituximab by the tumor was observed. In addition, the radiolabeling of rituximab with ^{131}I using Iodogen as oxidizing agent, did not affect the biological clearance of ^{131}I -rituximab as the half-life of ^{131}I -rituximab corresponded to the half-life of unlabeled rituximab.

Acknowledgements

The authors wish to thank prof. dr. L.A. Aarden, K. van Houten and H. de Vrieze, from the Department of Immunopathology, for their help with the sample analysis.

References

1. Maloney DG, Grillo-Lopez AJ, White CA et al. IDEC-C2B8 (Rituximab) anti-CD20 monoclonal antibody therapy in patients with relapsed low-grade non-Hodgkin's lymphoma. *Blood* 1997;90(6):2188-2195
2. Fisher RI, Kaminski MS, Wahl RL et al. Tositumomab and iodine-131 tositumomab produces durable complete remissions in a subset of heavily pretreated patients with low-grade and transformed non-Hodgkin's lymphomas. *J Clin Oncol* 2005;23(30):7565-7573
3. Witzig TE. Efficacy and safety of 90Y ibritumomab tiuxetan (Zevalin) radioimmunotherapy for non-Hodgkin's lymphoma. *Semin Oncol* 2003;30(6 Suppl 17):11-16
4. Kaminski MS, Zasadny KR, Francis IR et al. Radioimmunotherapy of B-cell lymphoma with [¹³¹I]anti-B1 (anti-CD20) antibody. *N Engl J Med* 1993;329(7):459-465
5. Press OW, Eary JF, Appelbaum FR et al. Phase II trial of 131I-B1 (anti-CD20) antibody therapy with autologous stem cell transplantation for relapsed B cell lymphomas. *Lancet* 1995;346(8971):336-340
6. Fraker PJ, Speck JC, Jr. Protein and cell membrane iodinations with a sparingly soluble chloroamide, 1,3,4,6-tetrachloro-3a,6a-diphrenylglycoluril. *Biochem Biophys Res Commun* 1978;80(4):849-857
7. Bolton AE, HUNTER WM. A new method for labelling protein hormones with radioiodine for use in the radioimmunoassay. *J Endocrinol* 1972;55(2):
8. Nikula TK, Bocchia M, Curcio MJ et al. Impact of the high tyrosine fraction in complementarity determining regions: measured and predicted effects of radioiodination on IgG immunoreactivity. *Mol Immunol* 1995;32(12):865-872
9. Matzku S, Kirchgessner H, Nissen M. Iodination of monoclonal IgG antibodies at a sub-stoichiometric level: immunoreactivity changes related to the site of iodine incorporation. *Int J Rad Appl Instrum B* 1987;14(5):451-457
10. Lindmo T, Boven E, Cuttitta F et al. Determination of the immunoreactive fraction of radiolabeled monoclonal antibodies by linear extrapolation to binding at infinite antigen excess. *J Immunol Methods* 1984;72(1):77-89
11. Tran L, Baars JW, Maessen HJ et al. A simple and safe method for 131I radiolabeling of rituximab for myeloablative high-dose radioimmunotherapy. *Cancer Biother Radiopharm* 2009;24(1):103-110
12. Indik ZK, Park JG, Hunter S et al. Structure/function relationships of Fc gamma receptors in phagocytosis. *Semin Immunol* 1995;7(1):45-54
13. Kim JK, Firan M, Radu CG et al. Mapping the site on human IgG for binding of the MHC class I-related receptor, FcRn. *Eur J Immunol* 1999;29(9):2819-2825
14. Krapp S, Mimura Y, Jefferis R et al. Structural analysis of human IgG-Fc glycoforms reveals a correlation between glycosylation and structural integrity. *J Mol Biol* 2003;325(5):979-989
15. Tobinai K, Kobayashi Y, Narabayashi M et al. Feasibility and pharmacokinetic study of a chimeric anti-CD20 monoclonal antibody (IDEC-C2B8, rituximab) in relapsed B-cell lymphoma. The IDEC-C2B8 Study Group. *Ann Oncol* 1998;9(5):527-534

Chapter 4

^{124}I -rituximab in
patients with
rheumatoid arthritis

Chapter 4.1

The pharmacokinetics of
 ^{124}I -rituximab
as radio-diagnostic
in patients with rheumatoid arthritis

Ly Tran
Wouter V. Vogel
Martin H. van Rijswijk
Huib J. Dinant
Joke W. Baars
Jos H. Beijnen
Alwin D.R. Huitema

Submitted for publication

Abstract

Introduction

Rheumatoid arthritis is a destructive inflammatory joint disorder. Pre- and mature B-cells, characterized by CD20 antigen expression, play an important role in the inflammatory process. Rituximab, a chimeric monoclonal antibody against the CD20 antigen, has been approved since 2006 for the treatment of patients with rheumatoid arthritis. However, not all patients benefit from this treatment. Persistent activity of the disease has been reported despite treatment with rituximab. Imaging of radiolabeled rituximab can be used to monitor the biodistribution of rituximab, and potentially to predict the efficacy of the treatment. In this study, rituximab was radiolabeled with ^{124}I for positron emission tomography (PET) imaging. The aim of this study was to investigate the pharmacokinetics and biodistribution of ^{124}I -rituximab in patients with rheumatoid arthritis, to establish the optimal procedure for PET imaging.

Methods

Eligible patients received 50 MBq ^{124}I -rituximab, corresponding to approximately 1.5 mg rituximab. The first two patients received no pre-treatment with unlabeled rituximab, and no potassium iodide. The other five patients received 2.5 mg/kg unlabeled rituximab several hours prior to the administration of labeled rituximab. These five patients received potassium iodide for three days. Wholebody PET/CT imaging was performed at 10min, 24hrs, and 48hrs post injection. The total body activity, radioactivity in whole blood, and rituximab serum levels were determined.

Results

In the patients who did not receive pre-treatment, rituximab was eliminated from the circulation very fast and images at 10min showed localization of nearly all ^{124}I -rituximab in the spleen, indicating rapid targeting of the normal B-cell population. Scans at 24h and later showed that the uptake in the spleen was largely diminished while the radioactivity accumulated in the thyroid, consistent with induced lysis of the B-cell – tracer complex. Scans of patients pre-treated with unlabeled rituximab showed persistent tracer in the circulation with almost no splenic or bone marrow uptake, and an extended residence time in plasma. Still, accumulation of ^{124}I in the thyroid gland was observed.

Conclusion

^{124}I -rituximab has favorable pharmacokinetics for targeting of (pathological) B-cells and imaging over several days, but only after pre-treatment with unlabeled rituximab. In addition, protection of the thyroid is recommended to prevent uptake of released ^{124}I .

Introduction

Rheumatoid arthritis is a destructive inflammatory disorder, characterized by chronic inflammation in the synovial membrane of affected joints (1). The precise pathogenesis of rheumatoid arthritis is unknown, but it is evident that B-cells play an important role in the inflammatory process (2,3). Pre-B and mature B-cells are characterized by the presence of CD20 antigen, a cell surface nonglycosylated hydrophobic phosphoprotein.

Rituximab is a chimeric anti-CD20 monoclonal antibody that was initially approved for the treatment of low grade or follicular CD20 positive non-Hodgkin lymphoma. By binding to the CD20 antigen, rituximab causes B-cell depletion by induction of apoptosis, complement-mediated lysis, and antibody-dependent cellular toxicity (4). As rituximab binds to the CD20 antigen, imaging with radiolabeled rituximab may reflect the level of CD20 antigen expression at pathological sites. Imaging of the CD20 antigen has already been applied in patients with CD20 positive non-Hodgkin lymphoma for imaging, dosimetric purposes prior to radioimmunotherapy, and for treatment monitoring (5-7).

Since 2006, rituximab has also been approved for the treatment of patients with rheumatoid arthritis who do not respond to tumor necrosis factor antagonists. Randomized controlled trials have demonstrated the efficacy of rituximab in rheumatoid arthritis refractory to other treatments (1,8,9). However, in these three studies, deterioration of the disease was reported in 12-21% of the patients despite treatment with rituximab. The mechanisms that explain the variable efficacy of rituximab treatment are currently not known. As rituximab binds to the CD20 antigen, imaging with radiolabeled rituximab may also represent the level of CD20 antigen expression, and thus B-cell infiltration, in inflamed joints. In addition, visualization of targeting of radiolabeled rituximab to the B-cell population may allow prediction of the efficacy of rituximab treatment.

To assess the disposition of rituximab, monitoring for several days is required. Several approaches for radiolabeling and imaging of rituximab have been published, including labeling with ^{99m}Tc for gamma camera imaging, and ^{89}Zr for positron emission tomography (PET) imaging (7,10). The labeling technique has an impact on the immunoreactivity and possibly the biodistribution of the tracer, and on the image quality that can be achieved. In the study outlined herein, rituximab was labeled with ^{124}I , which enables CD20 antigen imaging with PET, offering wholebody imaging with high sensitivity and spatial resolution in a 3-dimensional and quantitative approach. The half-life of ^{124}I (4.2 days) allows imaging over several days. On the other hand, the relatively long half-life also induces a radiation burden that limits the dose to be administered, and the physical decay properties of ^{124}I are not ideal for PET imaging. It is unknown if the pharmacokinetics of diagnostic doses of ^{124}I -rituximab are favorable for in vivo monitoring of rituximab for several days.

In this study, we investigated the disposition of diagnostic doses of ^{124}I -rituximab in patients with rheumatoid arthritis with or without pretreatment with unlabeled rituximab. Factors that were plausible to influence the biodistribution and pharmacokinetics of ^{124}I -rituximab were investigated to determine the study protocol for optimal imaging of ^{124}I -rituximab in patients with rheumatoid arthritis.

Materials and Methods

Eligible patients were rituximab naive patients with active rheumatoid arthritis as determined by a disease activity score (DAS28) higher than 3.5 (11). Written informed consent was obtained from all patients. The study protocol was approved by the medical ethics committee of the hospital.

Radiolabeling of rituximab with ^{124}I

The radiolabeling procedure and quality control was based on the lodogen radiolabeling procedure, as described earlier for ^{131}I with rituximab (12). In brief, 10 μL of (not-radioactive) Na^{127}I (0.116 mg/mL in 0.05 mol/L NaOH) was added to 185 MBq Na^{124}I solution in 0.02 mol/L NaOH (>740 MBq/mL) (IBA, Louvain-la-Neuve, Belgium). 500 μL rituximab (10 mg/mL) was added. The labeling reaction was initiated by addition of 35 μL 1 mg/mL lodogen (Sigma-Aldrich, St. Louis, MO, USA) in acetonitrile (Merck, Darmstadt, Germany). After 3 minutes, 100 μL 50 mg/mL ascorbic acid (BUFA, Uitgeest, The Netherlands) was added. The reaction was completed after 10 minutes. Purification and buffer exchange was conducted with a tangential flow filtration system (Midgee, GE Healthcare, Diegem, Belgium). Volume was adjusted to 20 mL, followed by sterile filtration using a sterile filter (0.2 μm , Sartorius, Goettingen, Germany). The final formulation consisted of approximately 120 MBq ^{124}I -rituximab in 20 mL of 5 mg/mL ascorbic acid in 0.9% NaCl (Braun Medical, Melsungen, Germany).

Tracer administration

The first two patients did not receive any pretreatment. The other 5 patients received 2.5 mg/kg unlabeled rituximab several hours prior to labeled rituximab according to local treatment protocols. All patients received acetaminophen 1000 mg orally and clemastine 2 mg intravenously as premedication on the day of rituximab administration, to prevent infusion reactions. All patients received 50 MBq ^{124}I -rituximab intravenously as a bolus injection. Patients received a daily oral dose of 200 mg potassium iodide for 3 days.

PET imaging

Wholebody PET imaging was performed at 10min, 24h, 48h, and if possible, 72-96h post injection, using a hybrid PET/CT scanner (Gemini TF, Philips, Cleveland,

USA). Images were acquired from top to toes, with 1:30 minutes per bedposition in the body and 1:00 minutes per bedposition in the legs, for a total acquisition time of about 30 minutes. Images were reconstructed with optimized settings for ^{124}I , with attenuation correction based on CT images. Accompanying low-dose CT images were acquired at all imaging time points, scan parameters included 40 mAs with dose optimization, 5 mm slice thickness and spacing, and no oral or intravenous contrast. Image sets were fused and visualized in 3-dimensional orthogonal slices using the Osirix software (13) on an Apple Mac Pro system (Apple, USA).

Total body activity

Quantification of the total amount of ^{124}I -rituximab in the body is not straightforward due to the physical decay properties of ^{124}I . Besides a positron, ^{124}I also emits photons at 602 keV (abundance 60%) and 722 keV (abundance 10%). The energy window of the PET/CT scanner was not narrow enough to exclude these photons from detection, and thus these photons contributed to the scatter and coincidence events. These extra scatter and coincidences had opposing effects on the measured counts. Scatter resulted in an underestimation of the measured counts, extra coincidences in an overestimation (14,15). Dependent on scanner and, more importantly, the used algorithms to correct for scatter and randoms, the net result could be an under- or overestimation of the measured counts. On condition that the total number of measured counts from scan to scan was not too large, the above mentioned effects were both proportional to the injected activity (14,15). Because of this proportionality, it was possible to make a reliable estimation of the relative change in the activity over time per patient. To this end, per patient the relative change of the total activity from the first scan was calculated. For the total activity, all the voxels within the field of view (FOV) were summed. Data was processed using Osirix (13). Contribution of noise outside the contours of the body was negligible (less than 0.5 % of the voxel values in the body).

Pharmacokinetic blood sampling and analysis

Blood samples were taken before administration of the infusion with 2.5 mg/kg unlabeled rituximab, before administration of ^{124}I -rituximab, and before each scan.

Radioactive measurements

1 mL heparinized blood was counted for 60 seconds in an automatic gamma counter (Wizard 1480, Perkin Elmer, Waltham, MA, USA). The acquired data, expressed in counts per minute, were corrected for physical decay to the time of administration. The data obtained 10 minutes post injection was set at 100%.

Rituximab serum levels and antibodies against rituximab

Rituximab concentrations in serum were measured by an enzyme-linked immunosorbent assay. The assay was designed and performed as described by Damen et al for the monoclonal antibody trastuzumab under identical conditions (16). In brief, anti-idiotypic antibodies raised in rabbits immunized with F(ab)₂ fragments of rituximab were coated on Maxisorp plates (Nunc, Roskilde, Denmark). After washing, patient sera, diluted in high performance ELISA buffer (HPE, Sanquin, Amsterdam, The Netherlands), were incubated with biotinylated rabbit anti-idiotypic IgG. Subsequently, streptavidin–poly-horseradishperoxidase (Sanquin, Amsterdam, The Netherlands) was added. The samples were allowed to incubate for 30 minutes. After three washing steps, (3,5,3',5')-tetramethylbenzidine (TMB) ELISA peroxidase substrate (Uptima, Interchim, Montluçon, France) was added. The reaction was stopped by addition of 100 µL 2 M H₂SO₄ (Merck, Darmstadt, Germany). Rituximab levels were quantified by measuring the absorbance at 450 nm against a calibration curve. The minimum quantifiable concentration was 7.8 ng/mL. Samples above 5,000 ng/mL were diluted 10 times with HPE buffer. Samples above 50,000 ng/mL were diluted 100 times with HPE buffer. The accuracy was 12.7% and 5.78% for 10 and 100 times dilutions, respectively and the precision was 7.87% and 10.7% for the 10 and 100 times dilutions, respectively.

Antibodies against rituximab were measured by an antigen-binding test which as earlier described for adalimumab (17). Briefly, serum was incubated with sepharose-immobilised protein A (Pharmacia/GE Healthcare, Uppsala, Sweden) in Freeze buffer (Sanquin, Amsterdam, the Netherlands). Non-bound serum components were removed before ¹²⁵I labeled F(ab)₂ fragments of rituximab were added. After washing bound radioactivity was compared with a reference serum.

Results

Imaging

In the first two patients (patient 1 and 2) who did not receive pretreatment with unlabeled rituximab, images at 10min showed localization of nearly all radioconjugate in the spleen and to a lesser extent bone marrow, indicating very rapid targeting of the B-cell population. Scans at 24 hrs and later showed that the uptake in the spleen was largely diminished while the radioactivity accumulated in the thyroid (figure 1), indicating quick lysis of the B-cell-tracer complex. Scans of patients predosed with unlabeled rituximab (2.5 mg/kg) showed persistent tracer availability in the central circulation for multiple days, with almost no splenic uptake. In addition, scans performed at 72 hrs and later showed some accumulation of radioactivity in the thyroid gland.

Total body activity

Figure 2 depicts the total body activity in time. Patient 1 and 2 showed a rapid decline of total body activity within 24 hrs. 48 hrs after administration of the tracer, the remaining total body activity was only 36% for these patients. For the pre-treated patients, the total body activity 48 hrs post-injection ranged from 67-81%.

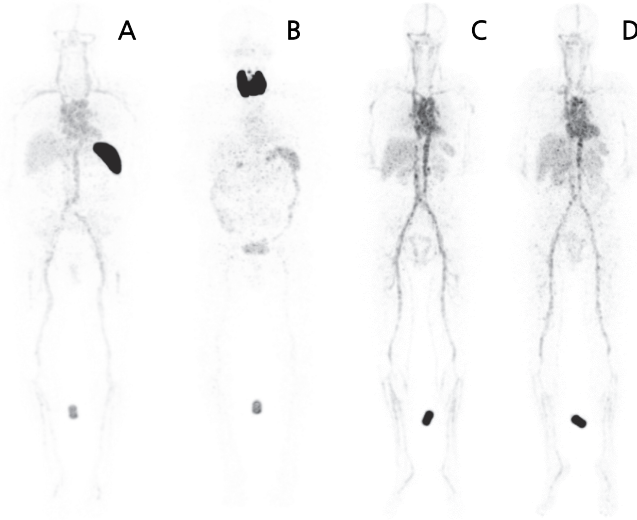


Figure 1 Image of patient 1 who was not pre-treated with unlabeled rituximab.

(A) 10 min after administration of ^{124}I -rituximab showed localization of nearly all radioconjugate in the spleen.

(B) 24 hrs after administration of ^{124}I -rituximab showed the uptake in the spleen was largely diminished while the radioactivity accumulated in the thyroid.

Images of patient 4 who was pre-treated with unlabeled rituximab showed persistent tracer availability in the central circulation for multiple days

(C) 10 min after administration of ^{124}I -rituximab,

(D) 24 hrs after administration of ^{124}I -rituximab

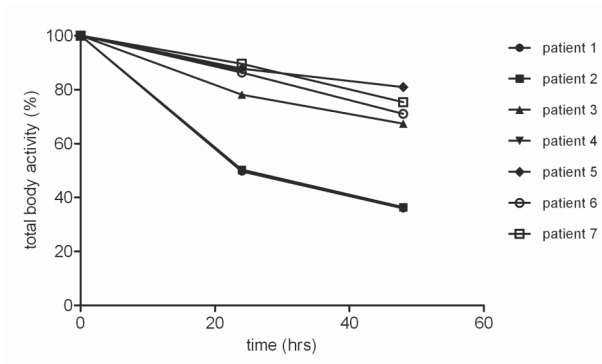


Figure 2 Total body activity, as percentage of the first analysis at 10 minutes set at 100%, in time (hrs)

Pharmacokinetic analysis

Radioactive measurements

Figure 3 shows the radioactivity measurements of whole blood in time (corrected for physical decay). Since free iodine is rapidly cleared from the circulation by the thyroid gland or renal excretion, this represents the biological elimination of ^{124}I -rituximab from the circulation. For patient 1 and 2, who received no pretreatment, rapid elimination within 24 hrs was observed consistent with the whole body imaging. The remaining radioactivity at 24 hrs post-injection was 15 and 16%, for patient 1 and 2 respectively. For the other patients, who did receive pretreatment, the remaining activity in the circulation at 24 hrs post injection ranged from 55-77%. For patient 3 and 4, data up to 120 hrs were available which allowed calculation of the biological half-life. The biological half-life of ^{124}I -rituximab of patient 3 was calculated to be 187 hrs, and for patient 4 at 267 hrs.

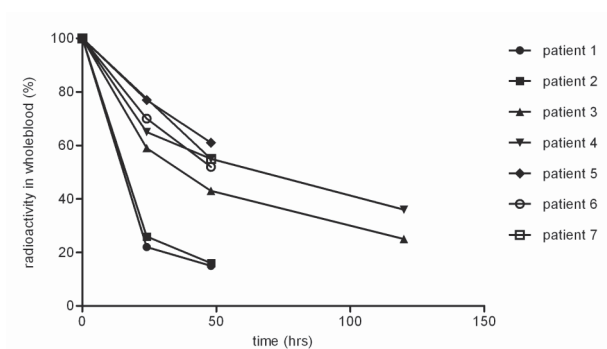


Figure 3 Radioactivity, as percentage of the first analysis at 10 minutes set at 100%, in whole blood in time (hrs)

Rituximab serum levels and antibodies against rituximab

The total amount ^{124}I -rituximab administered (approximately 1.5 mg) was negligible compared to the amount of unlabeled rituximab administered. Therefore, the measured serum concentration can be considered equal to the concentration of unlabeled rituximab (figure 4). Patient 1 and 2 did not receive pre-treatment with unlabeled rituximab, and therefore the rituximab levels of these patients were not detectable. The serum rituximab levels of patients 3-7 ranged from 31.5 to 60.8 $\mu\text{g}/\text{mL}$ at 24 hrs after administration. The half-life of rituximab for patient 3 was 267 hrs. Patient 4 had high levels of rituximab, and the half-life of rituximab was calculated to be 346 hrs. For all patients, no antibodies against rituximab were detected.

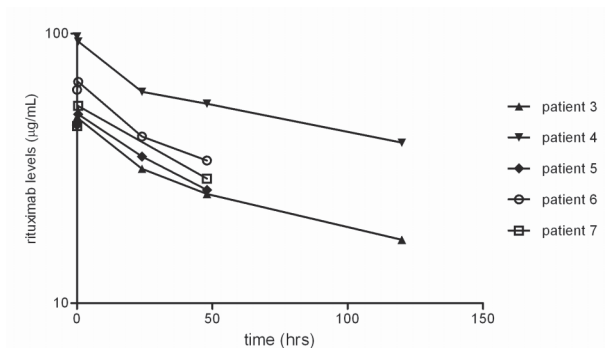


Figure 4 Rituximab serum levels ($\mu\text{g/mL}$) in time (hrs)

Discussion and conclusion

In this study, 50 MBq ^{124}I -rituximab was administered to seven patients with rheumatoid arthritis. The first two patients were not pre-treated with unlabeled rituximab. For these patients, total body activity as well as measurements in whole blood showed a rapid decrease within 24 hrs after administration of ^{124}I -rituximab. Images at 10 minutes demonstrated that nearly all administered ^{124}I -rituximab was already sequestered in the spleen. This biological behavior prevents adequate targeting of pathological B-cell populations that must be reached via the extravascular fluid pool. Therefore, the biodistribution of ^{124}I -rituximab was not suitable for imaging of rheumatoid arthritis without specific additional measures.

The spleen is a lymphatic organ interposed in the circulation, enriched with CD20 positive B-cells. By binding to the CD20 antigen, rituximab causes antigen mediated elimination by induction of apoptosis, complement-mediated lysis, and antibody-dependent cellular toxicity (11). Elimination of B-cells would also lead to destruction of bound ^{124}I -rituximab, resulting in deiodination and excretion of unbound iodine (18). Thus, specific measures are required to prevent splenic elimination of ^{124}I -rituximab.

CD20 antigen imaging has been applied in patients with CD20 positive non-Hodgkin's lymphoma for tumor imaging, dosimetric purposes prior to radioimmunotherapy, and for treatment monitoring (5-7). In this patient category, several studies have shown improved targeting and extended residence time of the radiolabeled compound by pre-treatment with the unlabeled compound. A pre-treatment dose of 2.5 mg/kg has been shown to have suitable pharmacokinetics, and to result in a more favorable biodistribution of the tracer in several studies (19-22).

As far as we know, the pharmacokinetics of rituximab with a single pretreatment dosage have not been reported before. Prior observed half-lives of rituximab in patients with rheumatoid arthritis were based on the standard treatment dosage (1000 mg on day 1 and 15) (23,24). For patients 3 and 4, of whom longer

measurements were available, the half-lives of unlabeled rituximab were calculated to be 267 and 346 hrs respectively.

In line with these findings, our data of the pre-treated patients also showed a prolonged residence time of the radiolabeled rituximab, as compared to patients without pre-treatment. We consider the measured half-life in plasma > 200 hours sufficient to allow adequate biodistribution for targeting of pathological B-cell populations.

The estimated half-lives of radiolabeled rituximab were shorter than the calculated half-lives of unlabeled rituximab. Another explanation may be structural changes of rituximab by the radiolabeling procedure, where ^{124}I atoms are introduced into the molecular structure of the antibody. Consequences of structural changes may be reflected by an impairment of the binding capacity, also known as the immunoreactivity (25). Besides immunoreactivity, the biological clearance and activity of rituximab can be affected due to the radiolabeling by modification of functional regions of the antibody. The Fc-region of a monoclonal antibody is glycosylated through asparagine residue 297. The Fc-region expresses interaction sites for ligands that activate clearance mechanisms (26,27). A correlation was found between Fc-region glycosylation and the binding to these ligands (28). A structural change in the glycan moiety could therefore also cause a change in biological clearance and immunogenicity of labeled rituximab.

Quality control of ^{124}I -rituximab showed a preservation of the binding capacity of 70% in our radiolabeled product, which is sufficient for a satisfactory binding to the CD20 antigen (12). In addition, the whole blood radioactivity measurements of ^{124}I -rituximab showed that the biological half-life of the radioconjugate was sufficient for imaging over several days.

Although pre-treatment minimizes splenic uptake and rapid lysis of the tracer, considerable deiodination of ^{124}I -rituximab has still to be taken into consideration. The presence of unbound ^{124}I results in poor-quality images due to the high background. But moreover, unbound radioactivity gives unnecessary radiation dose to the patient. Therefore, thyroid protection is considered necessary.

In conclusion, we have demonstrated that ^{124}I -rituximab has favorable pharmacokinetics for targeting of pathological B-cells and imaging over several days, but only after pre-treatment with unlabeled rituximab. In addition, protection of the thyroid is recommended to prevent uptake of deconjugated ^{124}I . Further research has to be performed to establish if ^{124}I -rituximab is clinically relevant for imaging of CD20 antigen expression in patients with rheumatoid arthritis.

Acknowledgements

The authors wish to thank prof. dr. L.A. Aarden, K. van Houten and H. de Vrieze, from the Department of Immunopathology, for their help with the sample analysis.

References

1. Edwards JC, Szczepanski L, Szechinski J et al. Efficacy of B-cell-targeted therapy with rituximab in patients with rheumatoid arthritis. *N Engl J Med* 2004;350(25):2572-2581
2. Zhang Z, Bridges SL, Jr. Pathogenesis of rheumatoid arthritis. Role of B lymphocytes. *Rheum Dis Clin North Am* 2001;27(2):335-353
3. Voswinkel J, Weisgerber K, Pfreundschuh M et al. The B lymphocyte in rheumatoid arthritis: recirculation of B lymphocytes between different joints and blood. *Autoimmunity* 1999;31(1):25-34
4. Maloney DG, Grillo-Lopez AJ, Bodkin DJ et al. IDEC-C2B8: results of a phase I multiple-dose trial in patients with relapsed non-Hodgkin's lymphoma. *J Clin Oncol* 1997;15(10):3266-3274
5. Rajendran JG, Fisher DR, Gopal AK et al. High-dose (131I)-tositumomab (anti-CD20) radioimmunotherapy for non-Hodgkin's lymphoma: adjusting radiation absorbed dose to actual organ volumes. *J Nucl Med* 2004;45(6):1059-1064
6. Wiseman GA, Leigh B, Erwin WD et al. Radiation dosimetry results for Zevalin radioimmunotherapy of rituximab-refractory non-Hodgkin lymphoma. *Cancer* 2002;94(4 Suppl):1349-1357
7. Gmeiner ST, Fettich J, Zver S et al. 99mTc-labelled rituximab, a new non-Hodgkin's lymphoma imaging agent: first clinical experience. *Nucl Med Commun* 2008;29(12):1059-1065
8. Emery P, Fleischmann R, Filipowicz-Sosnowska A et al. The efficacy and safety of rituximab in patients with active rheumatoid arthritis despite methotrexate treatment: results of a phase IIB randomized, double-blind, placebo-controlled, dose-ranging trial. *Arthritis Rheum* 2006;54(5):1390-1400
9. Cohen SB, Emery P, Greenwald MW et al. Rituximab for rheumatoid arthritis refractory to anti-tumor necrosis factor therapy: Results of a multicenter, randomized, double-blind, placebo-controlled, phase III trial evaluating primary efficacy and safety at twenty-four weeks. *Arthritis Rheum* 2006;54(9):2793-2806
10. Muylle K, Azerad MA, Perk LR, Meuleman N, Delrieu V, Ghanem G, Bourgeois P, Vanderlinden B, van Dongen GA, Flamen P, Bron D. Immuno-PET/CT imaging with ⁸⁹Zr-rituximab as a prelude for radioimmunotherapy with ⁹⁰Y-rituximab in patients with relapsed CD20+ B-cell non-Hodgkin's lymphoma. *Ann Oncol* 2008;19 Supp 4:179-180 (Abstract)
11. van der Heijde DM, Jacobs JW. The original "DAS" and the "DAS28" are not interchangeable: comment on the articles by Prevo et al. *Arthritis Rheum* 1998;41(5):942-945
12. Tran L, Baars JW, Maessen HJ et al. A simple and safe method for 131I radiolabeling of rituximab for myeloablative high-dose radioimmunotherapy. *Cancer Biother Radiopharm* 2009;24(1):103-110
13. Rosset A, Spadola L, Ratib O. OsiriX: an open-source software for navigating in multidimensional DICOM images. *J Digit Imaging* 2004;17(3):205-216
14. Gregory RA, Hooker CA, Partridge M et al. Optimization and assessment of quantitative 124I imaging on a Philips Gemini dual GS PET/CT system. *Eur J Nucl Med Mol Imaging* 2009;36(7):1037-1048
15. Jentzen W, Weise R, Kupferschlager J et al. Iodine-124 PET dosimetry in differentiated thyroid cancer: recovery coefficient in 2D and 3D modes for PET(CT) systems. *Eur J Nucl Med Mol Imaging* 2008;35(3):611-623
16. Damen CW, de Groot ER, Heij M et al. Development and validation of an enzyme-linked immunosorbent assay for the quantification of trastuzumab in human serum and plasma. *Anal Biochem* 2009;391(2):114-120
17. Bartelds GM, Wijbrandts CA, Nurmohamed MT et al. Clinical response to adalimumab: relationship to anti-adalimumab antibodies and serum adalimumab concentrations in rheumatoid arthritis. *Ann Rheum Dis* 2007;66(7):921-926
18. Cragg MS, Bayne MC, Illidge TM et al. Apparent modulation of CD20 by rituximab: an alternative explanation. *Blood* 2004;103(10):3989-3990
19. Press OW, Eary JF, Badger CC et al. Treatment of refractory non-Hodgkin's lymphoma with radiolabeled MB-1 (anti-CD37) antibody. *J Clin Oncol* 1989;7(8):1027-1038
20. Kaminski MS, Zasadny KR, Francis IR et al. Radioimmunotherapy of B-cell lymphoma with [131I]anti-B1 (anti-CD20) antibody. *N Engl J Med* 1993;329(7):459-465
21. Kaminski MS, Zasadny KR, Francis IR et al. Iodine-131-anti-B1 radioimmunotherapy for B-cell lymphoma. *J Clin Oncol* 1996;14(7):1974-1981
22. Knox SJ, Goris ML, Trisler K et al. Yttrium-90-labeled anti-CD20 monoclonal antibody therapy of recurrent B-cell lymphoma. *Clin Cancer Res* 1996;2(3):457-470

23. Ng CM, Bruno R, Combs D et al. Population pharmacokinetics of rituximab (anti-CD20 monoclonal antibody) in rheumatoid arthritis patients during a phase II clinical trial. *J Clin Pharmacol* 2005;45(7):792-801
24. Breedveld F, Agarwal S, Yin M et al. Rituximab pharmacokinetics in patients with rheumatoid arthritis: B-cell levels do not correlate with clinical response. *J Clin Pharmacol* 2007;47(9):1119-1128
25. Lindmo T, Boven E, Cuttitta F et al. Determination of the immunoreactive fraction of radiolabeled monoclonal antibodies by linear extrapolation to binding at infinite antigen excess. *J Immunol Methods* 1984;72(1):77-89
26. Indik ZK, Park JG, Hunter S et al. Structure/function relationships of Fc gamma receptors in phagocytosis. *Semin Immunol* 1995;7(1):45-54
27. Kim JK, Firan M, Radu CG et al. Mapping the site on human IgG for binding of the MHC class I-related receptor, FcRn. *Eur J Immunol* 1999;29(9):2819-2825
28. Krapp S, Mimura Y, Jefferis R et al. Structural analysis of human IgG-Fc glycoforms reveals a correlation between glycosylation and structural integrity. *J Mol Biol* 2003;325(5):979-989

Chapter 4.2

CD20 antigen imaging with ^{124}I -rituximab PET/CT in patients with rheumatoid arthritis

Ly Tran

Alwin D.R. Huitema

Martin H. van Rijswijk

Huib J. Dinant

Joke W. Baars

Jos H. Beijnen

Wouter V. Vogel

Abstract

Introduction

Rheumatoid arthritis is an autoimmune disorder characterized by chronic inflammation of the synovial membrane. B-cells play a major role in the inflammatory process of rheumatoid arthritis. As the CD20 antigen is exclusively expressed on B-cells, the CD20 antigen is a specific molecular target for B-cell populations. Visualization of the CD20 antigen expression could provide a tool to localize sites of inflammation and could be of additive value in the diagnosis, and subsequently, in the treatment follow-up of patients with rheumatoid arthritis. In this study, an approved chimeric anti-CD20 monoclonal antibody, rituximab (Mabthera®), was radiolabeled with ¹²⁴I. We report the first results of ¹²⁴I-rituximab PET/CT in patients with rheumatoid arthritis.

Methods

Eligible patients received 50 MBq ¹²⁴I-rituximab corresponding with approximately 1.5 mg rituximab. Wholebody PET/CT imaging was performed at 10min, 24hrs, 48hrs and 72-96hrs post injection. Images were evaluated primarily on a visual basis and were correlated with disease activity as determined by physical examination and clinical measures.

Results

Joints with visually detectable targeting of ¹²⁴I-rituximab were observed in 4 out of 5 evaluable patients. Only the images at 24hrs and later showed accumulation in joints, indicating that the visualized signal represented active targeting of rituximab to the CD20 antigen. Several images showed CD20 positive B-cell infiltration in joints which were clinically normal, while a few clinically diagnosed arthritis localizations were not visualized. This discrepancy suggests that infiltration of CD20 positive B-cells in synovium is a phenomenon that is at least partially independent of clinical inflammation. The level of uptake in joints was generally very low, representing less than 0.5% of the injected dose.

Conclusion

We have shown the feasibility of CD20 antigen imaging using ¹²⁴I-rituximab in patients with rheumatoid arthritis. Further research is needed to elucidate the clinical significance of demonstrated B-cell infiltration in rheumatic joints.

Introduction

Rheumatoid arthritis is a destructive inflammatory joint disorder characterized by chronic inflammation of the synovial membrane. Clinical manifestations include pain, tenderness and symmetrical swelling of joints, and eventually loss of function (1). Determination of the clinical status of rheumatoid arthritis and therefore the treatment strategy is primarily based on clinical evaluation (2,3). Studies have shown the additive value of imaging modalities, e.g. computed tomography (CT), magnetic resonance imaging (MRI), and ultrasound (US). These anatomical imaging modalities provide information about bone structure and soft tissue abnormalities, with superior sensitivity compared to conventional radiography, but are limited by lack of specificity with regard to activity of inflammation (4,5). The radiolabeled glucose analogon ^{18}F -fluorodeoxyglucose (FDG) accumulates in activated macrophages and granulocytes, and thus uptake ^{18}F -FDG on a positron emission tomography (PET) scan reflects joint inflammation. However, uptake of ^{18}F -FDG is increased in infectious and degenerative forms of osteoarthritis as well, and therefore is not specific for rheumatoid arthritis (6).

B-cells are involved in the inflammatory process of rheumatoid arthritis (7,8). The precise contribution of B-cells is not fully elucidated, but it is known that the synovial membrane in patients with rheumatoid arthritis contains an abundance of B-cells. B-cell development occurs through several stages, accompanied by the evolvement of different B-cell membrane receptors. Both pre-B and mature B-cells express the CD20 antigen, a cell surface nonglycosylated hydrophobic phosphoprotein, that is not expressed in other cell populations (9). Therefore, CD20 is a specific molecular target for certain B-cell populations. Rituximab (Mabthera®) is a chimeric anti-CD20 monoclonal antibody that induces complement activation and subsequent cell death after binding to its ligand. It was originally approved for the treatment of low grade or follicular CD20 positive non-Hodgkin lymphoma. Rituximab has also been applied successfully to eradicate B-cell populations in rheumatoid arthritis, aiming to reduce inflammation and to limit joint damage (10-12). Since 2006, rituximab has been FDA approved for the treatment of patients with rheumatoid arthritis non-responsive to tumor necrosis factor antagonists.

The level of expression of the CD20 antigen in joints may be of clinical relevance in patients with rheumatoid arthritis, providing a tool to localize sites of inflammation, and possibly indicating the degree of inflammation by reflecting the local number of infiltrating B-cells. In addition, the level of CD20 expression in inflamed joints may be predictive for the efficacy of subsequent treatment with rituximab, as it represents the binding target for the antibody.

Antibodies and their biodistribution can be visualized in vivo by labeling them with a radionuclide suitable for imaging (13,14). Radiolabeled anti-CD20 ligands have been linked to gamma emitting radionuclides, mostly iodine isotopes such as ^{123}I or ^{131}I (15-17). Hence, application of these radioconjugates is limited to gamma-camera

imaging, with inherently limited spatial resolution, overprojection and poor quantification. For this study, rituximab was labeled with ^{124}I for PET imaging, a technique that allows wholebody imaging with better sensitivity and spatial resolution, in a 3-dimensional and quantitative approach. Furthermore, using a combined PET and computed tomography (PET/CT) system, the biodistribution can be correlated with anatomical structures.

Aim

The aim of this study was to determine the feasibility of wholebody PET/CT imaging of CD20 antigen expression in rheumatoid arthritis using ^{124}I labeled rituximab.

Methods

Patients

Eligible patients were rituximab naive patients with active rheumatoid arthritis as measured by a disease activity score (DAS28) greater than 3.5 (18). Between January 2009 and June 2009, 6 patients were included. Informed written consent was obtained from all patients. The study protocol was approved by the medical ethics committee.

Radiolabeling rituximab with ^{124}I

The production and quality control of ^{124}I labeled rituximab based on the radiolabeling procedure of rituximab with ^{131}I as described earlier (19). In brief, 10 μL of not-radioactive Na^{127}I (0.116 mg/mL in 0.05 mol/L NaOH) was added to 185 MBq Na^{124}I solution. 500 μL rituximab (10 mg/mL) was then added. The labeling reaction was initiated by addition of 35 μL 1 mg/mL Iodogen in acetonitrile. After 3 minutes, 100 μL 50 mg/mL ascorbic acid was added. The reaction was completed after 10 minutes. Purification and buffer exchange was conducted with a tangential flow filtration system (Midgee, GE Healthcare, Diegem, Belgium), followed by sterile filtration using a sterile filter (0.2 μm , Sartorius, Goettingen, Germany). The final formulation consisted of ^{124}I -rituximab in 5 mg/mL of ascorbic acid in 0.9% NaCl.

Tracer administration

Patients received acetaminophen 1000 mg orally and clemastine 2 mg intravenously as premedication on the day of rituximab administration, to prevent infusion reactions. Patients received 2.5 mg/kg unlabeled rituximab several hours prior to labeled rituximab, to block targeting of the normal B-cell populations in the bone marrow and spleen (20). Subsequently, patients received 50 MBq ^{124}I -rituximab by an intravenous bolus injection. For thyroid protection, a daily oral dose of 200 mg potassium iodide was given to the patient for 3 days.

PET/CT image acquisition

Wholebody PET/CT imaging was performed at 10min, 24hrs, 48hrs, and 72-96hrs post injection, using a hybrid PET/CT scanner (Gemini TF, Philips, Cleveland, USA). Images were acquired from top to toes, with 1:30 minutes per bedposition of the body and 1:00 minutes per bedposition of the legs, for a total acquisition time of about 30 minutes. Images were reconstructed with optimized settings for ^{124}I , with attenuation correction based on CT images. Accompanying low-dose CT images were acquired at all imaging time points, scan parameters included 40 mAs with dose optimization, 5 mm slice thickness and spacing, and no oral or intravenous contrast was used. Image sets were fused and visualized in 3-dimensional orthogonal slices using the Osirix software (21) on an Apple Mac Pro system (Apple, USA).

Clinical evaluation

Physical examination, conducted by the rheumatologist, consisted of a tender joint and a swollen joint count of 28 joints. The erythrocyte sedimentation rate (ESR), the assessment of general health on a visual analog scale, and the tender en swollen joint count were used to determine the DAS28 (18).

Image evaluation

The images were evaluated primarily on a visual basis. Uptake of the tracer in joints was correlated with active joints as determined using physical examination, conducted by the rheumatologist. The level of uptake in joints was calculated by determination of the counts within a region of interest, and was expressed as percentage of the total body counts at 10 minutes after administration of the tracer.

Results

In total, 6 patients were included, with a mean age of 56 years (range 50-63 years). One patient was not able to undergo imaging due to adverse events after administration of the unlabeled rituximab (pyrexia, rigor, hypotension, and nausea). Another patient had an adverse event during post-infusion observation of unlabeled rituximab (hypotension, syncopation) but this patient recovered quickly and the administration of ^{124}I -rituximab and imaging could be completed according to schedule. Thus, data of 5 patients were ultimately available for evaluation. Table 1 shows an overview of patient characteristics and the study results.

Joints with visually detectable targeting of ^{124}I -rituximab were found in 4 out of 5 patients (table 1). Images shortly after administration (bloodpool phase) did not show accumulation of the tracer in joints, while images at 24hrs and later did show accumulation in joints, indicating that the visualized signal represents active targeting of the antibody to the CD20 epitope and not mere perfusion (figure 1). The uptake in joints relative to background activity was similar in images after 24hrs, 48hrs and

later. Combined PET/CT images allowed confirmation of localization of the tracer in thickened synovia in joints (figure 2). The presence of CD20 positive B-cells in joints, as represented by ^{124}I -rituximab binding, correlated only partially with active joints as determined by physical examination. ^{124}I -rituximab PET demonstrated CD20 expression in several joints that were not clinically inflamed, while a few clinically diagnosed localizations did not show tracer uptake (table 1). The level of uptake in joints was generally very low, representing no more than 0.5% of the injected dose, in all detected joints at all timepoints (data not shown).

Table 1 Patient characteristics, disease activity parameters, and specific uptake of ^{124}I -rituximab

Patient	Age	Gender	ESR	VAS	DAS28	Active joints	Specific uptake of ^{124}I -rituximab
1	55	m	110	75	6.89	R shoulder, R elbow, R wrist, <u>R ankle</u> , B hands	R shoulder, R elbow, <u>R knee</u> , <u>B wrists</u>
2	56	f	24	63	5.48	<u>B wrists</u> , <u>B hands/fingers</u> , <u>B ankles</u> , <u>B feet/toes</u>	none
3	63	f	64	75	6.52	<u>B knees</u> , B hands/fingers, B ankles	<u>B shoulders</u> , <u>B elbows</u> , <u>B wrists</u> , B hands, B feet
4	52	m	36	70	6.05	B wrists, B hands/fingers, B ankles, B feet/toes	<u>R shoulder</u> , <u>B elbows</u> , B wrists, B hands/fingers, <u>B ankles</u> , B feet/toes
5	61	f	24	80	5.86	L knee, <u>B hands/fingers</u>	L knee

R = right side, L = left side, B = both sides.

Underlined = unique finding, not detected by other method of investigation.

ESR = Erythrocyte sedimentation rate (mm/hr), VAS = visual analog scale (0-100)

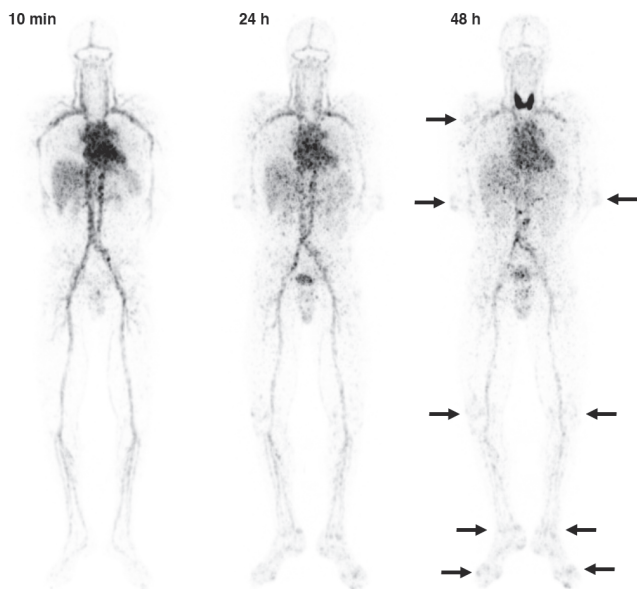


Figure 1

Wholebody PET images of patient 4, at 10 min, 24 hrs and 48 hrs post-injection.

The arrows indicate limited but specific accumulation of ^{124}I -rituximab in joints with B-cell infiltration

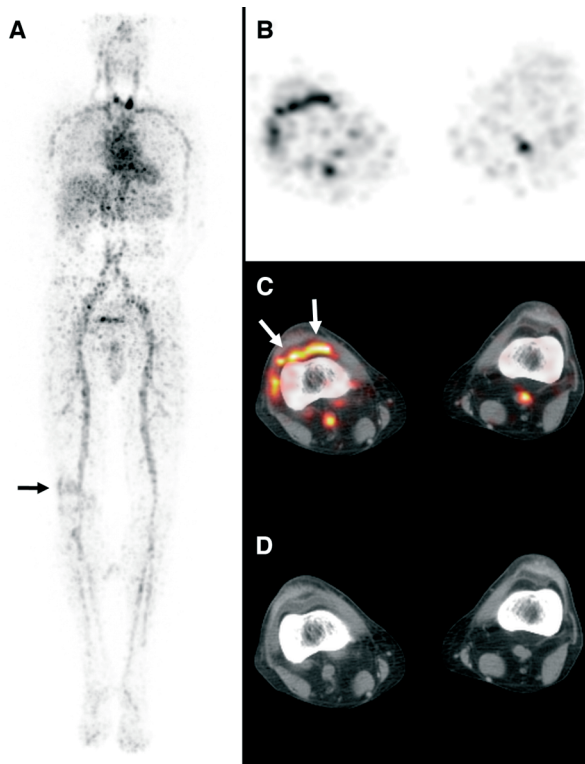


Figure 2

(A) Wholebody PET image 24 hrs post-injection of patient 1, focused on the right knee; Transverse slice through the knees of
 (B) PET;
 (C) PET/CT;
 (D) CT images. Arrows indicate CD20 positive B cell infiltration in the thickened synovia of the right knee.

Discussion

Five patients received ^{124}I -rituximab PET for whole body imaging of rheumatoid disease activity. The locations of tender joints were visually compared to scans after administration of ^{124}I -rituximab. Several images showed CD20 positive B-cell infiltration in joints which were not established by the rheumatologist as actively inflamed. On the other hand, the images could not confirm all the locations of the active joints. In addition, scans of patient 2 did not show any specific uptake.

Quantitative count of swollen and tender joints is the primary measure to evaluate patients with rheumatoid arthritis. However, there are some limitations of physical examination, including a poor reproducibility (3,22,23). Additionally, a number of studies indicated that swollen joint and tender joint counts are not very sensitive, at least compared to ultrasound (24,25). Ultrasound, however, has the disadvantage of lacking specificity (25). Therefore, a more specific approach is required, preferably in a wholebody approach. The results from this feasibility study suggest that ^{124}I -rituximab PET/CT can detect inflamed joints in rheumatoid arthritis, with a seemingly reasonable sensitivity, and with a thusfar unknown specificity. Further investigations would be required to determine the diagnostic accuracy of this procedure, and to establish the clinical value of the findings.

There may be several reasons why the ^{124}I rituximab PET findings do not always correlate with clinical findings. Rituximab is an IgG monoclonal antibody with a size of approximately 150 kDa. Possibly, the accessibility of certain joints is hindered for such a large molecule. Another possibility would be the absence of CD20 positive B-cells in certain active joints. Plasma cells are differentiated from B-cells and produce immunoglobulins such as rheumatoid factor, of which high levels have been associated with more aggressive articular disease, a higher frequency of extraarticular manifestations and increased mortality (26,27). Plasma cells lack CD20 antigen expression, and therefore cannot be visualized by ^{124}I -rituximab. Arthroscopic biopsy of joint synovium will be required for elucidation of this issue.

Rituximab is primarily used for the treatment of patients with CD20 positive non-Hodgkin lymphoma (B-cell NHL). As more than 90% of the B-cell NHL show CD20 antigen expression, ^{124}I -rituximab can also be applied in these patients, for whole body tumor detection and staging. Proof of concept of this approach has been provided using $^{99\text{m}}\text{Tc}$ -rituximab for gammacamera imaging (14) and ^{89}Zr -rituximab for PET imaging. Whether ^{124}I -rituximab can achieve similar image quality and sensitivity in detection of lymphoma, or whether $^{99\text{m}}\text{Tc}$ -rituximab or ^{89}Zr -rituximab can visualize rheumatoid activity (28), needs to be determined in separate investigations.

The uptake of ^{124}I -rituximab in joints was not high, and it did not seem to increase further over time after the first 24 hours. This may be explained by the therapeutic effect of the antibody. By binding to the CD20 antigen, rituximab causes B-cell eradication by induction of apoptosis, complement-mediated lysis, and antibody-dependent cellular toxicity (9). Elimination of the B-cell would also result in destruction and removal of the radioconjugate-B-cell complex (29). For optimal imaging with high synovial background contrast, a ligand is preferred that does not loose binding to its target and that leaves its target intact, resulting in cumulative uptake over time. A ligand without biological activity could circumvent the elimination effects of rituximab. Rituximab, an IgG molecule, consists of two identical Fab regions and a Fc-region. The Fc-region contains interaction sites for ligands that activate clearance mechanisms (30). The Fab-region determines the antigen specificity of the IgG molecule. By constructing anti-CD20 Fab fragments, the apoptotic effect of rituximab may be circumvented. Thus, for improvement of imaging, the application of Fab-fragments may be considered. However, as far as we know, no anti-CD20 Fab fragments are currently available for clinical use, and complications due to administration of the radioconjugate would have to be considered. In addition, (pre)clinical studies have reported the accumulation of radioconjugated Fab fragments in the bladder, stomach and kidneys, that could interfere with imaging (31-33).

Exposure to rituximab can lead to the formation of antibodies against rituximab and can have consequences for further treatment with rituximab. Human antibodies against chimeric antibodies (HACAs) can induce an immune response by evoking systemic inflammatory effects. In addition, HACAs could affect rituximab

pharmacokinetics, and subsequently reduce the efficacy of further rituximab treatment. The development of HACAs has occurred in a higher rate in patients with auto-immune diseases who are treated with rituximab than in patients with B-cell non-Hodgkin's lymphoma (10,34-37). The development of HACAs has been reported with high incidence after four cycles of rituximab (34). The included patients were all rituximab naive, and thus HACAs will not have influenced our results.

The ^{124}I -rituximab PET/CT imaging procedure is demanding, both for the patient and for involved personnel and imaging facilities. The patient first received unlabeled rituximab at an out-patient facility, whereafter the patient received labeled ^{124}I -rituximab, followed by image acquisitions for several days. This poses a significant time burden for the patient. However, our results showed that the number of scans can be reduced to one scan at 24 hrs or 48 hrs post-injection to evaluate the specific tracer uptake in joints. Two of the six (rituximab naive) patients had an adverse event after administration of unlabeled rituximab, in one case with a severity that prohibited administration of ^{124}I -rituximab. The events were infusion reactions, commonly observed after rituximab administration. Furthermore, the procedure carries a theoretical radiation dose of 0.6 mSv/MBq in a worst-case scenario with no excretion of the ^{124}I labeled antibody. These factors underline that the procedure should be validated further prior to clinical implementation, and its use should be limited to clinically relevant cases.

In conclusion, we have shown the feasibility of CD20 antigen imaging using ^{124}I -rituximab, for detection of inflamed joints in rheumatoid arthritis patients, albeit with limited uptake and sensitivity. The results are encouraging and form a fundament for more research, especially with regard to the interesting occurrence of discrepancies between ^{124}I -rituximab and clinical evaluation.

References

1. Shaw T, Quan J, Totoritis MC. B-cell therapy for rheumatoid arthritis: the rituximab (anti-CD20) experience. *Ann Rheum Dis* 2003;62 Suppl 2:ii55-9.ii55-ii59
2. Wolfe F, Cathey MA. The assessment and prediction of functional disability in rheumatoid arthritis. *J Rheumatol* 1991;18(9):1298-1306
3. Ward MM. Clinical measures in rheumatoid arthritis: which are most useful in assessing patients? *J Rheumatol* 1994;21(1):17-27
4. Bruyn GA, Naredo E, Moller I et al. Reliability of ultrasonography in detecting shoulder disease in patients with rheumatoid arthritis. *Ann Rheum Dis* 2009;68(3):357-361
5. Dohn UM, Ejbjerg BJ, Hasselquist M et al. Detection of bone erosions in rheumatoid arthritis wrist joints with magnetic resonance imaging, computed tomography and radiography. *Arthritis Res Ther* 2008;10(1):R25-
6. Elzinga EH, van der Laken CJ, Comans EF et al. 2-Deoxy-2-[F-18]fluoro-D-glucose joint uptake on positron emission tomography images: rheumatoid arthritis versus osteoarthritis. *Mol Imaging Biol* 2007;9(6):357-360
7. Zhang Z, Bridges SL, Jr. Pathogenesis of rheumatoid arthritis. Role of B lymphocytes. *Rheum Dis Clin North Am* 2001;27(2):335-353
8. Voswinkel J, Weisgerber K, Pfreundschuh M et al. The B lymphocyte in rheumatoid arthritis: recirculation of B lymphocytes between different joints and blood. *Autoimmunity* 1999;31(1):25-34
9. Maloney DG, Grillo-Lopez AJ, White CA et al. IDEC-C2B8 (Rituximab) anti-CD20 monoclonal antibody therapy in patients with relapsed low-grade non-Hodgkin's lymphoma. *Blood* 1997;90(6):2188-2195
10. Edwards JC, Szczepanski L, Szechinski J et al. Efficacy of B-cell-targeted therapy with rituximab in patients with rheumatoid arthritis. *N Engl J Med* 2004;350(25):2572-2581
11. Cohen SB, Emery P, Greenwald MW et al. Rituximab for rheumatoid arthritis refractory to anti-tumor necrosis factor therapy: Results of a multicenter, randomized, double-blind, placebo-controlled, phase III trial evaluating primary efficacy and safety at twenty-four weeks. *Arthritis Rheum* 2006;54(9):2793-2806
12. Emery P, Fleischmann R, Filipowicz-Sosnowska A et al. The efficacy and safety of rituximab in patients with active rheumatoid arthritis despite methotrexate treatment: results of a phase IIB randomized, double-blind, placebo-controlled, dose-ranging trial. *Arthritis Rheum* 2006;54(5):1390-1400
13. Perik PJ, Lub-de Hooge MN, Gietema JA et al. Indium-111-labeled trastuzumab scintigraphy in patients with human epidermal growth factor receptor 2-positive metastatic breast cancer. *J Clin Oncol* 2006;24(15):2276-2282
14. Gmeiner ST, Fettich J, Zver S et al. 99mTc-labelled rituximab, a new non-Hodgkin's lymphoma imaging agent: first clinical experience. *Nucl Med Commun* 2008;29(12):1059-1065
15. Behr TM, Wormann B, Gramatzki M et al. Low- versus high-dose radioimmunotherapy with humanized anti-CD22 or chimeric anti-CD20 antibodies in a broad spectrum of B cell-associated malignancies. *Clin Cancer Res* 1999;5(10 Suppl):3304s-3314s
16. Blauenstein P, Locher JT, Seybold K et al. Experience with the iodine-123 and technetium-99m labelled anti-granulocyte antibody MAB47: a comparison of labelling methods. *Eur J Nucl Med* 1995;22(7):690-698
17. Wiseman GA, Leigh B, Erwin WD et al. Radiation dosimetry results for Zevalin radioimmunotherapy of rituximab-refractory non-Hodgkin lymphoma. *Cancer* 2002;94(4 Suppl):1349-1357
18. van der Heijde DM, Jacobs JW. The original "DAS" and the "DAS28" are not interchangeable: comment on the articles by Prevoo et al. *Arthritis Rheum* 1998;41(5):942-945
19. Tran L, Baars JW, Maessen HJ et al. A simple and safe method for 131I radiolabeling of rituximab for myeloablative high-dose radioimmunotherapy. *Cancer Biother Radiopharm* 2009;24(1):103-110
20. Illidge TM, Bayne M, Brown NS et al. Phase 1/2 study of fractionated (131I)-rituximab in low-grade B-cell lymphoma: the effect of prior rituximab dosing and tumor burden on subsequent radioimmunotherapy. *Blood* 2009;113(7):1412-1421
21. Rosset A, Spadola L, Ratib O. OsiriX: an open-source software for navigating in multidimensional DICOM images. *J Digit Imaging* 2004;17(3):205-216
22. Wolfe F, Kleinheksel SM, Cathey MA et al. The clinical value of the Stanford Health Assessment Questionnaire Functional Disability Index in patients with rheumatoid arthritis. *J Rheumatol* 1988;15(10):1480-1488

23. Pincus T. Limitations of a quantitative swollen and tender joint count to assess and monitor patients with rheumatoid arthritis. *Bull NYU Hosp Jt Dis* 2008;66(3):216-223
24. Roben P, Barkmann R, Ullrich S et al. Assessment of phalangeal bone loss in patients with rheumatoid arthritis by quantitative ultrasound. *Ann Rheum Dis* 2001;60(7):670-677
25. Levy G, Chow C, Cimmino MA et al. RA Imaging Study Group: which imaging in rheumatoid arthritis? *Joint Bone Spine* 2009;76(4):438-439
26. Youinou P, Taher TE, Pers JO et al. B lymphocyte cytokines and rheumatic autoimmune disease. *Arthritis Rheum* 2009;60(7):1873-1880
27. Reparon-Schuijt CC, van Esch WJ, van Kooten C et al. Presence of a population of CD20+, CD38- B lymphocytes with defective proliferative responsiveness in the synovial compartment of patients with rheumatoid arthritis. *Arthritis Rheum* 2001;44(9):2029-2037
28. Muylle K, Azerad MA, Perk LR, Meuleman N, Delrieu V, Ghanem G, Bourgeois P, Vanderlinden B, van Dongen GA, Flamen P, Bron D. Immuno-PET/CT imaging with ⁸⁹Zr-rituximab as a prelude for radioimmunotherapy with ⁹⁰Y-rituximab in patients with relapsed CD20+ B-cell non-Hodgkin's lymphoma. *Ann Oncol* 2008;19 Supp 4:179-180 (Abstract)
29. Kaminski MS, Zasadny KR, Francis IR et al. Radioimmunotherapy of B-cell lymphoma with [131I]anti-B1 (anti-CD20) antibody. *N Engl J Med* 1993;329(7):459-465
30. Krapp S, Mimura Y, Jefferis R et al. Structural analysis of human IgG-Fc glycoforms reveals a correlation between glycosylation and structural integrity. *J Mol Biol* 2003;325(5):979-989
31. Brouwers A, Mulders P, Oosterwijk E et al. Pharmacokinetics and tumor targeting of 131I-labeled F(ab')₂ fragments of the chimeric monoclonal antibody G250: preclinical and clinical pilot studies. *Cancer Biother Radiopharm* 2004;19(4):466-477
32. Burvenich IJ, Schoonoghe S, Blanckaert P et al. Biodistribution and planar gamma camera imaging of (123)I- and (131)I-labeled F(ab')₂ and Fab fragments of monoclonal antibody 14C5 in nude mice bearing an A549 lung tumor. *Nucl Med Biol* 2007;34(3):257-265
33. Carter T, Sterling-Levis K, Ow K et al. Biodistributions of intact monoclonal antibodies and fragments of BLCA-38, a new prostate cancer directed antibody. *Cancer Immunol Immunother* 2004;53(6):533-542
34. Pijpe J, van Imhoff GW, Spijkervet FK et al. Rituximab treatment in patients with primary Sjogren's syndrome: an open-label phase II study. *Arthritis Rheum* 2005;52(9):2740-2750
35. Looney RJ, Anolik JH, Campbell D et al. B cell depletion as a novel treatment for systemic lupus erythematosus: a phase I/II dose-escalation trial of rituximab. *Arthritis Rheum* 2004;50(8):2580-2589
36. Berinstein NL, Grillo-Lopez AJ, White CA et al. Association of serum Rituximab (IDEC-C2B8) concentration and anti-tumor response in the treatment of recurrent low-grade or follicular non-Hodgkin's lymphoma. *Ann Oncol* 1998;9(9):995-1001
37. McLaughlin P, Grillo-Lopez AJ, Link BK et al. Rituximab chimeric anti-CD20 monoclonal antibody therapy for relapsed indolent lymphoma: half of patients respond to a four-dose treatment program. *J Clin Oncol* 1998;16(8):2825-2833

Conclusions and perspectives

The research described in this thesis shows that the chimeric monoclonal anti-CD20 antibody rituximab can be radiolabeled for diagnostic and therapeutic purposes in humans.

The labeling chemistry of antibodies with iodine is already known for several decades. Since its introduction in 1978 by Fraker and Speck, the Iodogen method is the most frequently utilized method for the radioiodination of monoclonal antibodies. The coated vial method is the most used variant of the Iodogen method. However, application of this method resulted in an unacceptable decrease of the immunoreactivity of rituximab. We have demonstrated that structural changes due to the oxidizing effect of Iodogen are the cause of this deterioration of the immunoreactivity of rituximab. We have also evaluated the potential role of three spectroscopic analytical techniques to characterize the structural changes emerging after iodination of rituximab. Using liquid chromatography coupled to mass spectrometry, we have shown a mass increase of the iodinated compound. Next to incorporation of iodine atoms, heterogeneous oxidation of amino acid moieties could contribute to the mass increase. Although the differences in circular dichroism spectra were subtle, the circular dichroism data of iodinated rituximab supports these results by showing an alteration in secondary structure of the monoclonal antibody after iodination. In addition, we have shown that fluorescence emission spectrophotometry can be a tool for rapid stability monitoring.

We have developed and validated an improved method for labeling and purification of radiolabeled rituximab. The integrity and immunoreactivity of rituximab were largely preserved (70%) and thus the radiolabeled product could be used for further clinical studies. The method is applicable for low doses as well as high doses of radioactivity. The labeling process was accompanied by a low and acceptable radiation exposure to involved personnel.

Radioimmunotherapy has emerged as a promising treatment modality in patients with a CD20 positive non-Hodgkin's lymphoma. Based on encouraging results published elsewhere, rituximab radiolabeled with ^{131}I was used for radioimmunotherapy in patients with relapsed or refractory non-Hodgkin lymphoma. In an ongoing clinical trial, 2 patients received ^{131}I -rituximab. The first patient was scheduled for radioimmunotherapy as consolidation therapy after remission induction treatment, unexpectedly showed no targeting of ^{131}I -rituximab in a remaining proven vital and CD20 positive lymphoma lesion. In the second patient, acceptable targeting was found after which he received a therapeutic dose. This case demonstrated the feasibility of this therapy, and the predictable pharmacokinetics of ^{131}I -rituximab supports the safe use of this treatment strategy. However, no response to the radioimmunotherapy was found. The exact mechanisms that prevents binding of radiolabeled rituximab in pretreated patients who still express the CD20 antigen has not been elucidated. Moreover, it is questionable if a therapeutic dose of ^{131}I -rituximab can be efficacious as consolidation therapy in patients who have received

extensive pretreatment with rituximab. These patients had lesions that showed progression during rituximab treatment. Treatment selection could exclude patients with unfavorable biodistribution. For this, radiolabeled rituximab can be used as scouting agent in order to select patients with proper binding. Thus, more studies are required to estimate the optimal patient populations and time point for radioimmunotherapy, before this technique can be applied.

Radiolabeling rituximab with ^{124}I allows imaging with positron emission tomography, a technique that provides wholebody imaging with better sensitivity and spatial resolution than conventional scintigraphy, in a 3-dimensional and quantitative approach. Furthermore, using a combined PET and computed tomography (PET/CT) system, the biodistribution of the antibody can be correlated with anatomical structures.

We have investigated the disposition of diagnostic doses of ^{124}I -rituximab in patients with rheumatoid arthritis with or without pretreatment with unlabeled rituximab. We have shown that a diagnostic dose of 50 MBq of ^{124}I -rituximab has favorable physical properties and pharmacokinetics for imaging over several days. However, our results also indicated that prior dosing with unlabeled rituximab is crucial, to avoid elimination of the tracer molecule due to targeting of the normal CD20 positive B-cell population in the spleen. Using this strategy, we were able to demonstrate the feasibility of CD20 antigen imaging using ^{124}I -rituximab, for the detection of inflamed joints in rheumatoid arthritis patients. Whether ^{124}I -rituximab can achieve good image quality and sensitivity in detection of lymphoma needs to be determined in further investigations.

However, the uptake of ^{124}I -rituximab in joints was not high, and it did not seem to increase further over time after the first 24 hours. For optimization of the imaging procedures, it would be preferable to use a ligand with no biological activity, that will result in cumulative uptake over time. Rituximab, an IgG molecule, consists of two identical Fab regions and a Fc-region. The Fc-region contains interaction sites for ligands that activate clearance mechanisms. The Fab-region determines the antigen specificity of the IgG molecule. By constructing anti-CD20 Fab fragments, the apoptotic effect of rituximab may be circumvented. Thus, for improvement of imaging, the application of Fab-fragments may be considered. However, as far as we know, no anti-CD20 Fab fragments are currently available for clinical use.

In this thesis, the pharmaceutical development and clinical application of radiolabeled rituximab is described. We have demonstrated a robust product for both therapy and imaging. The clinical application of the radioconjugate as radioimmunotherapeutic agent revealed unexpected new insights that emphasize the need for further research to find the optimal target population and time point. For this, radiolabeled rituximab can be used for diagnostic imaging to assist in optimal treatment selection.

¹²⁴I-rituximab as radioimmunosintigraphic agent for PET/CT imaging of the CD20 antigen is feasible and is promising for several clinical purposes. Interesting challenges lie ahead for further improvement of this application for imaging.

Summary

Monoclonal antibodies have proven their significant role in the treatment of malignant and benign diseases. Next to their therapeutic role, monoclonal antibodies also offer the application of radioimmunoscinigraphy and radioimmunotherapy. The basic concept is to use monoclonal antibodies as a carrier to transport a radionuclide to the target sites, exploiting the mechanism of selective binding of the antibody to an antigen. These antibody based modalities require the development and the use of radiolabeled monoclonal antibodies. **Chapter 1.1** describes selected methods for the preparation of radiolabeled monoclonal antibodies for human use emphasizing on issues such as manufacturing, validation, quality control and radiation safety.

As more than 90% of the B-cell non-Hodgkin lymphoma show CD20 antigen expression, the CD20 antigen is an ideal target for the treatment of B-cell non-Hodgkin lymphoma. Rituximab is a chimeric monoclonal antibody that specifically targets the CD20 antigen and induces B-cell eradication through antibody-mediated mechanisms. ^{131}I is a suitable nuclide for radioimmunotherapy. The β -emitting characteristics promote cytotoxic activity while the γ -rays enable diagnostic imaging. Hence, ^{131}I -rituximab was considered an appropriate agent for radioimmunotherapy for the treatment of B-cell non-Hodgkin lymphoma. In **chapter 1.2**, a radiolabeling and purification procedure is described for manufacturing high dose ^{131}I -rituximab. The described method offers a reproducible product with high (radio)chemical purity and retained immunoreactivity with minimal radiation exposure for involved personnel.

The radiolabeling procedure can affect the structural integrity of the monoclonal antibody. Subsequently, structural changes may influence the biological integrity, and thus the biological targeting, of the monoclonal antibody. In **chapter 1.3**, the potential role of three spectroscopic analytical techniques is demonstrated to characterize structural changes of rituximab emerging after iodination. Liquid chromatography coupled to mass spectrometry, fluorescence emission spectrophotometry, and circular dichroism can provide valuable information about structural changes of a radiolabeled compound, e.g. during pharmaceutical development and for quality control. The effects of different labeling conditions on the integrity of the protein can elegantly be studied using these techniques.

In **chapter 2** the pharmacokinetics of unlabeled rituximab in patients with CD20 positive non-Hodgkin lymphoma is described. The pharmacokinetics of unlabeled rituximab were investigated to get more insight into the factors that influence the pharmacokinetics of rituximab. Considerable inter-individual variability of rituximab levels was observed. For patients with circulating tumor cells and a high tumor burden, loading doses of rituximab could be considered for neutralizing the circulating antigen. The pharmacokinetics of rituximab were not influenced by the

development of antibodies against rituximab as the formation of these antibodies was not observed in our patient population.

Chapter 3.1 describes a case report of a 69-year old male with a relapsed mantle cell lymphoma scheduled for radioimmunotherapy. Images with a diagnostic dose of ^{131}I -rituximab did not show any uptake of the tracer, even though subsequent cytological analysis unequivocally confirmed a CD20 positive B-cell population in the lesion. The administration of a therapeutic dose of ^{131}I -rituximab was therefore cancelled. In this chapter, mechanisms that may explain lack of targeting in a proven CD20 positive lymphoma are discussed. Based on these results it is questionable if ^{131}I -rituximab would be efficacious as consolidation therapy for patients who have received extensive pretreatment with rituximab. Moreover, this case emphasizes the need for treatment selection for radioimmunotherapy.

Chapter 3.2 illustrates the case of a 65-year-old male with a relapsed CD20 positive follicular non-Hodgkin Lymphoma. After induction therapy the patient was in partial remission. Following administration of a diagnostic dose of 185 MBq ^{131}I -rituximab, remaining lesions were identified on the wholebody scans. The patient then received a therapeutic dose of 1000 MBq ^{131}I -rituximab. Whole body scans demonstrated localization of ^{131}I -rituximab in the tumor area. The half-life of ^{131}I -rituximab corresponded to the half-life of unlabeled rituximab. The pharmacokinetics of ^{131}I -rituximab were not different from unlabeled rituximab. This case demonstrates the feasibility of this therapy and the predictable pharmacokinetics of ^{131}I -rituximab supports the safe use of this treatment strategy.

Next to radioimmunotherapy, radioiodinated rituximab can serve as an imaging agent. **Chapter 4** illustrates the application of ^{124}I -rituximab for wholebody PET/CT imaging of CD20 antigen expression in patients with rheumatoid arthritis.

Rheumatoid arthritis is a destructive inflammatory joint disorder. Pre- and mature B-cells, characterized by CD20 antigen expression, play an important role in the inflammatory process. As the CD20 antigen is the biological target of rituximab, imaging of radiolabeled rituximab can be used to monitor the level of expression of the CD20 antigen in joints, and possibly indicating the degree of inflammation by reflecting the local number of infiltrating B-cells. **Chapter 4.1** demonstrates that ^{124}I -rituximab has favorable pharmacokinetics for targeting of (pathological) B-cells, and is suitable for imaging over several days, but only after pre-treatment with unlabeled rituximab. In addition, protection of the thyroid is recommended to prevent uptake of ^{124}I released from the radiolabeled antibody.

Chapter 4.2 reports the first results of ^{124}I -rituximab PET/CT in patients with rheumatoid arthritis. Images shortly after administration did not show accumulation of the tracer in joints, while images at 24h and later did show accumulation in joints, indicating that the visualized signal represents active targeting of the antibody to the

CD20 epitope and not mere perfusion. Although the determined level of uptake in joints was generally low, we have shown the feasibility of CD20 antigen imaging using ¹²⁴I-rituximab in rheumatoid arthritis patients.

In this thesis, we have shown that the manufacturing process of radiolabeled rituximab is safe for involved personnel, and moreover, results in a product with high preservation of the integrity of rituximab. The radioconjugate has favorable pharmacokinetics for radioimmunotherapy and radioimmunoscintigraphy.

However, its current position in the treatment strategy for patients with a CD20 positive non-Hodgkin lymphoma is not clear. More studies have to be performed to evaluate the optimal timing and the use of radioimmunotherapy for patients with CD20 positive non-Hodgkin lymphoma who are present treated with rituximab containing regimens and rituximab maintenance therapy. This might have impact upon the efficacy of radiolabeled anti-CD20 antibodies. In addition, we have shown that, apart from application in patients with non-Hodgkin lymphoma, the radioconjugate is feasible as radioimmunoscintigraphic agent for CD20 antigen imaging in patients with rheumatoid arthritis.

Samenvatting

Monoklonale antilichamen spelen een belangrijke rol in de behandeling van o.a. auto-immuunziekten en een aantal maligniteiten. Gekoppeld aan een radionuclide, kunnen monoklonale antilichamen ook gebruikt worden voor radioimmunosintigrafie en radioimmunotherapie. Gebruikmakend van de binding van een monoklonaal antilichaam aan een bepaald antigen, kunnen monoklonale antilichamen worden ingezet om radionucliden specifiek te richten op bepaalde processen en/of plaatsen in het lichaam. Hiervoor is het nodig om radioactief gelabelde antilichamen te ontwikkelen. Dit proefschrift beschrijft de ontwikkeling en toepassing van radioactief gelabeld rituximab.

In **hoofdstuk 1.1** wordt een aantal methoden beschreven voor de bereiding van radioactief gelabelde antilichamen voor humaan gebruik. Productie, validatie, kwaliteitscontrole en stralingsveiligheid zijn hierbij belangrijke aandachtspunten.

Rituximab is een chimeer monoklonaal antilichaam dat specifiek is gericht op een eiwit dat uitsluitend aanwezig is op de celwand van pre- en rijpe B-cellen: het CD20 antigen. Bij meer dan 90 procent van de B-cel non-Hodgkin lymfomen is het CD20 antigen aanwezig waardoor dit antigen een ideaal doelwit is voor de behandeling van B-cel non-Hodgkin lymfomen (non-Hodgkin lymfomen). Wanneer rituximab bindt aan een B-cel met het CD20 antigen, kunnen een aantal processen in werking treden waardoor de B-cel vernietigd kan worden: complementactivatie en hierdoor celdood, stimulatie van apoptose en het optreden van *antibody dependent cytotoxicity* (ADCC). Het is reeds aangetoond dat dit middel in combinatie met chemotherapie de responskans en de ziektevrije periode van patiënten met bepaalde B-cel non-Hodgkin lymfomen kan verbeteren.

^{131}I is een geschikt radionuclide voor radioimmunotherapie. De uitgezonden β -straling bevordert celdodende activiteit, terwijl de uitgezonden γ -stralen gebruikt kunnen worden voor diagnostische doeleinden. Hierdoor werd ^{131}I -rituximab beschouwd als een geschikt middel voor radioimmunotherapie voor de behandeling van B-cel non-Hodgkin lymfoom. In **hoofdstuk 1.2** wordt een procedure beschreven voor het radioactief labelen en opzuiveren van hoge dosis ^{131}I -rituximab. Toepassing van de beschreven methode resulteert in een product met een reproduceerbare hoge (radio)chemische zuiverheid en een voldoende immunoreactiviteit. Het product is te maken met minimale blootstelling aan straling voor het betrokken personeel.

De labelingprocedure kan de structuur van het monoklonaal antilichaam aantasten. Structuurveranderingen kunnen de biologische activiteit van het monoklonaal antilichaam (negatief) beïnvloeden. In **hoofdstuk 1.3** wordt de potentiële rol van drie spectroscopische analytische technieken bestudeerd om structuurveranderingen van rituximab te karakteriseren, die kunnen ontstaan na jodering van het monoklonaal antilichaam. Vloeistof chromatografie gekoppeld aan massa spectrometrie, fluorescentie emissie spectrofotometrie en circulair dichroïsme kunnen waardevolle informatie leveren over structuurveranderingen van een radioactief

gelabeld monokonaal antilichaam, bijvoorbeeld tijdens de farmaceutische ontwikkeling of als kwaliteitscontrole. De effecten van verschillende labelingsomstandigheden op de integriteit van het eiwit kan met behulp van deze technieken goed bestudeerd worden.

Hoofdstuk 2 beschrijft de farmacokinetiek van ongelabeld rituximab in patiënten met een CD20 positieve non-Hodgkin lymfoom. De farmacokinetiek van ongelabeld rituximab werd onderzocht om meer inzicht te krijgen in de factoren die de farmacokinetiek van rituximab kunnen beïnvloeden. Aanzienlijke interindividuele variabiliteit in rituximab spiegels werden waargenomen. Voor patiënten met circulerende tumorcellen en een hoge tumorlast kunnen oplaaddoses worden overwogen om circulerend antigen snel te neutraliseren en daardoor sneller een therapeutisch effect te bereiken. De farmacokinetiek van rituximab werd niet beïnvloed door de ontwikkeling van antilichamen tegen rituximab, aangezien het ontstaan van deze antilichamen niet werd waargenomen in onze patiëntenpopulatie, dit in tegenstelling tot patiënten met auto-immuunziekten waar dit werd waargenomen met een vrij hoge frequentie. Opvallend was dat bij de twee patiënten die een recidief kregen of niet goed op de therapie reageerden, de rituximab spiegel weer daalde of laag bleef: kennelijk bonden de tumorcellen de rituximab wel, maar werden er niet door gedood.

In **hoofdstuk 3** worden die eerste resultaten van de toepassing van ¹³¹I-rituximab voor radioimmuntherapie bij patiënten met recidief B-cel non-Hodgkin lymfoom weergegeven.

Hoofdstuk 3.1 beschrijft een casus van een 69-jarige man met een recidief mantelcel lymfoom die gepland stond voor radioimmunotherapie. Beeldvorming met een diagnostische dosis van ¹³¹I-rituximab liet echter geen opname van het radiofarmacon zien, terwijl gelijktijdige cytologische analyse een duidelijk CD20 positieve B-cel populatie toonde. De toediening van een therapeutische dosis van ¹³¹I-rituximab werd hierdoor geannuleerd aangezien er geen therapeutische voordelen voor de patiënt te verwachten waren. In dit hoofdstuk worden mechanismen voorgelegd die mogelijkerwijs een verklaring kunnen geven voor het ontbreken van *targeting* in een aangetoonde CD20 positieve laesie. Gebaseerd op deze resultaten, is het ook twijfelachtig of ¹³¹I-rituximab een plaats heeft als consolidatietherapie voor patiënten die uitgebreid zijn voorbehandeld met rituximab. Bovendien benadrukt deze casus de behoefte voor patiëntselectie voor radioimmunotherapie.

Hoofdstuk 3.2 belicht een casus van een 65-jarige man met een recidief CD20 positief folliculaire non-Hodgkin lymfoom. Na inductietherapie was de patiënt in partiële remissie. Na hier opvolgende toediening van een diagnostische dosis van 185 MBq ¹³¹I-rituximab werd duidelijke accumulatie van ¹³¹I-rituximab in de overgebleven laesies waargenomen. De patiënt kreeg een therapeutische dosis van

1000 MBq ^{131}I -rituximab. Vervolgens werd op verschillende manieren de farmacokinetiek van ^{131}I -rituximab onderzocht. Deze bleek niet te verschillen van ongelabeld rituximab. Deze casus toont aan dat deze therapie uitvoerbaar is en de voorspelbaarheid van de farmacokinetiek van ^{131}I -rituximab ondersteunt het veilige gebruik van deze benadering.

Naast radioimmunotherapie kan radioactief gelabeld rituximab dienen als diagnosticum. **Hoofdstuk 4** illustreert de toepassing van ^{124}I -rituximab voor visualisatie van CD20 antigen expressie in patiënten met reumatoïde artritis. Reumatoïde artritis is een chronische gewrichtsaandoening die gepaard gaat met ontstekingsreacties. De pre- en rijpe B-cellen, die door CD20 antigen expressie gekenmerkt worden, spelen een belangrijke rol in het ontstekingsproces.

Binding van rituximab aan het CD20 antigen kan worden gevisualiseerd door aan rituximab een hiervoor geschikt radionuclide te koppelen. ^{124}I is een radionuclide dat beeldvorming met behulp van positron emissie tomografie/computertomografie (PET/CT) mogelijk maakt. Binding van radioactief gelabeld rituximab aan het CD20 antigen kan worden gebruikt om het niveau van de CD20 antigen expressie aan te geven. Op deze manier kan eventueel de mate van ontsteking worden aangegeven.

Hoofdstuk 4.1 toont aan dat ^{124}I -rituximab gunstige farmacokinetische eigenschappen bezit voor het specifiek richten op (pathologische) B cellen. ^{124}I -rituximab is geschikt voor beeldvorming over verscheidene dagen, maar beeldvorming is slechts mogelijk na voorbehandeling met ongelabeld rituximab. Bovendien wordt het aanbevolen om de schildklier te beschermen tegen opname van ^{124}I dat vrijkomt van het radioactief gelabelde antilichaam. In **hoofdstuk 4.2** worden de eerste resultaten beschreven van ^{124}I -rituximab PET/CT beeldvorming in patiënten met reumatoïde artritis. De opgenomen beelden kort na toediening van het radiofarmacon toonden geen accumulatie van het radiofarmacon, terwijl de beelden vanaf 24 uur na toediening wel accumulatie in gewrichten toonden. Deze bevindingen kwamen merendeels overeen met de klinische bevindingen. Hoewel het niveau van opname van het radiofarmacon over het algemeen laag was, is de haalbaarheid aangetoond van visualisatie van CD20 antigeen expressie gebruikmakend van ^{124}I -rituximab in patiënten met reumatoïde artritis.

In dit proefschrift werd aangetoond dat het productieproces van radioactief gelabeld rituximab voor betrokken personeel veilig is en bovendien resulteert in een product met behoud van de integriteit van rituximab. Het radioconjugaat toonde gunstige farmacokinetiek voor de toepassing van radioimmunotherapie en radioimmunosintigrafie. Nochtans is de huidige positie van radioimmunotherapie met radioactief gelabelde antilichamen gericht tegen het CD20 antigen in de behandelingsstrategie voor patiënten met B-cel non-Hodgkin lymfomen die voorbehandeld zijn met het ongelabeld monoklonaal antilichaam gericht tegen het CD20 antigen (rituximab is het meest gebruikt) niet duidelijk. Meer studies moeten

worden uitgevoerd voor de evaluatie van het optimale tijdpunt en plaats van radioimmunotherapie in het behandelingsplan voor patiënten met non-Hodgkin lymfomen.

Radio-actief gelabeld rituximab kan ook gebruikt worden voor diagnostische doeleinden bij patiënten met non-Hodgkin lymfomen of auto-immuunziekten zoals reumatoïde artritis. Uit het onderzoek beschreven in dit proefschrift blijkt de toepassing van radioactief gelabeld rituximab voor visualisatie van het CD20 antigeen in patiënten met reumatoïde artritis goed mogelijk te zijn.

Dankwoord
&
Curriculum vitae

Op de voorkant van een proefschrift staat altijd maar één naam. Echter, een proefschrift - zeker dit proefschrift - is het resultaat van het werk van velen. Ik wil iedereen bedanken die heeft bijgedragen aan het tot stand komen van deze dissertatie.

Allereerst wil ik de patiënten bedanken die hebben meegedaan aan de studies beschreven in dit proefschrift.

Een aantal personen wil ik in het bijzonder noemen. Ik hoop dat ik niemand tekort doe in dit dankwoord. Als dat wel het geval is, dan bied ik op voorhand mijn excuses aan.

Alwin Huitema, co-promotor en mijn directe begeleider. Dank voor vier jaar van topbegeleiding. Ik ben soms echt om achter het behang te plakken, maar gelukkig wist jij daar heel erg goed mee om te gaan.

Mijn andere co-promotor Joke Baars. Zonder jou was dit onderzoek nooit gestart. Bedankt voor het mogelijk maken van de onderzoeken die beschreven staan in dit proefschrift.

Jos Beijnen, promotor, dank voor je deskundigheid, je verfrissende doch kritische blik en je stille maar altijd aanwezige betrokkenheid bij het onderzoek.

Een groot deel van mijn onderzoek deed ik in samenwerking met de afdeling Nucleaire Geneeskunde. Ik wil alle medisch nucleair werkers bedanken voor al hun hulp op het hotlab en met het scannen van de patiënten.

En de drie nucleair geneeskundigen, drempelloos benaderbaar en gastvrij.

Wouter Vogel, je niet te temperen nieuwsgierigheid naar het nieuwe werkt aanstekelijk. Jij gaf een nieuwe dimensie aan mijn proefschrift. Mijn dank voor al je hulp is niet in een paar woorden uit te drukken.

Kees Hoefnagel en Renato Valdés Olmos, bedankt voor jullie interesse en jullie hulp. Bedankt dat jullie mij de mogelijkheid hebben gegeven om langer te blijven om mijn proefschrift in huis af te kunnen maken.

Martin van Rijswijk en Huib Dinant, de reumatologen, zijn van groot belang geweest bij het tot stand komen van hoofdstuk 4. Hiervoor mijn dank, het was mij een zeer groot genoegen om met jullie samen te werken.

I would like to thank Ilse Novak-Hofer and her team for giving me the first introduction into the radioiodination of monoclonal antibodies. Thank you for the hospitality during my stay at the Paul Sherrer Institute.

In een adem wil ik de hemato-oncologen Jan-Paul de Boer en Martijn Kerst, de stralingsdeskundigen Harry Maessen en Linda Jansen, de klinisch fysici Saar Muller en Michiel Sinaasappel, Henny van Rooy en Theo Lammers van het radionuclidencentrum, de dames van de bloedafname en alle verpleegkundigen van de dagbehandeling (zowel van het Antoni van Leeuwenhoek ziekenhuis als van het Slotervaartziekenhuis) bedanken voor hun hulp. Sietske de Vries en haar team, helaas is het RIT-project anders gelopen dan gehoopt. Desalniettemin, bedankt voor jullie hulp en inzet!

Ik wil de groep van John Haanen en Ton Schumacher bedanken voor hun gastvrijheid en voor hun hulp met de celproeven. Hierbij wil ik in het bijzonder Raquel Gomez en Willeke van den Kastele bedanken.

Guus van Dongen, Gerard Visser en Maria Vosjan ben ik zeer erkentelijk voor hun hulp toen mijn onderzoek tot stilstand kwam en een nieuwe boost nodig had.

Lucien Aarden, Kim van Houten, Henk de Vrieze van het Sanquin, hartelijk dank voor het meten van de rituximab spiegels.

Dick Pluim, bedankt voor het dag en nacht paraat staan voor al mijn HPLC problemen.

Bastiaan Nuijen, bedankt voor al je antwoorden op mijn productievragen. Edith Vermeij, dank voor jouw ondersteuning bij mijn productieactiviteiten. Natuurlijk wil ik de rest van de medewerkers van de apotheek bedanken voor al hun hulp.

Roel van Gijn, dank voor alles, vooral toen mijn computer begon te disfunctioneren. Iedereen van het BA lab en van het QC lab, bedankt voor al jullie hulp en sorry voor mijn destructieve karakter.

Mies van Steenberg van Universiteit Utrecht, bedankt voor de mogelijkheid om experimenten uit te voeren aan de universiteit.

Collega-onderzoekers van het eerste en het laatste uur: een unieke groep om nooit te vergeten. Een aantal collega-onderzoekers wil ik graag persoonlijk bedanken.

Allereerst mijn befaamde Slotervaartmannen: vakidioten van de bovenste plank. Lieve Dop, bedankt voor je advies en hulp. Bedankt voor je eeuwige geduld met mij en voor je altijd luisterend oor. Ronmen, dank je voor al je (computer)hulp en sorry dat ik je de laatste paar maanden gek heb gedraaid. Joost en Robbie! Jullie onuitputtelijke enthousiasme gaf de onderzoeker in mij weer moed als het even niet mee zat. Bedankt voor jullie ideeën en jullie pogingen om mij creatief te laten zijn.

Marie-Christine, Elke en Judith, dank jullie voor jullie oprechtheid en betrokkenheid. En inderdaad, jullie hadden gelijk: alles komt goed. Miek, succes met de laatste

loodjes en het komt allemaal goed. Carola, bedankt voor je hulp bij de MS analyse. Formuleringskamer, het epi-centrum van de GMP. Bedankt voor jullie hulp en tevens bedankt voor het aanbod om mij te adopteren als formulette. Mijn kamergenoten, mijn dank, jullie hadden het met mij zwaar te verduren, zeker in de laatste maanden. En de rest van de (oud-)collega's: bedankt voor alles!!

Op die ene dag in december word ik bijgestaan door twee paranimfen die zelf alle klappen van de zweep kennen. Lieve Rosie, begin dit jaar was ik jouw paranimf en nu sta je als mijn paranimf achter mij. Jij bent een bron van energie en dat werkt heel erg aanstekelijk. Je bent al een tijdje OIO-af, maar ik vind het echt top dat we elkaar nog vaak spreken. Lieve Anthe, het is voor ons beide een bijzonder jaar geweest, met veel onvergetelijke gebeurtenissen die ons nog dichter bij elkaar hebben gebracht. Ik mis de spontane "ik kom even een bakkie halen", maar een jaar is zo voorbij. En een rondje hardlopen in Central Park lijkt me wel wat!

Sander en Lars, de mannen achter deze dames: bedankt voor jullie interesse, betrokkenheid en het verzorgen van de catering.

Lieve Lot, mijn aller-oudste vriendinnetje. Van jou heb ik geleerd dat je niet altijd sterk hoeft te zijn. Bedankt dat je er altijd voor me bent.

Lieve Veronique en Femke, jullie lieten mij altijd weer lachen wanneer er weer een donderwolk boven mij hing. Met behulp van een zak M&M's en wijn, hielpen jullie mij om alles weer te relativeren, en vonden jullie op de juiste momenten de juiste woorden om te zeggen. Jullie zijn kanjers.

Lieve Pieter Frank, ik ben trots dat een echte Pieter Frank mijn voorkant siert. Dank!

In het laatste jaar van mijn onderzoek woonde ik meer op het werk dan thuis. Maar het was altijd fijn om thuis te komen, want daar was mijn lieve huisgenootje Anne-Marie, alias Siem. Lieve Siem, Tip is nu klaar en knal die flessen wijn maar open!

En alle andere vrienden en vriendinnen, teveel om op te noemen, mijn dank. Een mens mag zich gelukkig prijzen met zoveel vrienden om zich heen.

Lieve papa en mama, aan jullie draag ik dit proefschrift op. Jullie hebben toentertijd veel opgegeven en jullie zijn het onbekende tegemoet gegaan om ons een veilige haven te kunnen bieden. Bedankt voor de vrijheid om zelf keuzes te kunnen maken om te worden wie we nu zijn. Mijn lieve broer, zusjes, schoonzus en zwager, bedankt voor jullie vertrouwen en liefde.

Ly
Amsterdam, 2009

Ly Tran is op 12 december 1978 geboren in Vung Tau (Vietnam). Kort hierna besloten haar ouders om het land te verlaten. Haar jeugd bracht ze door in Enschede, waar ze in 1997 haar VWO diploma had behaald aan het Jacobus College. In datzelfde jaar startte ze met de studie farmacie aan de Rijksuniversiteit Groningen. De doctoraalopleiding werd afgesloten met een afstudeeronderzoek bij de afdeling Nucleaire Geneeskunde en de ziekenhuisapotheek van het Universitair Medisch Centrum Groningen, onder leiding van prof. dr. D.R.A. Uges en dr. M.N. Lub-de Hooge. Het project was de karakterisering van radioactief gelabelde trastuzumab. In 2005 behaalde ze het apothekersdiploma. Aansluitend begon ze met het promotieonderzoek dat is beschreven in dit proefschrift. Het onderzoek werd uitgevoerd in het Antoni van Leeuwenhoekziekenhuis en in het Slotervaartziekenhuis onder begeleiding van prof. dr. J.H. Beijnen, dr. A.D.R. Huitema en dr. J.W. Baars.

Ly Tran was born on December 12, 1978 in Vung Tau (Vietnam). Soon afterwards, her parents decided to leave the country. She spent her youth in Enschede, whereas she finished her secondary school at the Jacobus College in 1997. In that same year, she started to study pharmaceutical sciences at the University of Groningen. She completed her graduation project at the Department of Nuclear Medicine and the Hospital Pharmacy at University Medical Center Groningen. Dissertation subject was the characterisation of radiolabeled trastuzumab. The research was conducted under supervision of prof. dr. D.R.A. Uges and dr. M.N. Lub-de Hooge. In 2005, she received her PharmD degree and started her PhD project which is described in this thesis. This research was conducted in the Antoni van Leeuwenhoek hospital en the Slotervaart hospital under supervision of prof. dr. J.H. Beijnen, dr. A.D.R. Huitema and dr. J.W. Baars.

